



TECHNICAL UNIVERSITY OF CRETE

Study And Modeling of Pedestrian Walk With Regard to The Improvement of Stability And Comfort on Walkways

Author:

Pavlos Paris Giakoumakis

Thesis Committee:

Prof. Michalis Zervakis

Prof. George Karystinos

Assistant Prof. Fabrizio
Pancaldi (UNIMORE)

*A thesis submitted in partial fulfillment of the requirements for the Diploma in
Electrical and Computer Engineering*

in the

SCHOOL OF ELECTRICAL AND COMPUTER ENGINEERING

December 2020

TECHNICAL UNIVERSITY OF CRETE

Abstract

SCHOOL OF ELECTRICAL AND COMPUTER ENGINEERING

Diploma in Electrical and Computer Engineering

Study And Modeling of Pedestrian Walk With Regard to The Improvement of Stability And Comfort on Walkways

by Pavlos Paris Giakoumakis

The static stability of footbridges or pedestrian walkways can be effectively assessed through several approaches developed in the fields of mechanical and civil engineering. On the other hand, the dynamic stability of pedestrian walkways represents an underexplored field and only in the last 2 years, the comfort of such structures has been investigated. A walkway under the tendency to oscillate, provokes panic and insecurity of the users and needs to be appropriately addressed in order to guarantee the safety of pedestrians.

In this thesis, we introduce an innovative algorithm for modeling and simulation of human walk using Gaussian Mixture Models. Our model satisfies the requirements of simplicity, ease of use by engineers and is suitable to accurately assess the dynamic stability of walkways. Furthermore, we implement a simulator that can be used to provide reliable prediction and assessment of floor vibrations under human actions. Evaluation results are promising, showing that our simulator is capable of supplementing the experimental procedure in future research.

Η στατική ισορροπία των πεζογεφυρών ή πεζόδρομων μπορεί να εκτιμηθεί αποτελεσματικά μέσω διαφόρων προσεγγίσεων που έχουν αναπτυχθεί στα πλαίσια της μηχανολογίας και της πολιτικής μηχανικής. Αντίθετα, η δυναμική ισορροπία των πεζόδρομων αποτελεί ένα ανεξερεύνητο πεδίο και μόνο τα τελευταία 2 χρόνια ερευνάται το θέμα της άνεσης σε αυτές τις κατασκευές. Μία πεζογέφυρα που τείνει να ταλαντωθεί, προκαλεί πανικό και ανασφάλεια στους χρήστες και πρέπει να διευθετηθεί κατάλληλα ώστε να εγγυάται την ασφάλειας των πεζών.

Σε αυτή τη διπλωματική εργασία, παρουσιάζουμε έναν καινοτόμο αλγόριθμο για τη μοντελοποίηση και προσομοίωση του ανθρώπινου βαδίσματος χρησιμοποιώντας τα Gaussian Mixture Models. Το μοντέλο μας ικανοποιεί τις απαιτήσεις απλότητας, ευκολίας στη χρήση από μηχανικούς και είναι κατάλληλο για την εύστοχη εκτίμηση της δυναμικής ισορροπίας των πεζόδρομων. Επιπροσθέτως, υλοποιήσαμε έναν προσομοιωτή που μπορεί να χρησιμοποιηθεί για την αξιόπιστη πρόβλεψη και αξιολόγηση των δονήσεων του εδάφους που προκαλούνται από ανθρώπινες δράσεις. Η πειραματική αξιολόγηση της προσέγγισης μας είναι ενθαρρυντική καθώς υποδεικνύει ότι ο προσομοιωτής μας δύναται να ενισχύσει σημαντικά την πειραματική διαδικασία σε μελλοντική έρευνα.

Acknowledgements

As I finish my undergraduate studies, I would like to thank several people that have supported me through this period of my life.

First, I would like to thank Prof. Michalis Zervakis for the chance to work on this thesis and for his valuable guidance as well as Prof. Georgios Karystinos who devoted his valuable time to study and examine this work.

I would also like to express my gratitude to Assistant Prof. Fabrizio Pancaldi from the University of Modena & Reggio Emilia (UNIMORE) for providing me the chance to work on this subject at his laboratory. I will never forget the valuable help and happy memories he offered while living in Reggio Emilia.

Furthermore, I would like to thank my lab mates in UNIMORE for their advice and friendship: Behnoor Dianat and Manolis Kaditis.

My classmates in Technical University of Crete deserve special mention for the cooperation and friendship all these years: Aggelos Marinakis, Chris Kolomvakis, Manolis Kaditis, Nick Ghionis, Panagiotis Mpellonias, Petros Portokalakis, Thodoris Antoniadis and many others...

I would also like to thank my parents and my brother Giannis for their support and encouragement.

I would like to offer special thanks to my cousins Giannis and Pavlos Korkidis.

Last but not least, I would like to thank my friends for their emotional support and the fun times we spent together. To name a few: Akis Vagionakis, Antonis Lountzis, Elena Kornaraki, Evina Kappou, George Kolomvakis, Kostas Mantzouros, Kostas Tsoupakis, Michalis Voutsadakis, Nick Drakoulakis, Stamatia Volani and Stelios Apostolakis.

Contents

Abstract	iii
Acknowledgements	v
List of Figures	ix
List of Abbreviations	xi
1 Introduction	1
1.1 The Pedestrian Walkway	1
1.2 Issues to The Design - Vibration Serviceability	2
1.3 Thesis Contributions	3
1.4 Thesis Outline	3
2 Background	5
2.1 The Bipedal Walking	5
2.1.1 The Walking Cycle	5
2.1.2 The Walking Parameters	6
2.1.3 The Vertical Load Induced During a Walk	7
2.2 Problem Definition	10
2.2.1 The Statistical Model Deployed in This Work	10
2.2.2 Gaussian Mixture Modelling	12
3 Related Work	15
3.1 Time-Domain Deterministic Force Models	15
3.1.1 Low-Frequency Force Models	16
3.1.2 High-Frequency Force Models	18
3.1.3 Drawbacks in Deterministic Force Modeling	19
3.2 Frequency Domain Force Models	20
3.3 Probabilistic Force Models	22
3.3.1 Step Frequency of Probabilistic Force Models	22
3.3.2 Probabilistic Force Models Available in the Literature	22
4 Proposed Approach	27
4.1 Experimental Framework	29
4.1.1 Database Properties	29
4.1.2 Database Analysis	30
4.1.3 Variable Extraction	32

4.1.4	Extraction of Interarrival Time and Mean Force	33
4.1.5	Extraction of Length and Angle	36
4.1.6	Extraction of The Unified Table	37
4.2	Variable Modeling	39
4.2.1	Estimation of GMM Components	39
4.2.1.1	The Default Index Method	40
4.2.1.2	Exploring a Solution	40
4.2.1.3	Fitting on the Unified Walk Data	42
4.2.1.4	Fitting on the Pedestrian Walk Data	42
4.2.2	Distribution Fitting	44
4.3	Parameter Modeling	47
4.3.1	Statistical Description of the Mean Table	47
4.3.2	Statistical Description of the Mixing Probability (Component Proportion Coefficients)	55
4.3.3	Statistical Description of the Variance/Covariance Matrix Σ	59
4.4	Modeling Overview	61
4.5	The Simulator	63
4.5.1	Parameter Estimation	63
4.5.2	Extraction of the Random Walk	64
5	Experimental Setup	67
5.1	Instruments Used for the Analysis	67
5.2	Critical Factors in the Analysis	69
6	Simulations & Evaluation	71
7	Conclusion & Future Work	75
7.1	Conclusion	75
7.2	Future Work	75
	Bibliography	77

List of Figures

1.1	The Knokke Footbridge in Deerlyck, Belgium & The Millennium Bridge in London, UK	1
1.2	Components of vibration serviceability analysis	2
2.1	A Complete Walk Cycle	6
2.2	Vertical force induced in a single step	8
2.3	Vertical force induced for different modes of movement activity	9
2.4	The geometrical interpretation of the proposed model	11
3.1	Walking speed and DLF as a function of pacing rate	17
3.2	DLFs for the first four harmonics of the walking force	18
3.3	Response behavior comparison of successive steps in low and high frequency floors	19
3.4	Autospectral density (ASD) of the walking force	21
3.5	Representation of walking force in the frequency domain	21
3.6	Normal distributions of step frequency for normal tempo walking as extracted in several researches	23
3.7	Normal distribution of walking speed at 1.8 Hz of step frequency	23
3.8	DLFs of the first harmonic as a function of the number of persons and step frequency	24
3.9	80-step walking force time history for a single pedestrian, DLFs, phase angle and period of walking steps	25
3.10	Categorization of walking force signals based on pacing rate	25
4.1	A brief modeling plan	28
4.2	A brief simulation plan	28
4.3	Position measurements axis	29
4.4	Simplified form of the initial database	30
4.5	Simplified form of the modified database	31
4.6	An example of the force-time arrays before and after the "clear-out"	32
4.7	Construction of meanTime table	34
4.8	Dt extraction algorithm	35
4.9	Shifting the nans to the end of each row	36
4.10	Calculation of length and angle on 3 steps of a walk	37
4.11	The form of a random pedestrian's unified table	38
4.12	AIC and BIC values of GMMs varying components fitted on 11 pedestrians	41
4.13	AIC/BIC values of the GMM fitted on the unified walk data for 1-15 components	42

4.14	Mean index evaluation and score differential diagrams of the unified walk data	43
4.15	AIC/BIC values of the GMM fitted on a random pedestrian's data for 1-15 components	44
4.16	Mean index evaluation and score differential diagrams of the unified walk data	45
4.17	Multivariate GMM of 3 components fitted in random pedestrian's walk data	46
4.18	Univariate GMM of 2 components fitted on angle of step	47
4.19	Gaussians fitted on mean table for Dt, meanF and len - default method	49
4.20	Gaussians fitted on mean table for angle - default method	50
4.21	Mean table's modeling logic for Dt variable - part 1	51
4.22	Mean table's modeling logic devised in this work for Dt variable - part 2	52
4.23	Gaussians fitted on mean table for Dt, meanF and len	53
4.24	Gaussians fitted on mean table for angle	54
4.25	Mixing probability (Component Proportion Coefficients) modeling logic - part 1	56
4.26	Mixing probability (component proportion coefficients) modeling logic - part 2	57
4.27	Gaussians fitted on mixing probabilities	58
4.28	Variance/covariance matrix Σ modeling logic	59
4.29	Gaussians fitted in variance/covariance matrix Σ	60
4.30	An overview of modeling human walk	62
4.31	Generating a random mean table	63
4.32	Generating random mixing probability (component proportion coefficients)	64
4.33	Generating a random variance/covariance matrix Σ	64
4.34	Generating random parameters for the angle variable	65
4.35	An overview of the simulator	66
5.1	The instrumented floor used in the experiments	68
5.2	Force sensors installed beneath the vertices of the plates	68
6.1	A random walk	72
6.2	Scattering a random walk	73
6.3	First walk of a random subject	73

List of Abbreviations

AIC	Akaike Information Criterion
ASD	AutoSpectral Density
BIC	Bayesian Information Criterion
col	Column
dim	Dimension
DLF	Dynamic Load Factor
Dt	Interarrival Time
GM	Gaussian Mixture
GMM	Gaussian Mixture Model
GMMs	Gaussian Mixture Models
len	Length
meanF	Mean Vertical Force
ND	Normal Distribution
pdf	probability density function

*Dedicated to the memory of my friend Giorgos Paterakis
who will always remind me that life is too short to defy
your dreams. He did not have enough time to pursue his...*

Chapter 1

Introduction

1.1 The Pedestrian Walkway

Definition 1 *The pedestrian walkway or footbridge is a type of bridge designed solely for pedestrian crossings between two points. This type of infrastructure gained prominence in contemporary architecture of the 21st century because of the growing urban expansion and the push towards a “greener” mobility [53].*

Despite the desire of the human species to overcome the obstacles of nature, there has been a considerable spread of walkways dedicated exclusively to pedestrians and cyclists only after the Second World War, following the development of the road network. This has paved the way for numerous projects of pedestrian walkways climbing over canals, rivers or roads. The design of this type of bridge requires the development of a sustainable approach aimed at encouraging human's approach to the living environment, even in highly urbanized tissues as well as promoting the use of bicycles and walking not only for recreational use but also for basic needs.

Nowadays, pedestrian walkways are very widespread and are not only built for crossing the obstacles of nature but also as a means to traverse road networks and complex railways safely. **Figure 1.1**, depicts two pedestrian walkways, designed to overcome a road and a river, respectively.



FIGURE 1.1: (a) The Knokke Footbridge in Deerlyck, Belgium - (b) The Millennium Bridge in London, UK.

1.2 Issues to The Design - Vibration Serviceability

Lightness and **slenderness** are substantive aesthetic characteristics in the design of a modern footbridge. This is corollary given the fact that the loads these structures must support are generally low (about $400\text{-}500 \text{ kg/m}^2$).

An emblematic example of this is the **London Millennium Footbridge** in London, UK. It is a steel suspension footbridge crossing the River Thames, linking Bankside with the City of London that initially opened in June 2000. On this day, thousands of pedestrians crossed it to celebrate the grand opening and was closed for modifications only two days later because of unexpected **lateral vibration** due to **resonant structural response** that was not adequately considered and analyzed during the design phase. For this reason, residents of London often refer to it by the nickname "Wobbly Bridge".

These **excessive vibrations** are a common under-researched phenomenon that also applies to other infrastructures e.g., stadiums [24] theaters [63], building floors [14, 21], and staircases [13]. In this case, the pedestrians crossed a bridge with lateral oscillation and unconsciously matched their footsteps to the sway, exacerbating it. A well-known example of this phenomenon is when troops march over a suspension bridge in a synchronized step and therefore are required to break step when crossing such a bridge.

Definition 2 *Vibration serviceability analysis* is in fact to ensure the human comfort when crossing such a walkway i.e., the study of the comfort of walkways.

Consequently, the so-called **vibration serviceability** has become a dominant design aspect to consider over the last few years and has been increasingly the focus of researchers worldwide [61, 54, 34, 43]. This factor is firmly linked to the possible deformation and vibration of the structure even though these vibration phenomena generally do not pose a risk to the safety of the structure. It is therefore of vital importance to monitor and evaluate the mode of vibration to avoid discomfort situations.

The two main parameters typically used to quantitatively describe vibration response are **amplitude** and **frequency** [9]. More specifically, if the amplitude exceeds a tolerance limit at the frequency of vibration, it is considered excessive i.e. the frequencies of vibrations induced in the bridge must be distant from the low frequencies that are perceived by humans.

Vibration serviceability analysis can be broken down into three key components as depicted in **Figure 1.2**. These are the **input** (excitation source), the **system** (floor structure), and the **output** (vibration receiver) [41, 42, 40, 50, 70]. The pedestrian is a typical receiver of vibrations in the walkway but also represents the excitation source that this work will focus on, due to the induced dynamic load. Human activities such

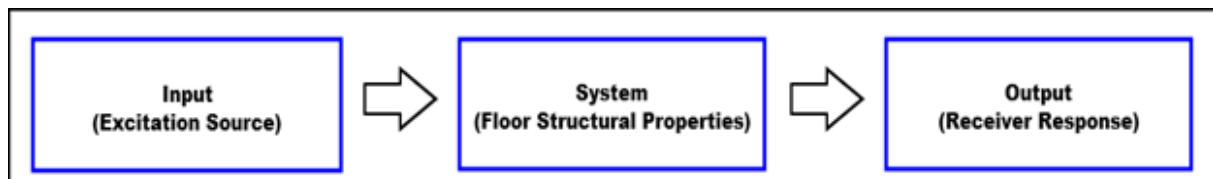


FIGURE 1.2: Components of vibration serviceability analysis.

as walking [10], jogging [45], jumping [49], and running [36] commonly create the vibration problems.

Over the years there have been several studies planning to establish a **natural frequency threshold**. An example of these is the NTC 2008 that concluded in the fact that a higher natural frequency to 5Hz ensures a good level of comfort to the pedestrian. However, the evaluation of vibrations induced by humans is still widely debated and poorly understood despite the importance of vibration serviceability in the design of the structure. In fact, there is a wide variety of contradictory dynamic load models due to many uncertainties associated with human walking [37]. This problem would be surpassed by an acceptable uniform model of the human walk.

1.3 Thesis Contributions

The scope of this thesis is to provide a reliable and efficient **uniform model of human walk** as well as a simulator for the sake of establishing an experimental procedure and a reference dataset for future researches taking its probabilistic nature into consideration. More specifically, the measurements resulting by more than 200 subjects crossing an instrumented floor were provided and calibrated in a walk database (see [chapter 5](#)). The appropriate variables describing human gait were then extracted from these measurements in order to statistically describe them. Then, a statistical model describing the parameters of the variable models is estimated therefore creating our uniform model of human walk. Furthermore, a gait **simulator** has been developed based on this statistical model. The output of this simulator are the n appropriate variables describing a random walk of n steps.

1.4 Thesis Outline

The remainder of this thesis is structured as follows:

- In [chapter 2](#), we introduce some basic background concerning the bipedal walking as well as some key ideas used throughout the thesis. Furthermore, a definition of the problem beneficial to understanding the mathematical models implemented is described.
- In [chapter 3](#) we investigate the history and some related work in the field of modeling human-induced walking excitation.
- In [chapter 4](#) we discuss the proposed approach, starting from the experimental framework and the calibration of the walk database, moving on to the statistical description of the variables describing human walk, then the modeling of the parameters describing these variables, and finally describing the implementation of the simulator.
- In [chapter 5](#) we elaborate on the experimental setup and more specifically on the instruments used for the analysis as well as the critical factors we should consider in the measurements.

- In [chapter 6](#) we provide an evaluation of the simulations and the simulated results.
- Finally, [chapter 7](#) provides a conclusion for our work and suggests possible future work.

Chapter 2

Background

In section 2.1, we are going to give a short introduction to the key ideas used throughout the thesis as well as present the basic concept of bipedal walking, while in section 2.2 we will present the statistical model deployed in this work.

2.1 The Bipedal Walking

2.1.1 The Walking Cycle

In most people's eyes, walking is a simple and automatic act. However, if we focus on the dynamics of human movement, we find that it is rather a complex mechanism. It is therefore important to understand what constitutes a complete walk cycle in this first analysis.

Definition 3 *A complete walk cycle consists of the human body movement starting from the beginning of a step with one foot, up to the beginning of the next step with the same foot, as shown in Figure 2.1.*

While walking, each foot passes through two phases during a single step: the swing phase and the stance (or contact) phase.

Definition 4 *The swing phase refers to the period when the foot is off the floor, while the stance phase refers to the period during which the foot is in contact with the ground [4].*

Concurrently, the human body goes through two stages during the walking process: the double-support and the single-support stage.

Definition 5 *When the body is on the double-support stage, the feet are in contact with the ground [32]. This stage usually comprises less than 20% of the walking cycle while as the walking speed increases, it comprises a smaller percentage. On the contrary, the human body is at the single-support stage when one foot is in contact, while the other is off the ground [59].*

A **complete walk cycle** can be explained as a series of consecutive events as follows [22, 20, 57, 44]:

1. The left foot is straying from the ground ("left toe-off" in Figure 2.1) in the direction of walking. At the same time, the right foot provides the essential support. Thus, the left foot is in a swing phase, while the human body is in a right single-support stage.

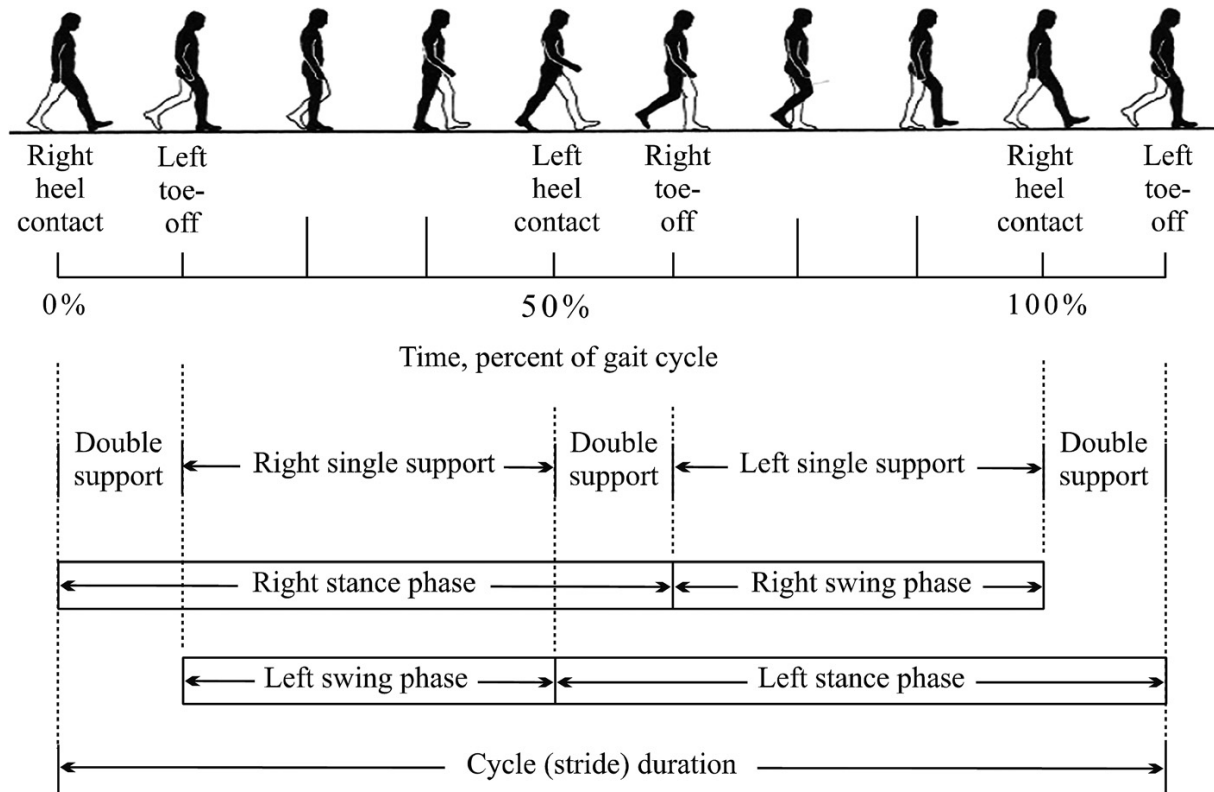


FIGURE 2.1: A Complete Walk Cycle. [22]

2. Subsequently, the left foot contacts the floor ("left heel contact" in Figure 2.1) and starts the contact phase, while the human body passes through a stage of double support once again.
3. Next, the right foot moves off the floor and starts a swing phase, while the left foot is still in contact phase providing left single support for the body.
4. Then the right foot contacts the floor and the body is on double support phase.
5. Finally, the left foot moves off the ground (left toe-off in Figure 2.1), and the walking cycle is completed.

2.1.2 The Walking Parameters

The parameters used to describe human gait are divided into two types: the **temporal (time)** and **spatial (distance or location)** parameters [younis].

Some typical **temporal parameters** are:

- **The walking speed:** The magnitude of horizontal velocity in the gait direction, expressed in meters per second.
- **Cycle time:** Represents the period during which a complete cycle occurs.

- **Pacing rate (walking frequency):** The number of steps in a specific duration, usually expressed in steps per minute or Hz [57].

Some typical **spatial parameters** are:

- **Step length:** The distance measured during a single step between both heels in the direction of walking.
- **Step width:** The distance measured transversely between the two lines which describe the paths taken by the right and the left foot, where these lines pass through heel midpoints.
- **Stride length:** The distance measured along the gait direction between two consecutive contacts of the same foot. It also represents the total distance traveled during one cycle period [44].

2.1.3 The Vertical Load Induced During a Walk

Regarding the various parameters that characterize the human walking process, we can identify the presence of two types of randomness: The intersubject and the intra-subject variability [35].

Definition 6 *The intersubject variability exists because different persons will have different key parameters directly related to the induced forces, such as subject weight, step frequency, walking speed, and so on [68]. So, the resultant walking forces vary from person to person. However, intrasubject variability exists because an individual never repeats two identical steps sequentially i.e., a person produces forces that are different at each footfall [67].*

A walking person causes dynamic forces that have components in three directions: the vertical the horizontal-parallel, and the horizontal-transverse to the direction of movement [5]. However, only the vertical force component will be addressed in this thesis, since it has the highest magnitude of all and is by far the most significant in vibration serviceability analysis.

Thorough studies conducted by several researchers starting with Harper [19] and followed by Galbraith and Barton [18], Blanchard et al. [7], Ohlsson [38], Andriacchi et al. [1], and Kerr [26], conclude that the vertical force typically has **two peaks and a trough** as shown in [Figure 2.2](#).

In this figure, the force is expressed as a percentage of the body weight, and the time is normalized with respect to the stance phase duration (see [Figure 2.1](#)). When the heel strikes the floor, the dynamic force increases until it reaches a peak value equal to F_1 at time T_1 which corresponds to approximately 25-30% of the stance phase's (or contact's) duration. After that, the dynamic force decreases until the mid-stance point, T_2 , at which both the heel and toe are in contact with the ground, while the other foot is in a swing phase. Subsequently, the heel rises, and the vertical force increases until it reaches another peak, F_3 , at time, T_3 , near the end of the stance phase and heel strike of the other foot. Finally, the foot rises from the floor and the force decreases rapidly to zero at the stance phase completion [50].

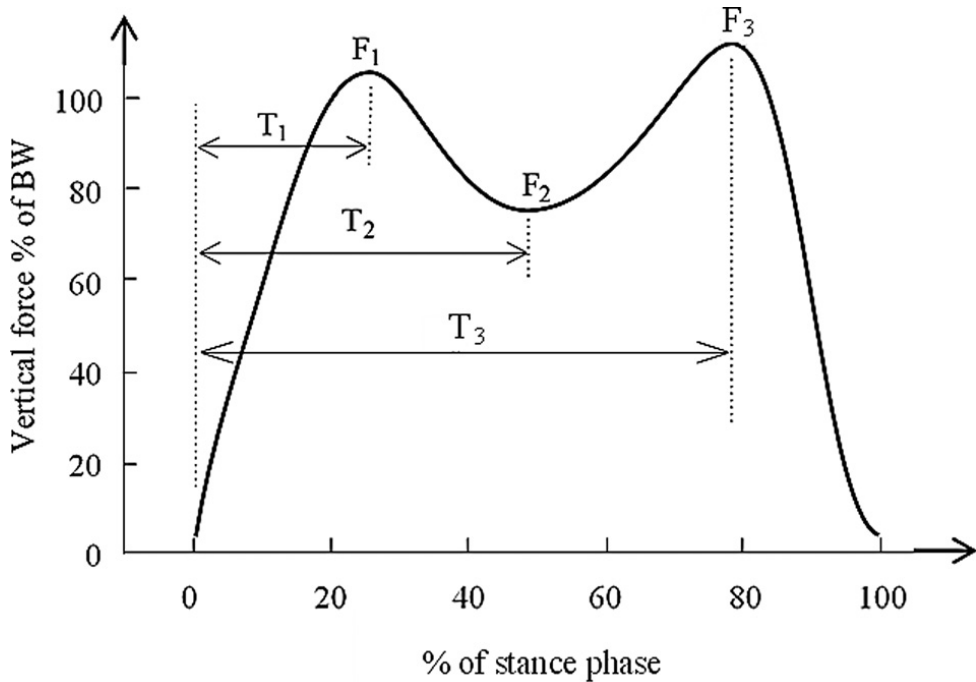


FIGURE 2.2: Vertical force induced in a single step. [50]

It was noted, however, that this graph changes considerably at different walking speeds. There are two main factors considered to affect the amplitude of the peak force: the **weight** of the person and the **frequency steps**. The increase of these factors leads to higher peak forces.

Wheeler [younis, 58] has conducted a wide-ranging study to classify different types of human movements, arranged from slow walking to running (Figure 2.3). Each of these categories had a unique peak amplitude single-step dynamic force, shape, and stance period. Additionally, the author stated that different parameters such as stride length, walking speed, contact time, peak force and step frequency are related. For example, increasing the step frequency leads to shortening the contact time and increasing the peak force.

This work will emphasize in normal tempo gaits (see Figure 2.2). Thus, running will not be discussed further as it is considered an extreme case of walking in terms of movement speed.

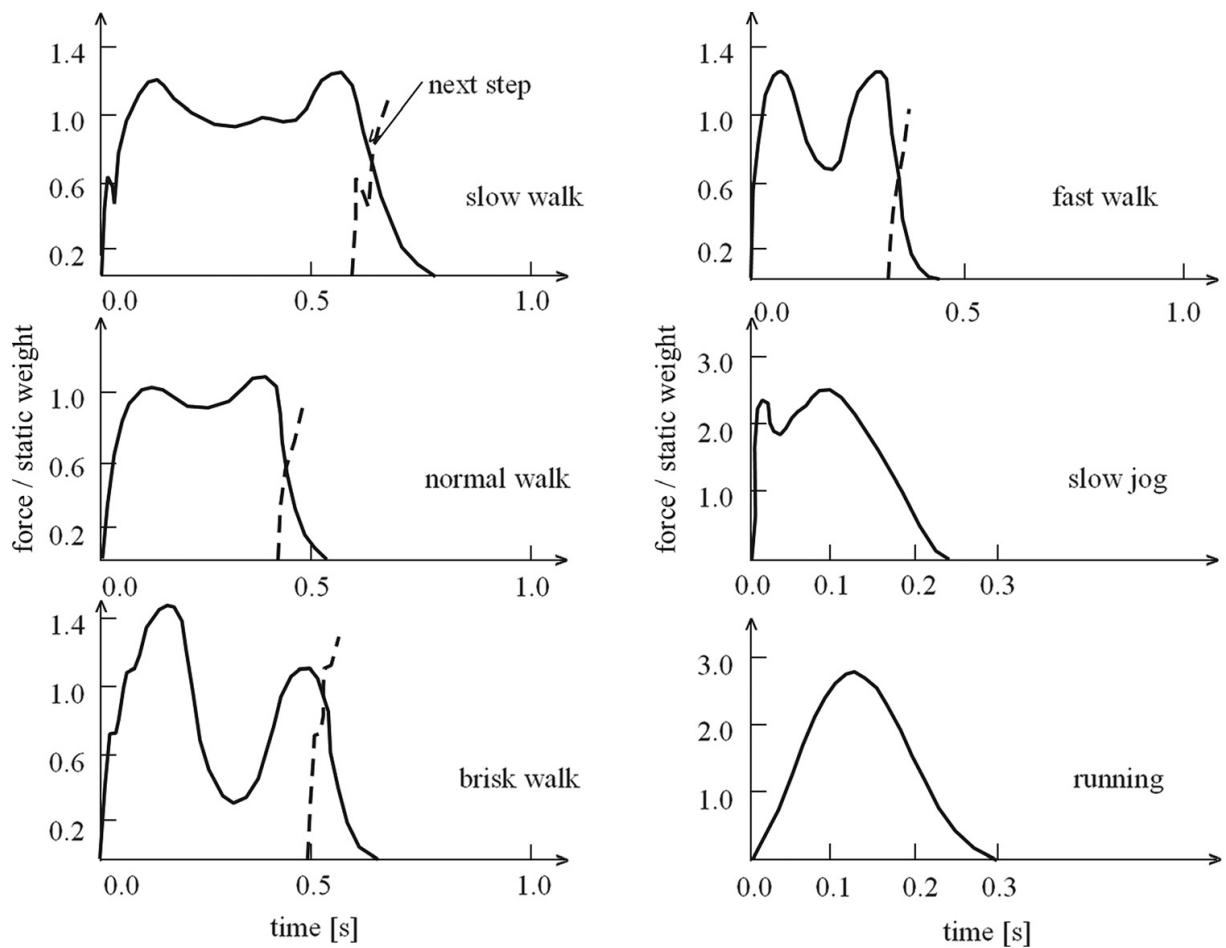


FIGURE 2.3: Vertical force induced for different modes of movement activity. [70]

2.2 Problem Definition

2.2.1 The Statistical Model Deployed in This Work

In this study, the human walk is described through four variables. Those are the **mean vertical force** (denoted as force), the **interarrival time** Δt (denoted as time), the **length**, and the **angle** of each step. Force is related to the weight and gait of the pedestrian and represents the excitation signal of a structure. For the sake of simplicity, it is assumed that each step's force is applied to a dimensionless point of the structure and the only forces considered are vertical.

The variables described above are related to each other. However, the steps of each person are never identical, as explained in [subsection 2.1.3](#) and thus, the pedestrian walk is modeled as a series of steps where each parameter of a given step is independent of those of the previous steps. The drawback of this method is the fact that due to this; the proposed model is **memoryless** and unable to describe some events i.e., a stumble or a collision.

The mathematical model used in this work takes inspiration from a Markov chain application called **random walk**. More specifically, the position of each pedestrian is described as a sequence where each step's position depends exclusively on the position of the previous step. In a classical random walk, the direction of each step is uniformly distributed between $[0, 2\pi)$. However, the pedestrian in our case is walking towards an endpoint, which means that its direction cannot be uniformly distributed.

In this scenario, the state of the Markov chain at the k^{th} step is described as:

$$S_k = \{F_k, \Delta t_k, l_k, \theta_k\} \quad (2.1)$$

where:

- F_k : The mean vertical force applied at the k^{th} step.
- Δt_k : The time between the $k - 1^{th}$ and k^{th} step.
- l_k : The length traversed between the $k - 1^{th}$ and k^{th} step.
- θ_k : The direction of the k^{th} step (angle between the $k - 1^{th}$ and k^{th} step)

[Figure 2.4](#) describes the geometrical interpretation of the proposed model. Since the process is represented by a countable sequence of steps, it can be inferred that the Markov chain is continuous in the state space S and discrete in time. Lastly, it is assumed that the steps are independent and identically distributed (i.i.d.) and thus, the Markov chain is described by the transition probability density function (pdf) which is devised by the experimental measurements contained in the provided database as:

$$p(S) = p(F, \Delta t, l, \theta) \quad (2.2)$$

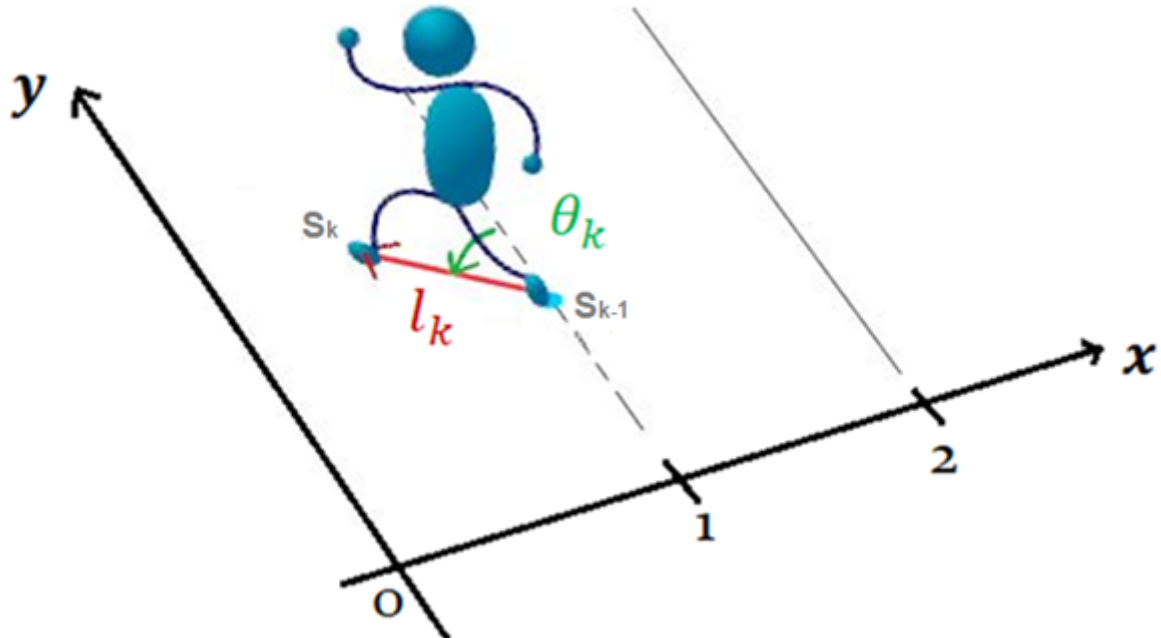


FIGURE 2.4: The geometrical interpretation of the proposed model. [39]

Consequently, the correlation between the 4 variables describing the human walk was extracted by Fornaciari [17], using some experimental measurements. More specifically, the correlation coefficients of distinct variables have been assessed for each student and then averaged over the number of students to devise general indications. Thus, the average matrix correlation \bar{R} arises as:

$$\bar{R} = [\bar{R}_{ij}] = \begin{bmatrix} 1 & -0.33 & -0.25 & 0.02 \\ -0.33 & 1 & 0.06 & 0.15 \\ -0.25 & 0.06 & 1 & 0.08 \\ 0.02 & 0.15 & 0.08 & 1 \end{bmatrix} \text{ for } i, j = 1, 2, 3, 4 \quad (2.3)$$

Where:

- $R_{12} = R_{21} = -0.33$: The time-force correlation coefficient
- $R_{13} = R_{31} = -0.25$: The time-length correlation coefficient
- $R_{14} = R_{41} = 0.02$: The time-angle correlation coefficient
- $R_{23} = R_{32} = 0.06$: The force-length correlation coefficient
- $R_{24} = R_{42} = 0.15$: The force-angle correlation coefficient
- $R_{34} = R_{43} = 0.08$: The length-angle correlation coefficient

As it occurs, the time-force, time-length, and force-angle correlations are important whereas any other correlation can be considered negligible. We consider that for

each step, time, force, and length are correlated, while the angle variable is statistically independent from the other variables. Thus, [Equation 2.2](#) can be written as:

$$p(S) = p(F, \Delta t, l, \theta) = p(F, \Delta t, l)p(\theta) \quad (2.4)$$

2.2.2 Gaussian Mixture Modelling

Definition 7 A **Gaussian Mixture Model (GMM)** is a probabilistic model for representing normally distributed subpopulations within an overall population. It is parameterized by the mixture component weights, the component means, and the variances/covariances.

For a Gaussian mixture model with K components, the k^{th} component has a mean of m_k and variance of σ_k for the univariate case and a mean of μ_k and covariance matrix of Σ_k for the multivariate case. The mixture component weights are defined as ϕ_k for component C_k , with the constraint that the total probability distribution normalizes to 1, thus:

$$\sum_{i=1}^K \phi_i = 1 \quad (2.5)$$

The component weights are the a-posteriori estimates of the component probabilities given the data.

As eventuated by the work of Caleri [11], a GMM is an interesting approach to this work since it depends on a limited number of parameters, can accurately approximate several practical distributions, can rely on simple algorithms, and represents the problem at hand successfully.

Assuming that the GM $p(F, \Delta t, l)$ fitting the **multivariate** pdf $p(F, \Delta t, l)$ is based on K components, the pdf is approximated through the GM:

$$\hat{p}(F, \Delta t, l) = \sum_{i=1}^K w_i N(\mu_i, \Sigma_i) \quad (2.6)$$

where ϕ_i is the weight of the i^{th} component and $N(\mu_i, \Sigma_i)$ is a multivariate normal distribution with mean μ_i and symmetric covariance matrix Σ_i , for $i = 1, 2, 3$ such that:

$$N(\mu_i, \Sigma_i) = \frac{1}{\sqrt{(2\pi)^3 |\Sigma_i|}} \exp\left(-\frac{1}{2} (\vec{x} - \vec{\mu}_i)^T \Sigma_i^{-1} (\vec{x} - \vec{\mu}_i)\right) \quad (2.7)$$

The pdf of the **step angle** $p(\theta)$ has been analyzed independently of the other variables (time, force, and step length). Assuming that the GM $p(\theta)$ fitting the **univariate** pdf $p(\theta)$ is based on M components, the pdf is approximated through the GM:

$$\hat{p}(\theta) = \sum_{i=1}^M \alpha_i N(m_i, \sigma_i) \quad (2.8)$$

where ϕ_i is the weight of the i^{th} component and $N(m_i, \sigma_i)$ is a univariate normal distribution with mean m_i and standard deviation σ_i , for $i = 1, 2, 3, 4$ such that:

$$N(m_i, \sigma_i) = \frac{1}{\sigma_i \sqrt{2\pi}} \exp\left(-\frac{(x - m_i)^2}{2\sigma_i^2}\right) \quad (2.9)$$

Concluding, the **transition pdf** $\hat{p}(S)$ is therefore approximated using eq: 2.4, 2.6 and 2.8 as:

$$\hat{p}(S) = \hat{p}(F, \Delta t, l) \hat{p}(\theta) = \left(\sum_{i=1}^K w_i N(\mu_i, \Sigma_i) \right) \left(\sum_{i=1}^M \alpha_i N(m_i, \sigma_i) \right) \quad (2.10)$$

Chapter 3

Related Work

In this chapter, we introduce some related work on the field of modeling human walking forces. The resulted models can be used to predict vibrations during the design phase. However, this modeling presents several challenges. First, due to many parameters being affected by the intersubject and intrasubject variability, a high variability in force waveform shapes is presented [58] as depicted in [Figure 2.3](#). Moreover, the dynamic forces induced by a pedestrian are narrowband random processes that are not completely understood yet and thus, not accurately assessed [8].

However, several force models have been implemented by researchers and are used during the design phase. Two types of models are most commonly used for human walking excitation. These are the time-domain models that are currently more widely used, and the frequency-domain models.

Time-domain force models are forked into two groups; the deterministic and probabilistic.

Definition 8 *Deterministic models aim to generate a uniform force model without directly considering the natural variability between people [6]. These models are based on assumptions such as perfect periodicity and uniformity of produced force for both feet. On the other hand, the probabilistic models consider the intersubject variability of each person i.e., each individual presents unique parameters influencing the produced forces e.g., weight, tempo etc. Each parameter is described by its pdf and hence, measured by the probability of occurrence [69].*

In the remaining chapter, we first discuss about time-domain deterministic force models available in the literature. Then, the frequency-domain models will be introduced and we conclude with some probabilistic force models that surfaced in the last years.

3.1 Time-Domain Deterministic Force Models

Bachmann and Ammann [5] indicated that the magnitude of human-induced vibration depends significantly on the ratio of walking frequency of the pedestrian and the lowest vertical natural frequency of the floor. There are two types of floors presented in the literature according to their natural frequency: the low-frequency and high-frequency floors [50]. This distinction has been applied as a result of significant variations in the dynamic responses, as ascertained in several studies. The threshold frequency values

defining the type of floor is calculated at **9-10 Hz** for floors having at least one natural frequency.

In the moment of writing, there is no deterministic walking force model that can be used for prediction of both low-frequency and high-frequency floor responses, due to the different response behavior. Therefore researchers have developed different force models for each.

3.1.1 Low-Frequency Force Models

Definition 9 *Low-frequency floors are typically regarded as floors having at least one responsive natural frequency below 9-10 Hz.*

Each periodic force with a period T can be represented by a Fourier series. The vertical dynamic force induced by a pedestrian can be expressed by a summation of harmonic components (i.e., Fourier series) being assumed as periodic in the time domain as:

$$F_p(t) = G + \sum_{i=1}^n G\alpha_i \sin(2\pi i f_p t - \phi_i) \quad (3.1)$$

where:

- G : The individual static weight (N).
- i : The order number of the harmonic.
- n : The number of all contributing harmonics.
- f_p : The step frequency (Hz).
- ϕ_i : The phase shift of the i^{th} harmonic (rads).
- α_i : The Fourier coefficient of the i^{th} harmonic, usually known as the dynamic load factor (DLF) i.e., The dynamic coefficient.

Many researchers have attempted to quantify the DLF α_i for the contributing harmonics over the last years as it is the key to generate an accurate deterministic force model. These studies resulted in the force models included in the major footbridge design guides used today.

Blanchard et al. [7] proposed a simple deterministic force model concerning the load exerted on footbridges by a pedestrian. In this model, it is concluded that if the fundamental frequency of the walkway does not exceed 4 Hz, resonance is presented in the first harmonic of the dynamic load with $\alpha_i = 0.257$ and $G = 700N$. If the fundamental frequency is between 4 and 5 Hz, the resonance is a result of the second harmonic and therefore applied some reduction factors.

Later in 1982, Kajikawa, according to Yoneda [64], improved the previous model. More specifically, he introduced a relationship between the correction coefficient i.e., DLF and walking pace (m/sec). The walking speed depending on step frequency was also added as an output of his model. His results are presented in [Figure 3.1](#).

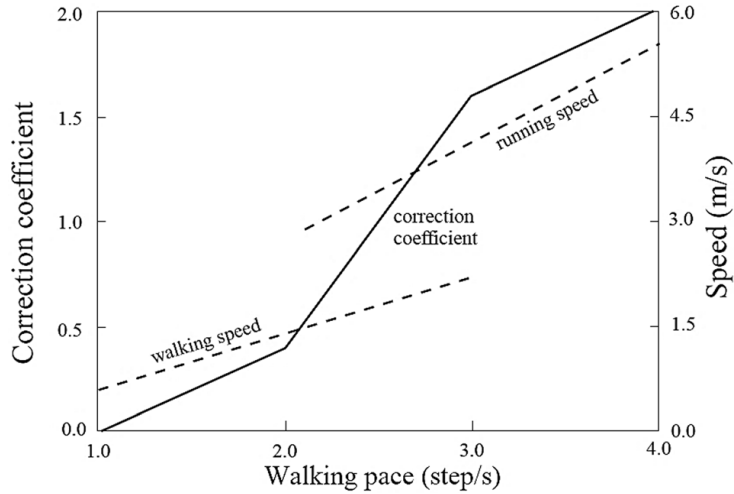


FIGURE 3.1: Walking speed and DLF as a function of pacing rate. [64]

Subsequently, Bachmann and Ammann [57] reported the Fourier coefficient values for the first five harmonics of the walking force and highlighted that the induced load is related to the step frequency. They specifically suggested DLFs of 0.4 and 0.5 for the first harmonic DLF at frequencies of 2.0 and 2.4 Hz, respectively, with linear interpolation for the frequencies in between, while a DLF value of 0.1 was proposed for a step frequency close to 2 Hz.

In late 80s, Rainer et al. [51] made a significant contribution by measuring the continuous waveform of force induced by walking, running and jumping on an instrumented floor. Through their studies, they also confirmed the strong bond between the DLF and the frequency. Interestingly, the dynamic forces reported for walking were found to be considerably higher than the ones suggested by previous researchers. However, the deficiency of this study is that it included measurements from only three test individuals and therefore cannot be considered statistically reliable [50, 70].

A very thorough work has been performed by Kerr [33] as part of his PhD thesis. He recruited 40 subjects and generated a very large database consisting of 1000 single-step force measurements of a single footfall on a force plate covering step frequencies ranging from 1 Hz, which is unnaturally low, to 3 Hz, which is unnaturally high. Each step was repeatedly appended and summed to create a waveform that represents a walk in a certain period of time, which was Fourier transformed to estimate the DLFs. The DLF values of the harmonics were characterized statistically simply by mean values and standard deviation with the exception of the first harmonic, in which the dynamic forces increase with step frequency. This study was partly criticized by Rasic et al. [18] due to its inability to represent the intrasubject variability.

Young [65] as well as Willford et al. [60] conducted a wide-ranging study to develop a reliable guide for modeling walking forces and the corresponding structural responses. More specifically, they applied statistical regression in the data of Figure 3.2 that were published by several researchers. Hence, they proposed DLF's mean and design values for the first four harmonics. Young [65] suggested the following set of

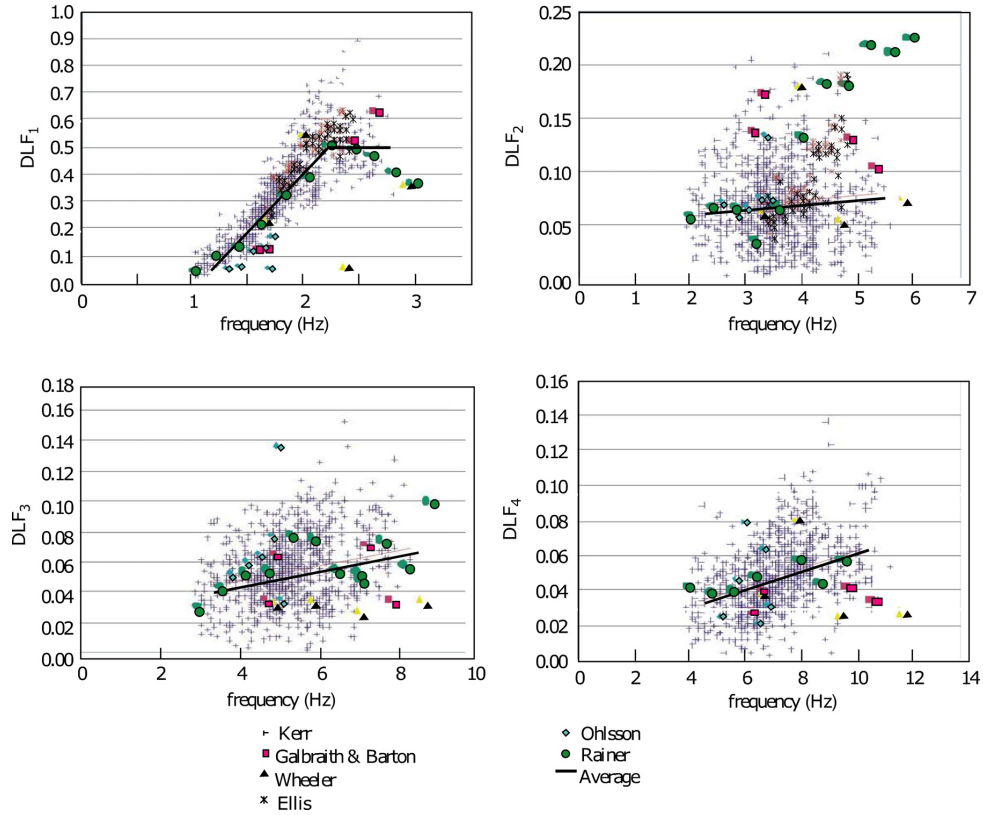


FIGURE 3.2: DLFs for the first four harmonics of the walking force gathered from different researchers. [65]

equations as a function of step frequency:

$$\begin{aligned}
 \alpha_1 &= 0.41(f - 0.95) \leq 0.56 & 1 \text{ Hz} \leq f \leq 2.8 \text{ Hz} \\
 \alpha_2 &= 0.069 + 0.0056f & 2 \text{ Hz} \leq f \leq 5.6 \text{ Hz} \\
 \alpha_3 &= 0.033 + 0.0064f & 3 \text{ Hz} \leq f \leq 8.4 \text{ Hz} \\
 \alpha_4 &= 0.013 + 0.0065f & 4 \text{ Hz} \leq f \leq 11.2 \text{ Hz}
 \end{aligned} \tag{3.2}$$

Where f represents the frequency of the harmonic which equals an integer multiple of the pacing rate. He also stated that the recommended design values have 25% probability of exceeding. This deduction classifies him as one of the first researchers that accounted the probabilistic nature of human walking.

3.1.2 High-Frequency Force Models

Definition 10 *High-frequency floors* are typically regarded as floors having no responsive natural frequency below 9-10 Hz i.e., floors with frequency higher than four times the average walking frequency.

The available literature on high-frequency force models is generally limited due to the fact that human discomfort in vibration phenomena is mainly found in low-frequency

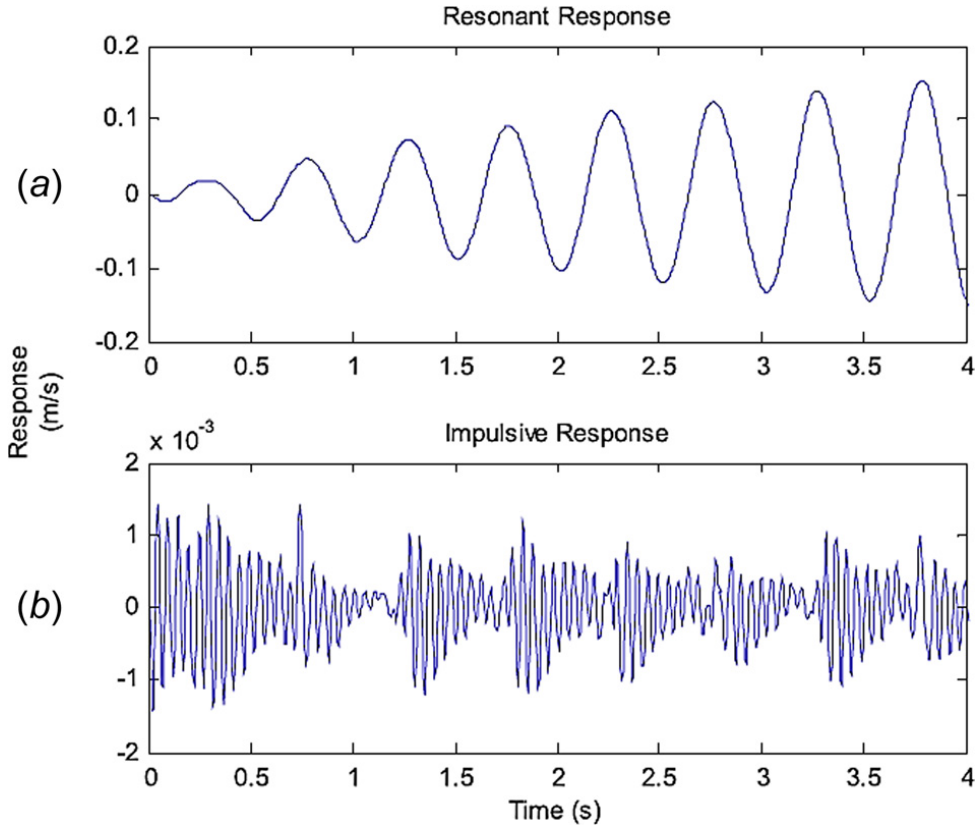


FIGURE 3.3: Response behavior comparison of successive steps in (a) low and (b) high frequency floors. [33]

floors. The response of these floors presents a transient or impulsive profile [33] unlike the resonant behavior found in the response of low-frequency counterparts. [Figure 3.3](#) illustrates this difference.

In this figure it is noted that, unlike the typical low-frequency resonant response which involves an accumulation in structure's response of successive step, in high-frequency floors the vibration responses of successive steps do not build up because of the structural damping decaying effect. More specifically, the first heel touch produces an initial peak response followed by floor oscillating at its natural frequency with a decaying rate associated with the damping ratio of the fundamental mode [28]. Similarly, another impulse response is generated at each subsequent step.

3.1.3 Drawbacks in Deterministic Force Modeling

Deterministic force models account for the most common approach in human walk modeling. Thus, the reliability of those models has been extensively tested and important drawbacks have been identified. First, these models usually do not consider the inter-and intrasubject variability of human walking. Secondly, the classification of floors by their natural frequency is not considered accurate in certain circumstances e.g., a floor with a fundamental frequency close to the 9-10 Hz threshold probably

exhibits a mixed response and thus cannot be classified [71]. Lastly, the vibration response computed in these models is a numeral usually compared with a selected limit of vibration tolerance. This results in a binary pass or fail criterion which does not provide enough information to make a decision in the design phase [72]. Therefore, Deterministic modeling is generally not considered very accurate or precise, leading to wrong estimation of the floor vibration response.

3.2 Frequency Domain Force Models

Continuous walking forces can be alternatively represented in the frequency domain, i.e. the walking history can be represented by the amplitudes gathered via Fourier transform decomposition [55]. Ohlsson [38] was one of the first researchers involved in frequency-domain representations of walking forces. He concluded that a single step contains excitation energy in the frequency range between 0 and 6 Hz and also extracted the autospectral density (ASD) of the walking force in the high frequency range of 6-50 Hz.

Eriksson [16] performed a similar study focusing on the low-frequency floors and produced the ASD of [Figure 3.4](#). In this figure, it is noted that the excitation energy at integer multiples of step frequency is smeared into the adjacent frequencies, producing a leakage at each peak. This leakage indicates that the human walking pattern presents imperfection and therefore force is **not perfectly periodic** [2]. The same author stated that human walking is a **random process** [16].

In another study, Sahnaci and Kasperski [52] stated that these imperfections result in what is known as **subharmonics**, which are intermediate load amplitudes holding a significant portion of excitation energy between the main harmonic frequency bands as presented in [Figure 3.5](#). The authors suggested that this phenomenon is presented due to the difference between left and right feet in the walking parameters e.g. step length, pacing tempo etc. Finally, they stated that the dynamic response without taking these subharmonics into consideration is significantly different [52].

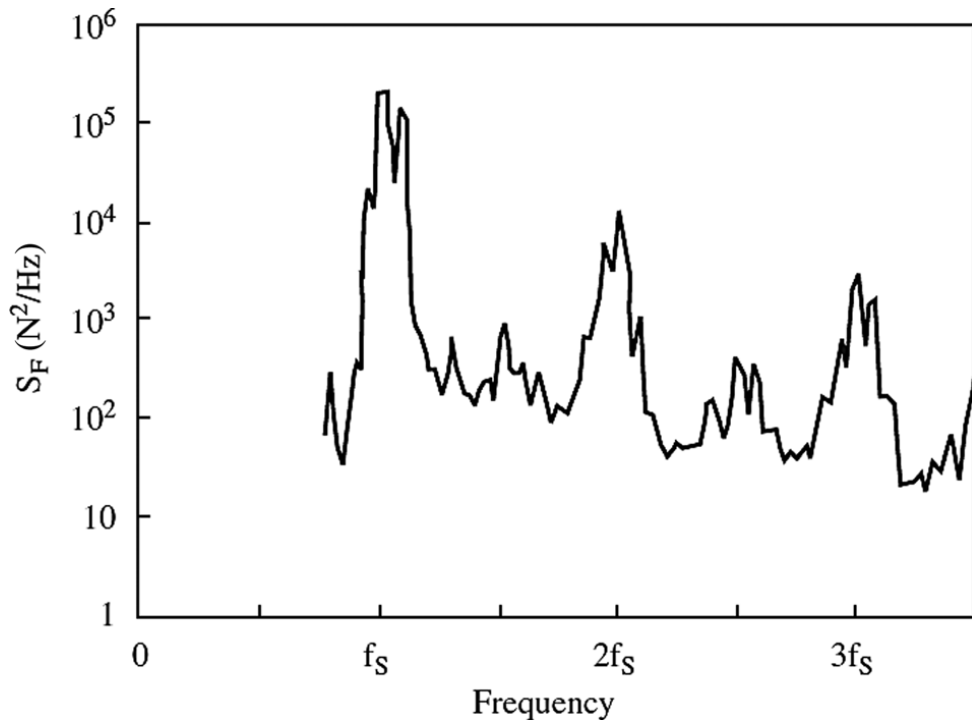


FIGURE 3.4: Autospectral density (ASD) of the walking force. [16]

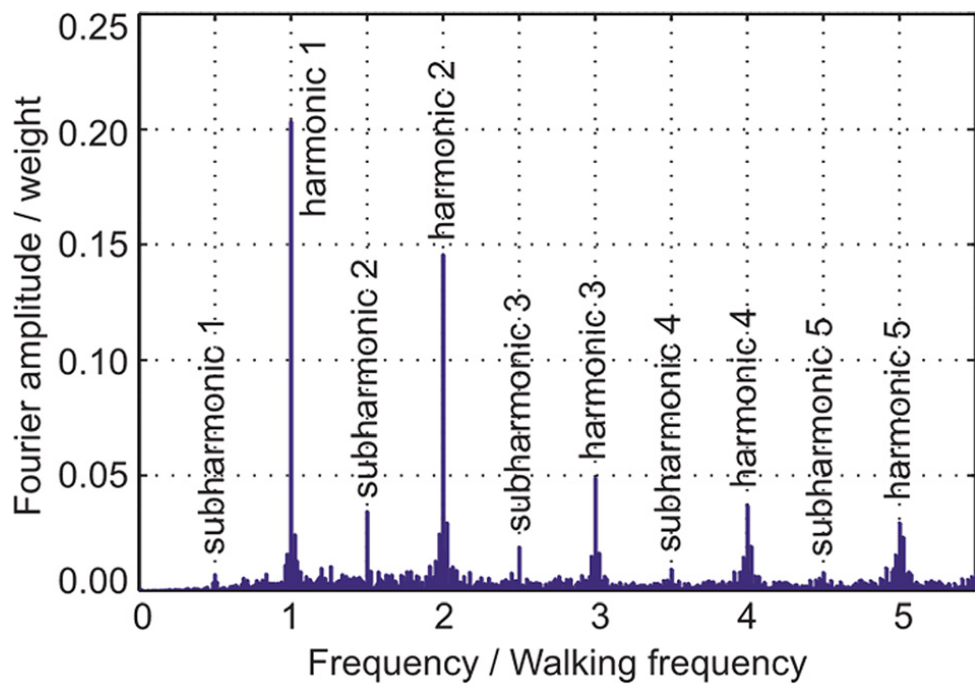


FIGURE 3.5: Representation of walking force in the frequency domain. [72]

3.3 Probabilistic Force Models

The probabilistic models were developed to respond to the need for more reliable approaches on the mathematical representation of the dynamic forces induced by human walking. These approaches take into account the intersubject and intrasubject variability i.e., a large database of measurements should be provided [47]. On reflection, according to these models, the human walking is considered a random or stochastic process with non deterministic behavior i.e., the next state cannot be predicted by the current state [12] and repeated experiments from the same person will be different [48]. The randomness can be expressed by the probability of the above variables density function. The output of these models are not a binary value generated from a comparison on a threshold but instead, the induced response can be expressed as a probability that will not exceed a certain value. This gives more space for engineers to make a decision on vibration serviceability [31].

3.3.1 Step Frequency of Probabilistic Force Models

There is a notable difference between step properties from several studies in the literature [72, 30, 25, 27]. Figure 3.6 depicts the normal distributions of step frequency for normal tempo walking as extracted in several researches. These differences occur because of the fact that step properties have been proven to depend on multiple factors such as gender, nation, culture [66, 62] and the environment [23]. Therefore, Racic et al. [50] suggested that in order to perform a reliable statistical analysis of walking parameters, a random sample of people from different genders, nations, and cultures should be collected.

Using statistical analysis, Zivanovic [66] noted that walking speed follows a normal distribution pattern, as illustrated in Figure 3.7. In this figure, the step frequency is adjusted at 1.8 Hz as this is the mean value of the normal probability distribution describing step frequency introduced by Pachi and Ji [23].

3.3.2 Probabilistic Force Models Available in the Literature

Ebrahimpour et al. [15] performed one of the first attempts to include the randomness into human induced walking forces. In the study about the dynamic loads induced by crowds of pedestrians, they achieved a model that can be used to determine the first harmonic DLF given the step frequency and the number of people (Figure 3.8). However, their model is not comprehensive and cannot be applied to predict the vibration response.

Later, Zivanovic [66] implemented a framework to predict the vertical response of a walkway excited by a single pedestrian. This was performed by first performing a statistical analysis on the walking parameters and finally extracting the pdfs of these parameters in order to calculate the cumulative probability that the vibration response

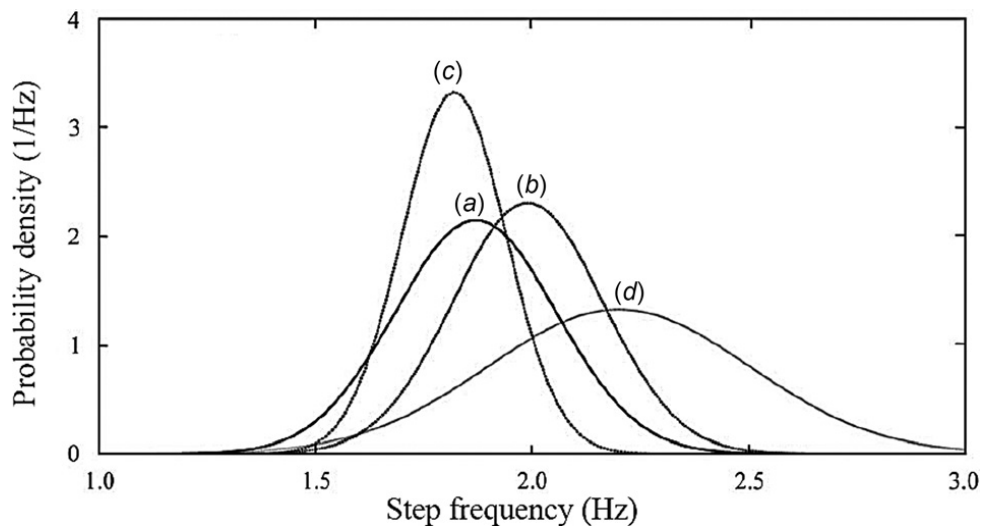


FIGURE 3.6: Normal distributions of step frequency for normal tempo walking as extracted from (a) Zivanovic' et al. [72], (b) Matsumoto et al. [30], (c) Kasperski and Sahnaci [25], and (d) Kramer and Kebe. [27]

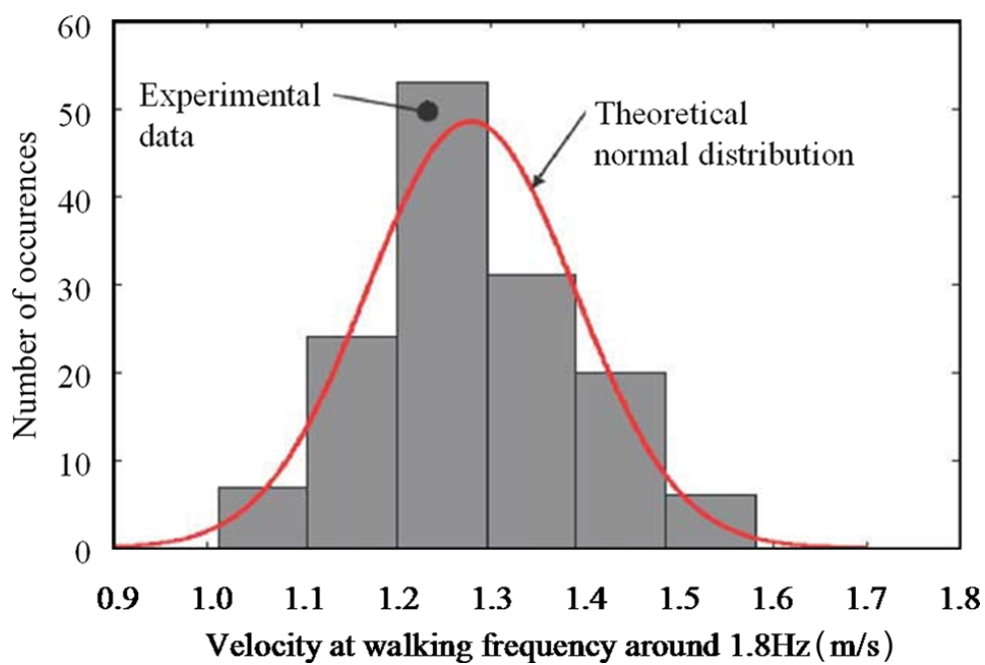


FIGURE 3.7: Normal distribution of walking speed at 1.8 Hz of step frequency. [66]

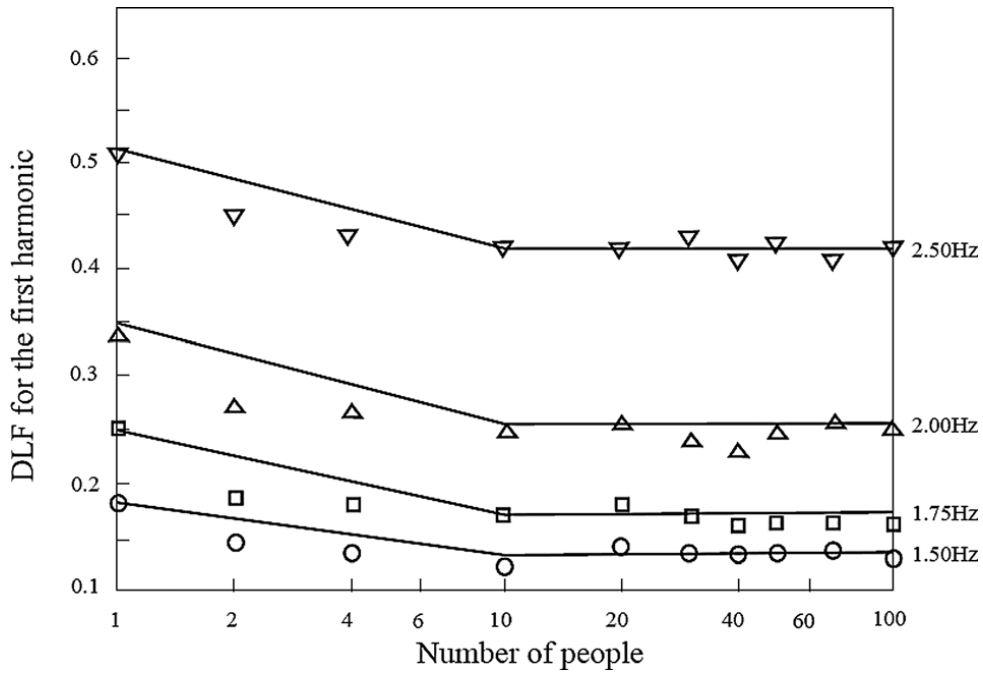


FIGURE 3.8: DLFs of the first harmonic as a function of the number of persons and step frequency. [15]

does not exceed a specified threshold. This framework however is bounded for footbridges presenting light traffic and only the first mode of vibrations is counted. Nevertheless, it is concluded that the first step to develop a reliable probabilistic model is to represent the single pedestrian excitation.

Consequently, Zivanovic et al. [72] have extended this model to include the subharmonics appearing in the frequency domain, unlike previous models considering the main harmonics only, as shown in Figure 3.9. The authors have accounted the inter-subject variability using the pdfs of the variables describing the human walk as well as the intrasubject variability via the phase angle, which was represented in the frequency domain with a random pattern uniformly distributed between $(-\pi, \pi)$. However, due to the lack of measurement database for subharmonics, the corresponding amplitudes were included as a function of the first harmonic's DLF. The accuracy of this model was proved to be adequate based on the experimental results.

Another model was introduced by Racic and Brownjohn [46]. This model emerged by an experimental campaign of 824 steps from about 80 subject of different physical characteristics. In this work, the authors categorized the walking signals into 20 clusters according to the pacing rate, each of 0.1 Hz, as depicted in Figure 3.10. Finally, they explained an algorithm for generating the walking force signals. However, the proposed modeling approach is numerically complicated thus making it impractical for the design engineers as the current techniques require simple calculations.

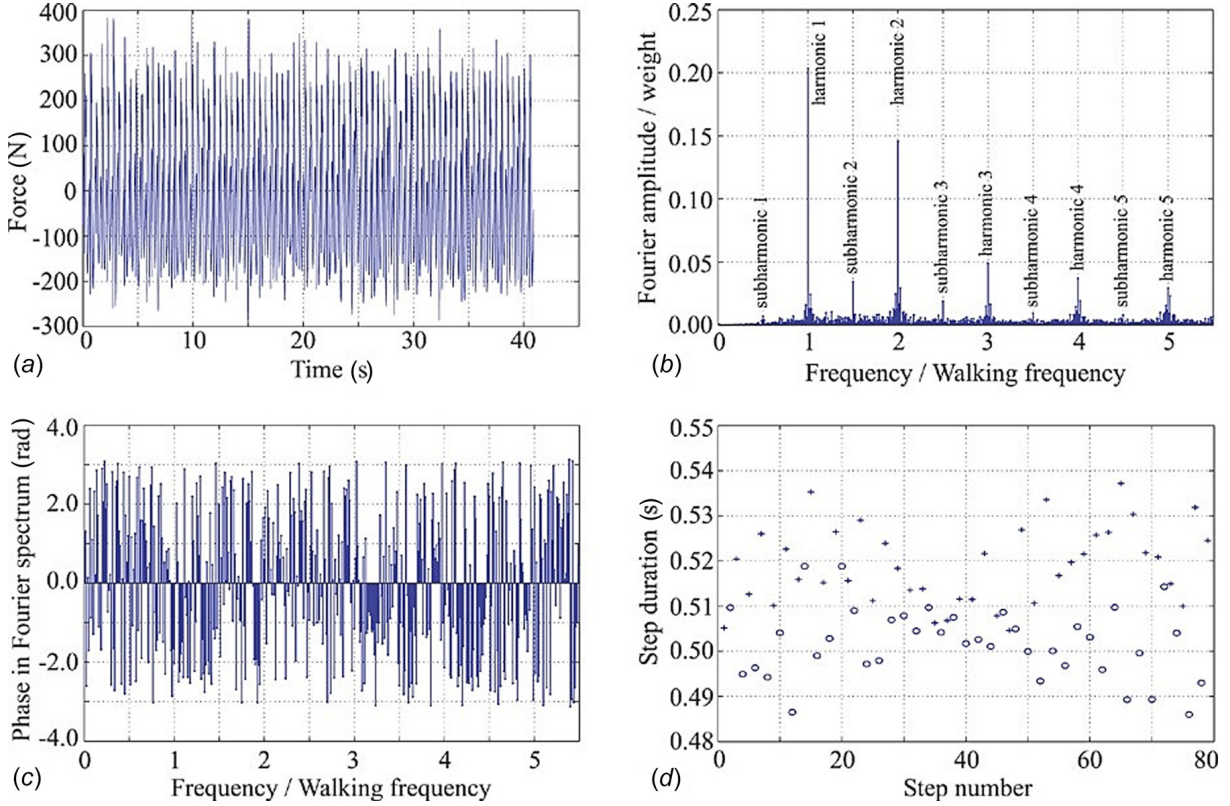


FIGURE 3.9: (a) 80-step walking force time history for a single pedestrian, (b) DLFs for the main harmonics and subharmonics in the frequency domain, (c) phase angle of forces in Fourier spectrum and (d) period of walking steps. [72]

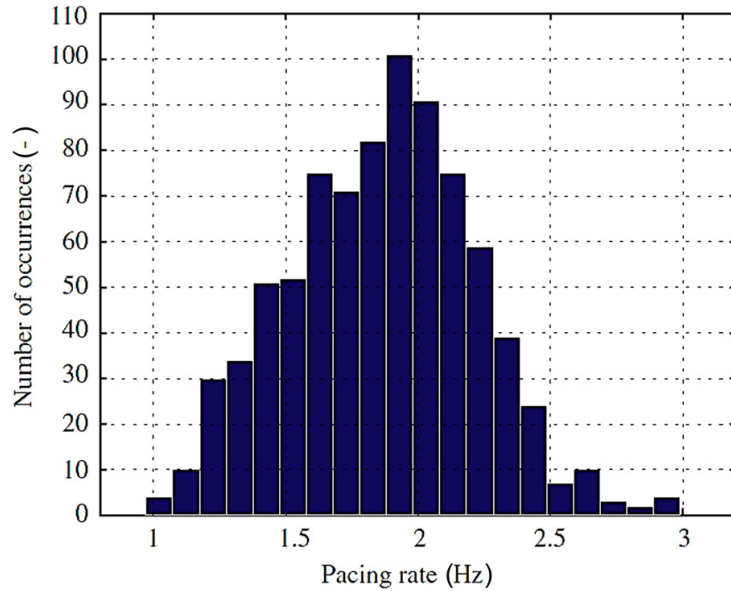


FIGURE 3.10: Categorization of walking force signals based on pacing rate. [46]

Chapter 4

Proposed Approach

In this chapter, we introduce the proposed approach to the problem. More specifically, in the first phase, we try to develop a **uniform model of human walk**. Therefore, the variables characterizing the walk of each subject in the database are modeled and then the parameters of the resulted models are fitted into new models to describe them uniformly as illustrated in the brief modeling plan of [Figure 4.1](#).

In second phase, a **simulator** of random human walk was implemented based on our models for the sake of establishing an experimental procedure as well as a reference dataset for future researches. Technically, this simulator uses the models describing the parameters, developed in the first phase, and generates random parameters. These parameters will be fitted into a new model that constitutes our simulator. This procedure is depicted in the brief simulation plan of [Figure 4.2](#).

The aforementioned are described analytically in the following sections.

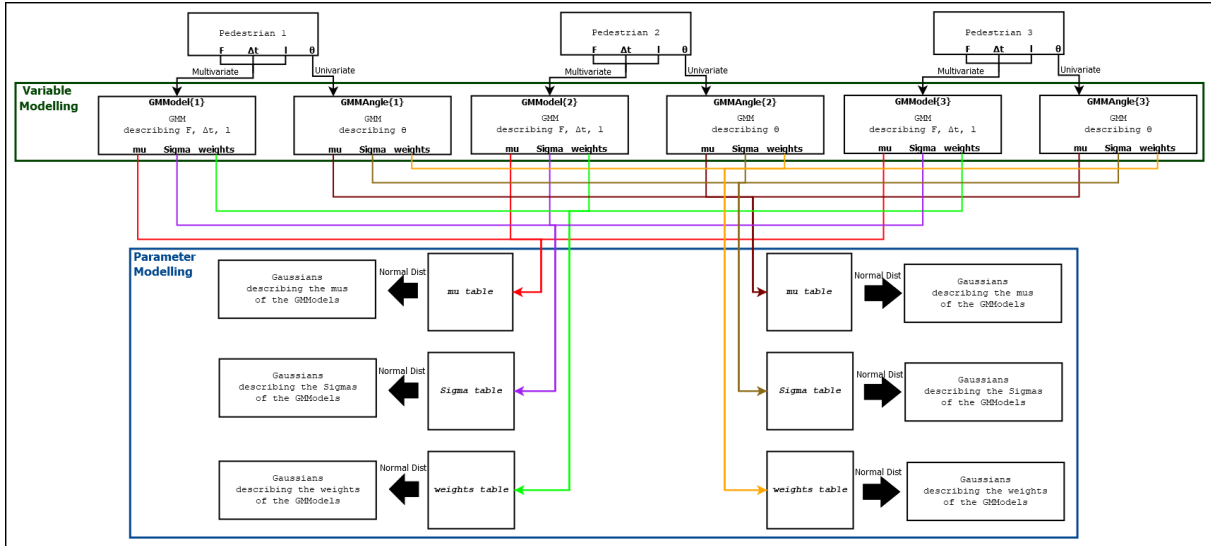


FIGURE 4.1: A brief modeling plan.

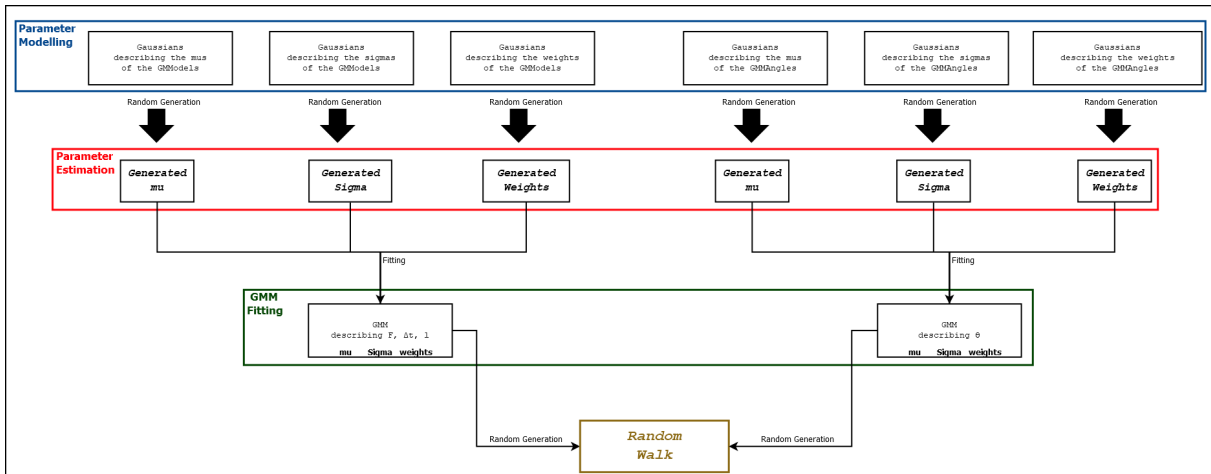


FIGURE 4.2: A brief simulation plan.

4.1 Experimental Framework

4.1.1 Database Properties

The database used for the modeling of human walk consists of valid measurements for **more than 200 pedestrians** in a variety of physical characteristics. More specifically, each subject was asked to cross a $10m^2$ plane walkway **twice at a normal tempo**. The equipment used to conduct the experiments included 10 plates along with the appropriate force sensors that occupy $1m^2$ each, as described in [chapter 5](#).

Subsequently, the database provided for the analysis was in the form of a cell table of 229 rows (subjects) and differed number of columns depending on the steps measured for each individual (minimum is 21 while maximum is 32 steps) for a sampling frequency of 50Hz. It is important to note that each subject (row) includes measurements of both walks for the specific individual e.g. if the first cross consisted of 14 steps and the second of 13, columns 1-14 include the measurements for the first walk and columns 15-27 include those of the second. Furthermore, some of the 229 rows are empty i.e., do not contain any measurements and as a result, will be considered **invalid for the analysis**.

Considering the subject (row) index as i and the step (column) index as j , each cell $\{i, j\}$ in the database matrix includes measured information about **force**, **time** and **position** on the plane for the i^{th} pedestrian at the j^{th} step.

Thus, database cell $\{i, j\}.\text{time}$ is an **array of measured times** that step j lasted corresponding to the forces induced during this step which are found on $\{i, j\}.\text{force}$ (maximum 70 measurements for each step). The time measurements were extracted by a timer used in the experimental procedure. Consequently, $\{i, j\}.\text{force}$ is an **array of vertical forces induced** during each step corresponding to the time array and measured in Newtons.

The $\{i, j\}.\text{x_step}$ and $\{i, j\}.\text{y_step}$ attributes are denoting the **relative position of feet** through the walkway on the x and y axis for the j^{th} step. By placing the center of axis in the middle of the plates on height and the start of the first plate on width (as depicted in [Figure 4.3](#)), it is concluded that y_step is a floating point number ranging in $[-0.5, 0.5]$ while x_step is a positive floating point number ranging in $[0, 10]$.



FIGURE 4.3: Position measurements axis.

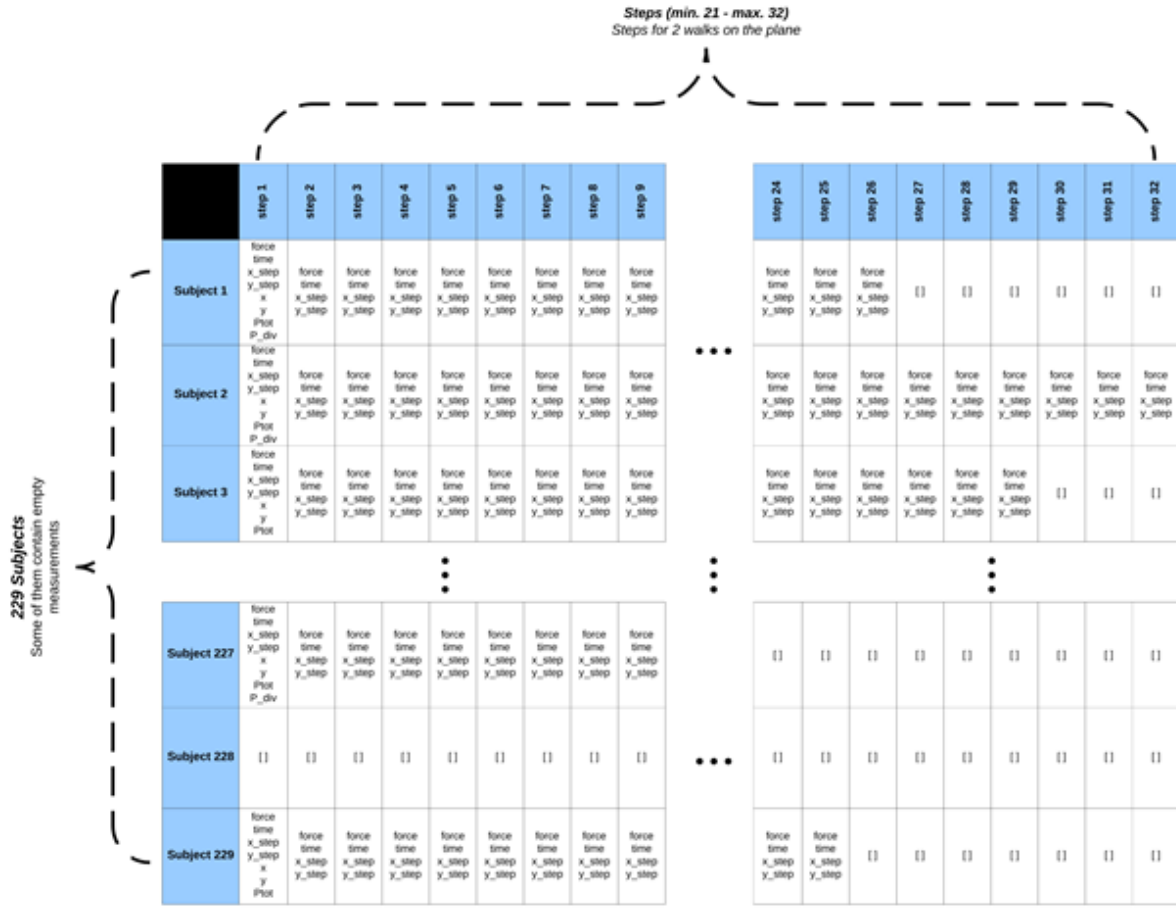


FIGURE 4.4: Simplified form of the initial database.

Finally, the first column of each pedestrian $\{i, 1\}$, includes some **extra measurement information**. More specifically, $\{i, 1\}.x$ and $\{i, 1\}.y$ contain the information about which points of each plate came in contact through the path, $\{i, 1\}.P_{tot}$ represents the sum of measurements acquired by all the force sensors beneath the instrumented floor and $\{i, 1\}.P_{div}$ collects the signals acquired by all the force sensors i.e., 10 plates and 4 sensors installed on each plate for a total of 40 measurements at each clock cycle. Those are raw data and **will not be used** on this work.

Figure 4.4 depicts a simplified form of the initial database which was provided for the analysis. In this example, it is obvious that each subject differs at number of steps performed on the 2 walks. Also, some subjects do not contain any measurements (subject 228 in this example) and ascribed to this, are considered invalid.

4.1.2 Database Analysis

The initial database, as described in subsection 4.1.1, needed some **modifications** in order to satisfy the requirements of the modelling. First of all, it needed to contain valid measurements only, but also force-time arrays contained in each cell are required to have the same indices on all cells on the basis that the measurements would later

Steps (min. 21 - max. 32)
Steps for 2 walks on the plane

215 Subjects
Empty measurements are deleted

	step 1	step 2	step 3	step 4	step 5	step 6	step 7	step 8	step 9
Subject 1	force time X_step Y_step x y Plot P_div								
Subject 2	force time X_step Y_step x y Plot P_div								
Subject 3	force time X_step Y_step x y Plot P_div								
...
Subject 213	force time X_step Y_step x y Plot P_div								
Subject 214	force time X_step Y_step x y Plot P_div								
Subject 215	force time X_step Y_step x y Plot P_div								
...
Subject 216	force time X_step Y_step x y Plot P_div								
Subject 217
Subject 218	force time X_step Y_step x y Plot P_div								
Subject 219
Subject 220	force time X_step Y_step x y Plot P_div								

FIGURE 4.5: Simplified form of the modified database.

be unified in tables for easier and more effective use. For this purpose, a "clear-out" is performed.

Initially, the subjects (rows) with empty measurements were identified and deleted. As a result, the database now contains measurements for **215 subjects** as opposed to the 229 initial subjects. This modification is depicted in [Figure 4.5](#). Furthermore, the force values are always be positive but due to some errors during the measurement procedure, this was not the case on some occasions. Hence, force measurements with negative values as well as the corresponding time values have been replaced with *nan* values in order to practically remove them from the database.

Finally, the force-time arrays were further modified to have the **same indices on all cells** as depicted in [Figure 4.6](#). These arrays initially had different indices on each cell but mutually the same. These modifications were crucial as a unified table would be needed for each of those variables. To do so, the maximum force-time array indices in the database were identified and each array was **modified to fit these indices** by adding *nan* values to the bottom of the array until the indices reach this maximum number. More specifically, the maximum array indices were calculated as 70 and therefore, each force-time array contains up to 70 measurements but always has 70 tuples.

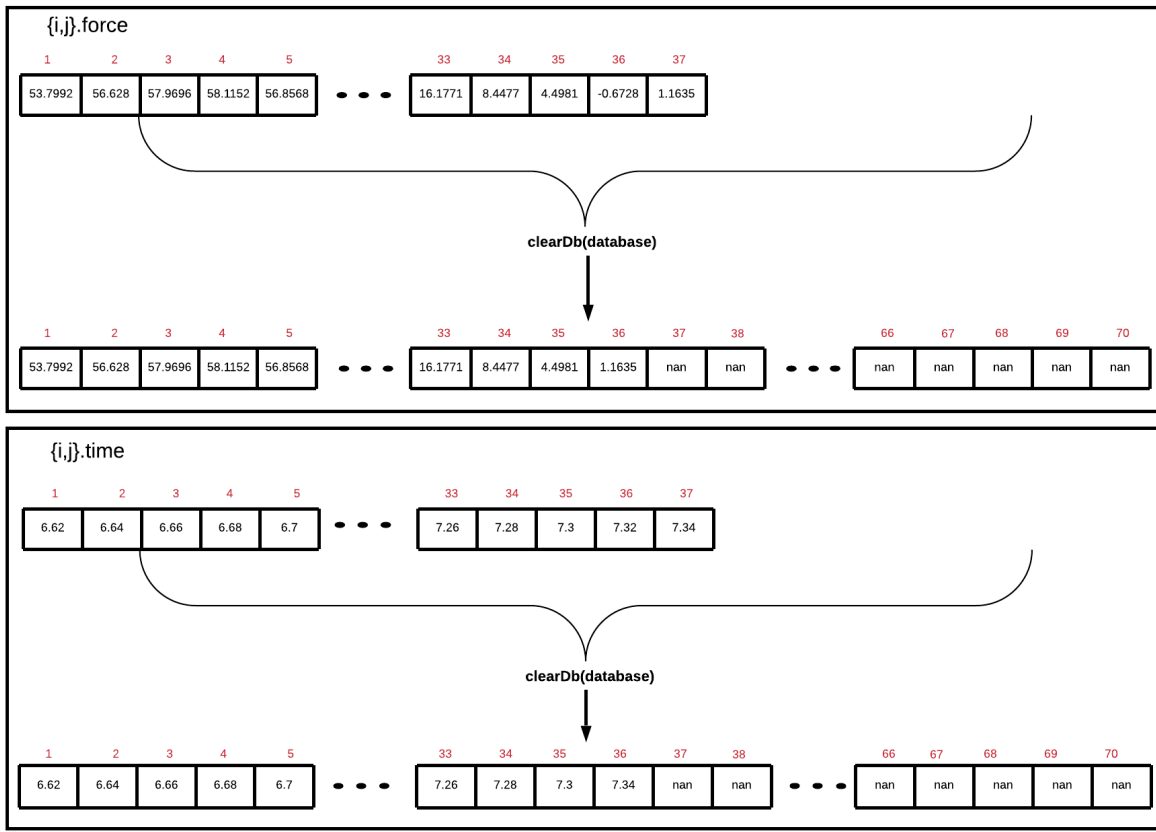


FIGURE 4.6: An example of the force-time arrays before and after the "clear-out".

Figure 4.6 shows an example of how the "clear-out" is implemented. In this example, it is visible that the pair of force-time will have a length of 70 tuples and all the negative forces, as well as their pairs in time, are deleted.

4.1.3 Variable Extraction

The next big step concerns the **extraction of the essential variables**. For this purpose, the 4 different variables contained in the database (force, time, x_step and y_step) were extracted in different tables. The 4 tables created had the following forms:

- **time:** $70 \times 32 \times 215$ (max measurements x steps x subjects)

The times in which measurements occurred (1st dim) for each step (2nd dim) and each subject (3rd dim).

- **force:** $70 \times 32 \times 215$ (max measurements x steps x subjects)

Vertical force induced on each moment (1st dim) for each step (2nd dim) and each subject (3rd dim).

- **x_coord:** 215×32 (subjects x steps)

The step coordinates in x axis for all subjects (rows) and steps (col).

- **y_coord:** 215×32 (subjects x steps)

The step coordinates in y axis for all subjects (rows) and steps (col).

However, these variables were not fitted to use for the statistical modeling of human walk. Indeed, the extraction of the following necessary variables is performed:

- **Interarrival time:** 215×32 (subjects x steps)

Interarrival time (Dt) between each step (col) for each subject (row).

- **Mean Vertical Force:** 215×32 (subjects x steps)

Mean vertical force ($meanF$) induced on each step (col) for each subject (row).

- **Length of step:** 215×32 (subjects x steps)

The distance between each step.

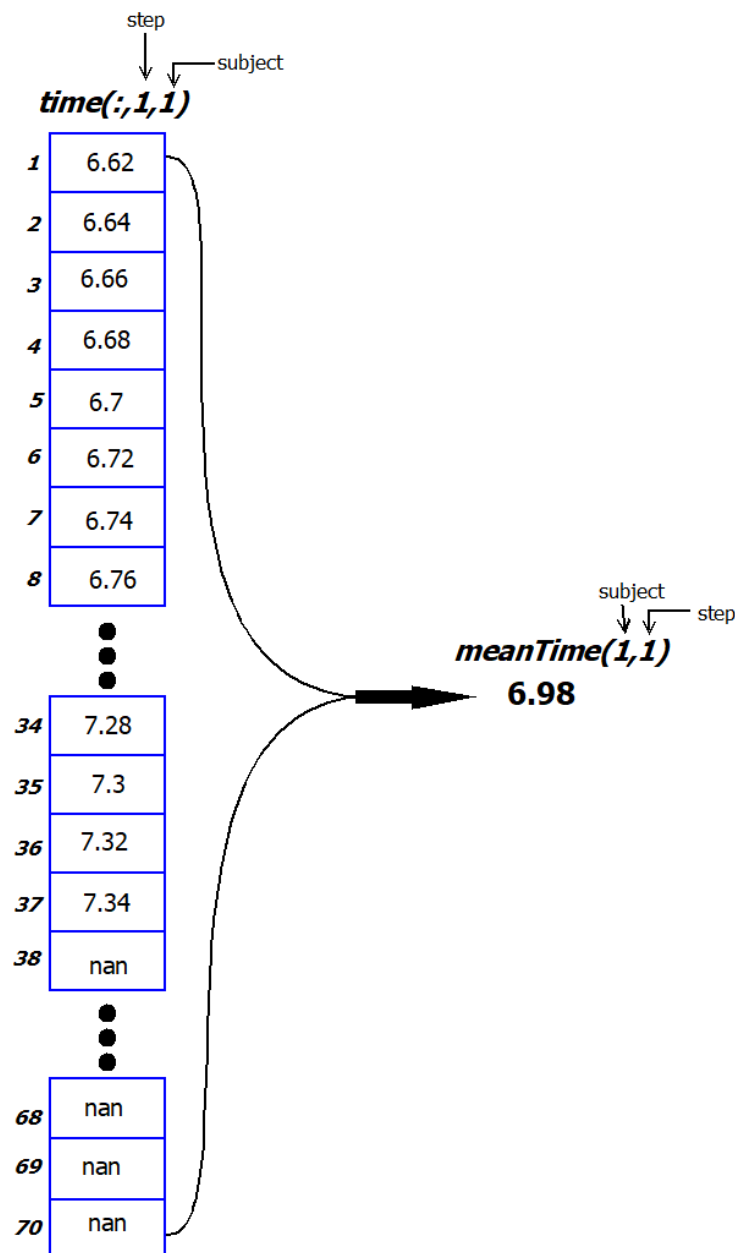
- **Angle of step:** 215×32 (subjects x steps)

The angle of each step along the gait horizontal direction.

4.1.4 Extraction of Interarrival Time and Mean Force

As denoted, the time table contains up to 70 time measurements for each step of each subject. These values are indicating the **duration of step**, but it would be preferable if there was only one time value characterizing the time in which a step is performed. The selected value for this was the mean time. Therefore, for each time array i.e., each step of each subject, the mean value ignoring the *nan* values, has been calculated and thus, the **mean time of each step** has been extracted as depicted in [Figure 4.7](#).

Let j be the current step of subject i . The **interarrival time (Dt)** of step j will be calculated as:

FIGURE 4.7: Construction of `meanTime` table.

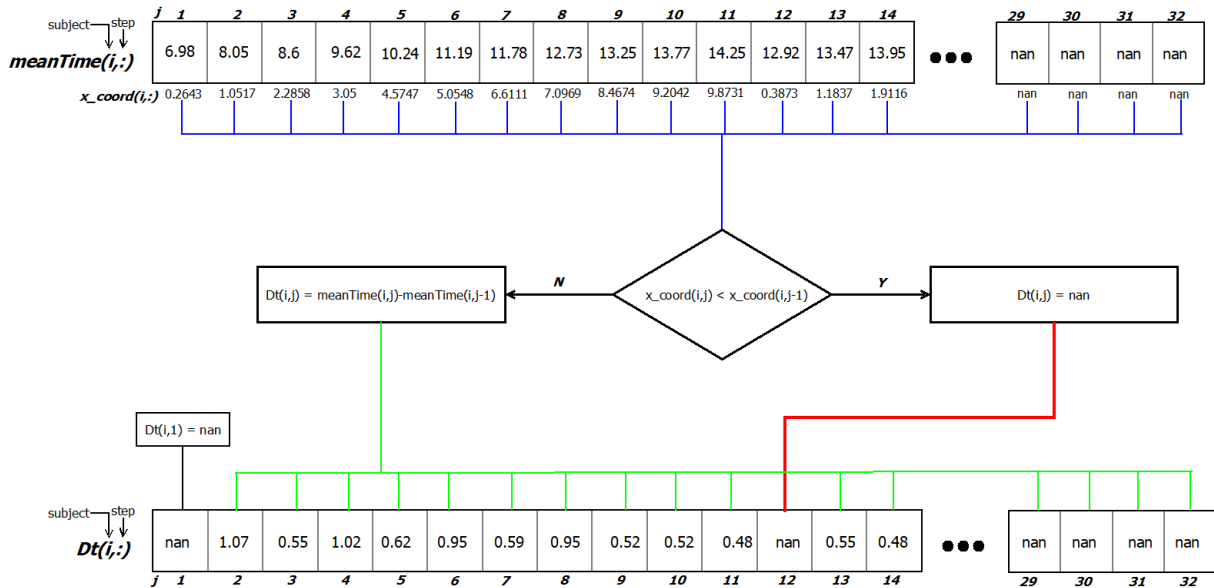


FIGURE 4.8: Dt extraction algorithm.

$$Dt(i,j) = \text{meanTime}(i,j) - \text{meanTime}(i,j-1) \quad (4.1)$$

Subsequently, each interarrival time between steps can be calculated using [Equation 4.1](#). This indicates that the first step ($Dt(i,1)$) has **no interarrival time**, although the mean time of the first step will be used to calculate the interarrival time between the first and second step. Therefore, $Dt(i,1)$ will be *nan*.

As stated above, each subject includes measurements for 2 walks on the pathway. Subsequently, each time a second walk starts, the analysis resets to zero and the first step of the second walk must **ignore the effect of previous steps** which belong to the first walk. The values in time, force, x_{coord} and y_{coord} arrays are continuous e.g. if the last step of the first walk was the 13th, the new walk starts at the 14th step. In order to identify in which step the new walk starts, the x_{coord} variable is used. More specifically, x_{coord} signifies the position of the subject on the plane and thus on the same walk: $x_{\text{coord}}(i,j) \geq x_{\text{coord}}(i,j-1)$. It can be inferred that a **new walk** has started when the subject has returned to the beginning of the walkway. In this case:

$$x_{\text{coord}}(i,j) < x_{\text{coord}}(i,j-1) \quad (4.2)$$

Using this condition, the step signifying the beginning of a new walk can be identified.

When a new walk is spotted, the first measurement will be used to calculate the interarrival time between the first and second step of this walk, while the equivalent interarrival time will take a *nan* value.

In order to extract the **mean vertical force induced in each step**, a similar procedure will be followed. This indicates that using the force table containing up to 70 measurements for each step of each subject, the mean vertical force induced in each step will be extracted similarly to the procedure followed for meanTime extraction ([Figure 4.7](#)). Using this method, the meanF table will be constructed.

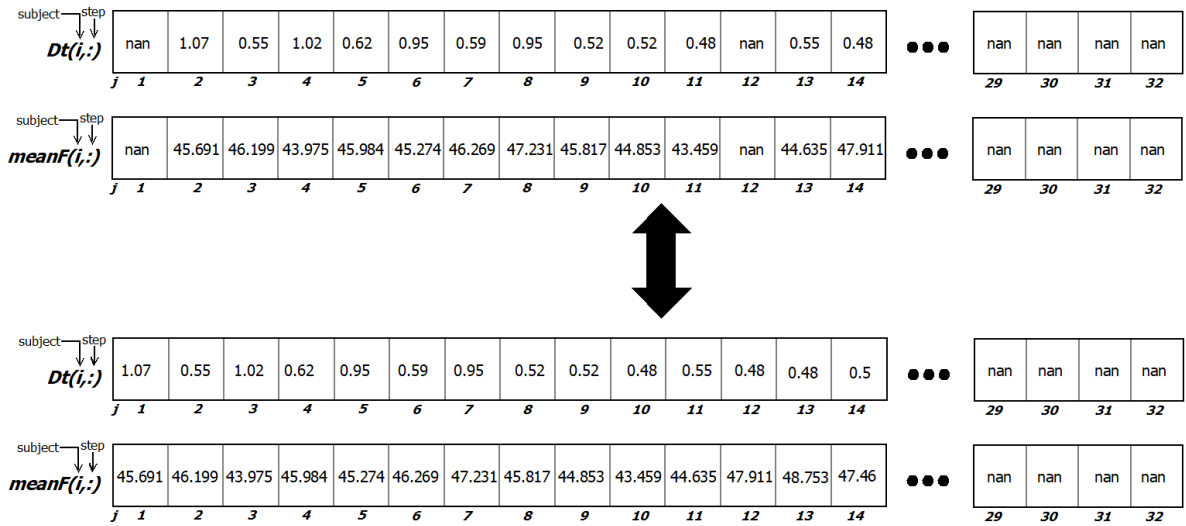


FIGURE 4.9: Shifting the nans to the end of each row.

However, in order to keep the necessary correspondence between Dt and meanF, the values of the first step of each walk will be erased. In other words, in whichever tuples Dt has the value of *nan*, meanF will get the *nan* value as well. Finally, the *nan* values of Dt and meanF tables are shifted to the end of each row as shown in Figure 4.9.

4.1.5 Extraction of Length and Angle

Concerning the extraction of **length** and **angle**, the *x_coord* and *y_coord* tables are used. More specifically, the length can be calculated as the **Euclidean distance** between one step and the next, while the angle is the **arctangent** of the traversed *x* and *y*.

This indicates that the first step of each walk will be used to calculate the length and angle between the first and second step. Nevertheless, there are no values corresponding to these steps and thus, their values will be ignored and shifted to the end of each row following the procedure described for Dt and meanF.

Figure 4.10 illustrates the way length and angle are calculated. In this example, 3 consecutive steps of a subject are depicted as circles in the *x* and *y* domain based on the coordinates taken by the *x_coord* and *y_coord* tables. x_{1-2} and y_{1-2} are the traversed *x* and *y* distances between the first and second step, respectively, and thus:

$$x_{1-2} = x_2 - x_1 \text{ and } y_{1-2} = y_2 - y_1 \quad (4.3)$$

The **distance** between the first and the second step i.e., length of the 1st step, can be calculated using the Euclidean distance as:

$$length_{1-2} = \sqrt{x_{1-2}^2 + y_{1-2}^2} \quad (4.4)$$

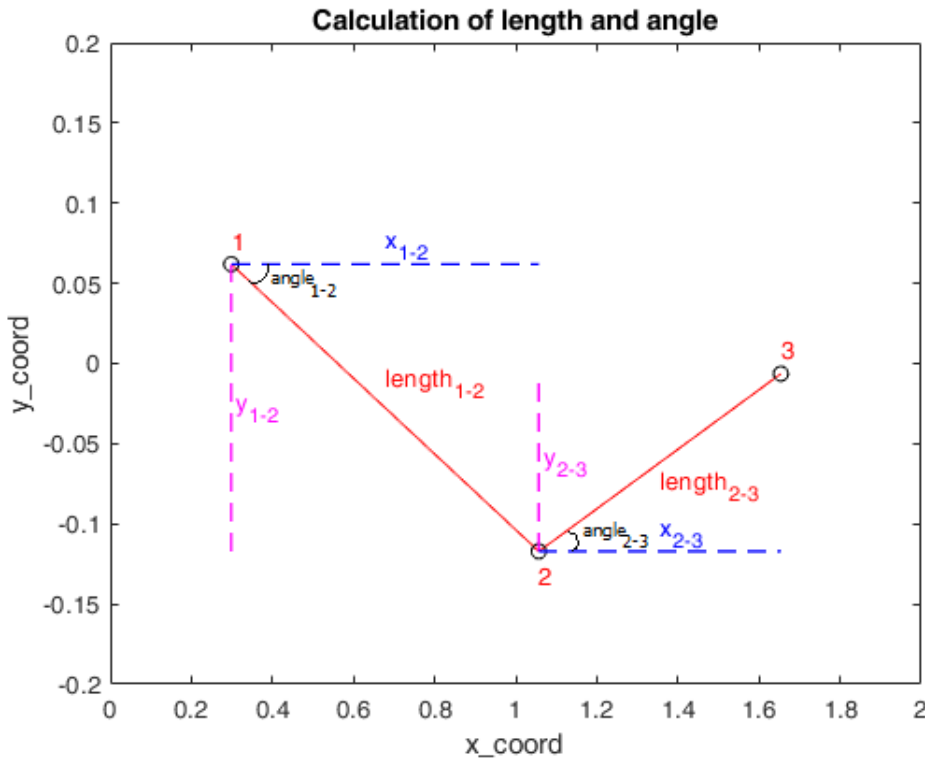


FIGURE 4.10: Calculation of length and angle on 3 steps of a walk.

While the **angle** (radians) between the first and the second step i.e., direction of the 1st step, can be calculated as:

$$\text{angle}_{1-2} = \arctan\left(\frac{x_{1-2}}{y_{1-2}}\right) \quad (4.5)$$

Using this procedure, all lengths and angles traversed on each step of a walk can be determined.

4.1.6 Extraction of The Unified Table

The 4 extracted variables were combined into table X which is a 32x4x215 table including meanF, Dt, len and angle for each step of each person. For each person represented in the 3rd dimension, 1st column represents the Dt while 2nd column is the meanF, 3rd column is the length and 4th is the angle for the specific step (row). An example of this table is shown in [Figure 4.11](#).

	Dt	meanF	len	angle
1	1.0400	55.9050	0.7674	-0.2926
2	0.5400	58.2194	1.2078	0.0309
3	0.4900	52.8682	0.6284	0.1795
4	0.5100	57.4001	0.6813	-0.1237
5	0.5100	54.8361	0.6217	0.1711
6	0.4900	55.1191	0.6935	-0.2096
7	0.5200	56.3619	0.6094	0.1723
8	0.5100	62.1039	0.7146	-0.2219
9	0.5000	56.3518	0.6571	0.2240
10	0.5500	57.2479	0.8875	-0.0232
11	0.4700	51.0994	0.4300	0.2670
12	0.4600	53.9626	0.6870	-0.2663
13	0.5200	57.5773	0.6099	0.1864
14	0.5600	59.5602	0.5453	-0.1783
15	1.1200	53.0572	0.7244	-0.1579
16	0.5200	56.6491	1.1545	-0.0263
17	0.5000	54.7379	0.6509	0.1994
18	0.5600	53.3399	0.8154	-0.0686
19	0.4800	52.2004	0.4658	0.2165
20	0.4900	56.3009	0.6532	-0.2190
21	0.5400	57.9725	0.5806	0.1357
22	1.0500	57.3230	0.7537	-0.2515
23	0.5300	59.5313	1.1034	0.0089
24	0.5100	60.9921	0.5955	0.1383
25	0.5400	52.7784	0.6227	-0.2184
26	1.0900	60.0655	0.7727	0.2390
27	NaN	NaN	NaN	NaN
28	NaN	NaN	NaN	NaN
29	NaN	NaN	NaN	NaN
30	NaN	NaN	NaN	NaN
31	NaN	NaN	NaN	NaN
32	NaN	NaN	NaN	NaN

FIGURE 4.11: The form of a random pedestrian's unified table X.

4.2 Variable Modeling

Fornaciari [17] has concluded that the angle does not present any correlation with the other three random variables (see subsection 2.2.1). Based on these results, it is clear that the mathematical model used to describe the human walk will need to encounter the angle variable **separately** than Dt, meanF and len. Using this deduction, Caleri [11] tried to fit a variety of distributions to identify which describes the process of human walk better (see subsection 2.2.2). He concluded that **Gaussian Mixture Models** were a good approach in most cases.

Based on this deduction, we decided to fit two GMMs on each subject i.e., a **multivariate describing the 3 correlated variables** and a **univariate describing the angle**. This resulted to a total of 430 GMMs to model the variables of walk. However, a decision on the number of components to use on these GMMs is considered essential.

4.2.1 Estimation of GMM Components

In this section we will present the procedure adopted to estimate the number of components used in the multivariate GMMs describing the three correlated variables (Dt, meanF and len). A similar procedure will be used for the estimation on all following GMMs. More specifically, the goal is to estimate the optimal number of GMM components i.e., the resulting GMMs should **describe the variables accurately** as well as **minimize the complexity**. The AIC and BIC criteria were used for this decision.

It must be noted here that the SharedCovariance property of the GMM has been set to true for all GMM fits described in this work, as setting it to false would not generate the GMM distribution due to the ill-conditioning of the covariance matrix. Also, the number of iterations performed by the fitting algorithm has been set to 1500.

Definition 11 *The Bayesian information criterion (BIC) is a criterion for model selection among a finite set of models. It is based, in part, on the likelihood function, and it is closely related to the Akaike information criterion (AIC).*

When fitting models, it is possible to increase the likelihood by adding parameters, but doing so may result in **overfitting**. The BIC resolves this problem by introducing a penalty term for the number of parameters in the model. The penalty term is larger in BIC than in AIC.

Mathematically BIC can be defined as:

$$BIC = \ln(n)k - 2\ln(\hat{L}) \quad (4.6)$$

While AIC can be defined as:

$$AIC = 2k - 2\ln(\hat{L}) \quad (4.7)$$

Where:

- \hat{L} : The maximized value of the likelihood function of the model.

- n : The number of data points.
- k : the number of parameters to be estimated.

A lower AIC and BIC value indicates lower penalty terms hence a **better model**.

Though AIC and BIC are derived from a different perspective, they are closely related. Apparently, the only difference is that BIC considers the number of observations in the formula, which AIC does not.

4.2.1.1 The Default Index Method

The **default method** for the estimation of the optimal number of GMM components describing the three variables (D_t , $meanF$, len), is based on fitting the GMMs using a variety of components. More specifically, each GMM is fitted using **1-15 components**. In each selection, the AIC and BIC scores are extracted. The number of components that achieve the **lowest score** describe the best model.

Figure 4.12 depicts the AIC and BIC values for a variety of components on 11 pedestrians. As observed, in most cases a bigger number of components leads to smaller scores. Consequently, the penalty AIC/BIC criteria give to complex models leads to **overfitting**. This phenomenon probably occurs due to the impact of **noise** in the data. More specifically, the data have an abnormal distribution which leads to overfitting the model to cover these values. Thus, this method is not optimal for the estimation as it leads to bigger complexity.

4.2.1.2 Exploring a Solution

Estimating the number of components can be regarded as an important factor in the accuracy of our model. Thus, it is significant to explore other techniques that will aid on this quest. By observing **Figure 4.12** we notice that the curve follows different slopes in different part of it. Hence, there is no need to find a global minimum of the AIC/BIC score and for this reason, we decided to check where the AIC/BIC curve change slope is big i.e., **detect the most drastic change of the AIC/BIC index**, as to signify a change of performance. This should denote the number of components that drastically impacts the fit and therefore could be accepted as a **descent point of focus**. This point will offer better **optimality - complexity payoff** in the GMMs.

It is important to note that each time a GMM is fitted on data the produced results will defer i.e., multiple GMMs fitted on the same data with the same number of components will produce **different results**. Therefore, in the selected method, we repeat the same procedure in order to get more representative results. In this case we abstractly repeat the fittings 12 times in each case. Thus, we decided to adopt the following technique:

- First, a **GMM is fitted** on the data and the AIC/BIC scores on 1-15 components are extracted.
- Then, a **mean index evaluation diagram** is created from all the 12 repetitions i.e., the mean AIC/BIC scores of the 12 GMMs are calculated for each point (component).

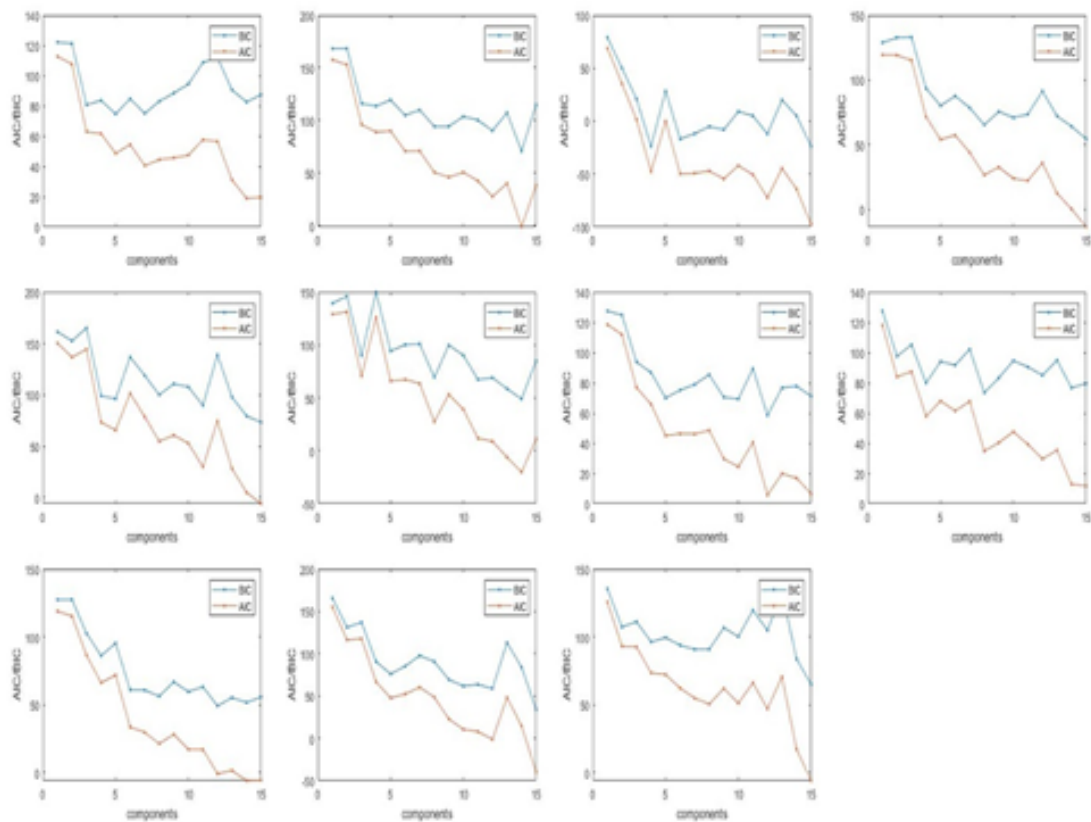


FIGURE 4.12: AIC and BIC values of GMMs varying components fitted on 11 pedestrians.

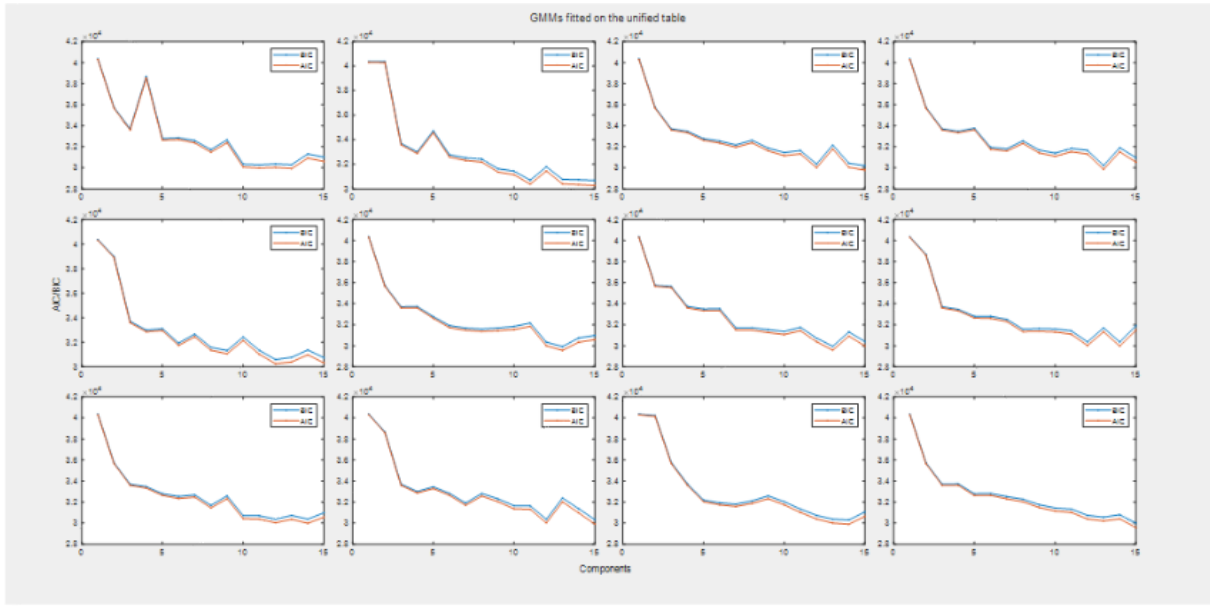


FIGURE 4.13: GMM fitted on the unified walk data for 1-15 components (12 repetitions).

- Lastly, the **score difference** is computed based on the mean index evaluation diagram and is graphically depicted. Note that large improvement in score implies large negative score difference.
- The **lowest pointy** in the Score differential diagram, depicting the largest improvement on the AIC/BIC scores, denotes the selected number of components.

To evaluate this point of interest we first follow this technique on a GMM fitted on the unified walk data and then the same procedure is followed on random separate pedestrians.

4.2.1.3 Fitting on the Unified Walk Data

In this step, a **unified table** containing all database steps is created for each person. More specifically, a GMM is fitted on the 3 variables (Dt , $meanF$, len) and the technique described at [subsubsection 4.2.1.2](#) is followed. [Figure 4.13](#) depicts the **AIC/BIC values of GMM** fitted on the unified walk data for 1-15 components for 12 repetitions while [Figure 4.14](#) presents the resulting mean index evaluation diagram and the score differential diagram. It can be noted that the biggest AIC/BIC score decrease i.e. largest improvement, is spotted on the **GMM using 3 components**.

4.2.1.4 Fitting on the Pedestrian Walk Data

The same procedure is followed on **random separate pedestrians** to verify the selection of the 3-component model. [Figure 4.15](#) depicts the AIC/BIC values of a GMM fitted on a random pedestrian's walk data for 1-15 components using 12 repetitions

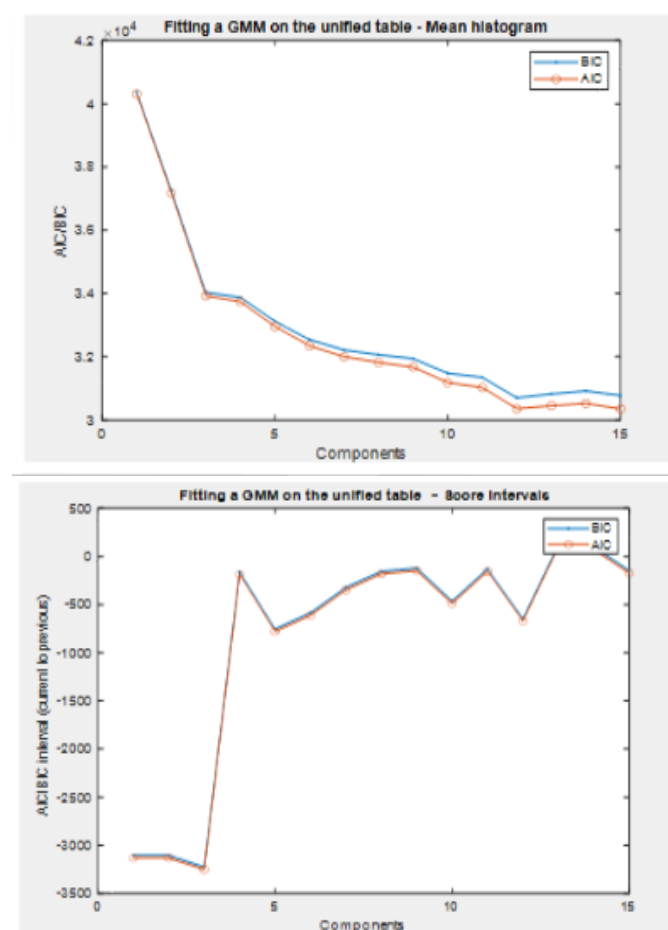


FIGURE 4.14: (a) Mean index evaluation diagram of unified walk data -
(b) Score differential diagram of the unified walk data.

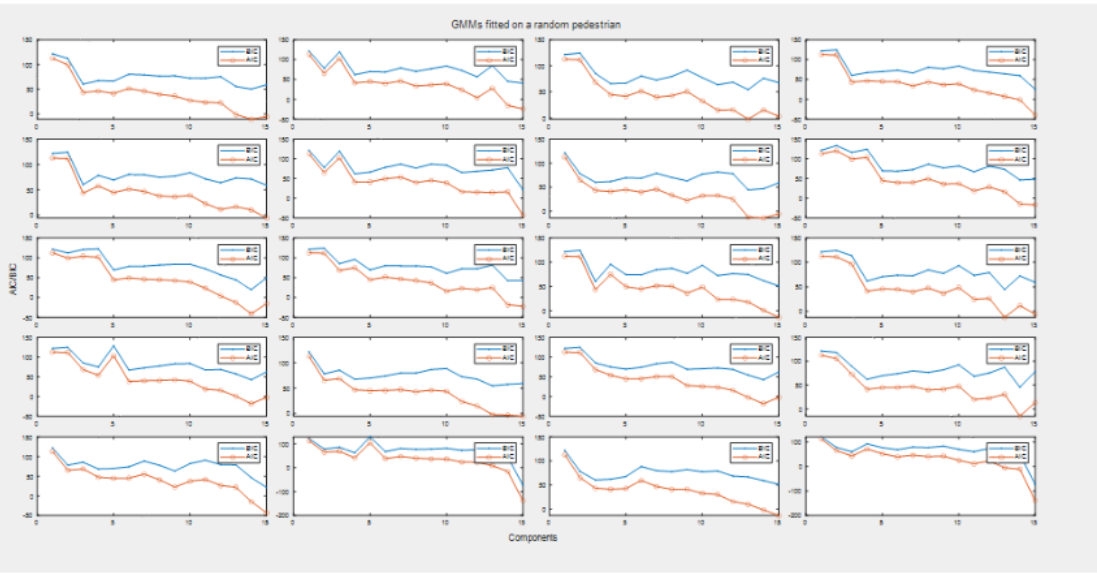


FIGURE 4.15: GMM fitted on a random pedestrian's data for 1-15 components (12 repetitions).

while [Figure 4.16](#) presents the resulting mean index evaluation diagram and the score differential diagram.

The results obtained verify that the 3-component GMM offers better payoff and thus we decided to use **3 components** on the fitting of the multivariate model describing Dt, meanF and len. These experiments were repeated on many random pedestrians with similar results in most cases.

Note: The procedures described in [subsection 4.2.1](#) are followed before every GMM fit reported in this work.

4.2.2 Distribution Fitting

Fitting of the 3-component multivariate GMM describing Dt, meanF and len in the respective walking data is performed in this section. [Figure 4.17](#) depicts this fitting for a random pedestrian on each variable. More specifically, [Figure 4.17a](#) presents the data fitted on the interarrival time of step, while [Figure 4.17b](#) and [Figure 4.17c](#) depicts the fitting on the mean vertical force induced in each step and the length traversed, respectively.

We note that the fittings presented in this figure are performed accurately on the significant parts of data while ignoring the values with low density. In this manner, we consider these values as **outliers or noise** in the data and we ignore them in the modeling while simultaneously achieving a **low complexity**.

Using the technique introduced at [subsection 4.2.1](#), we decided to use a 2-component GMM for the modeling of data describing the **angle of step** for each pedestrian. [Figure 4.18](#) depicts the fitting on the angle of step of a random pedestrian's data. It can be inferred that the 2-component GMM presents 2 curves in the form of a **bivariate**

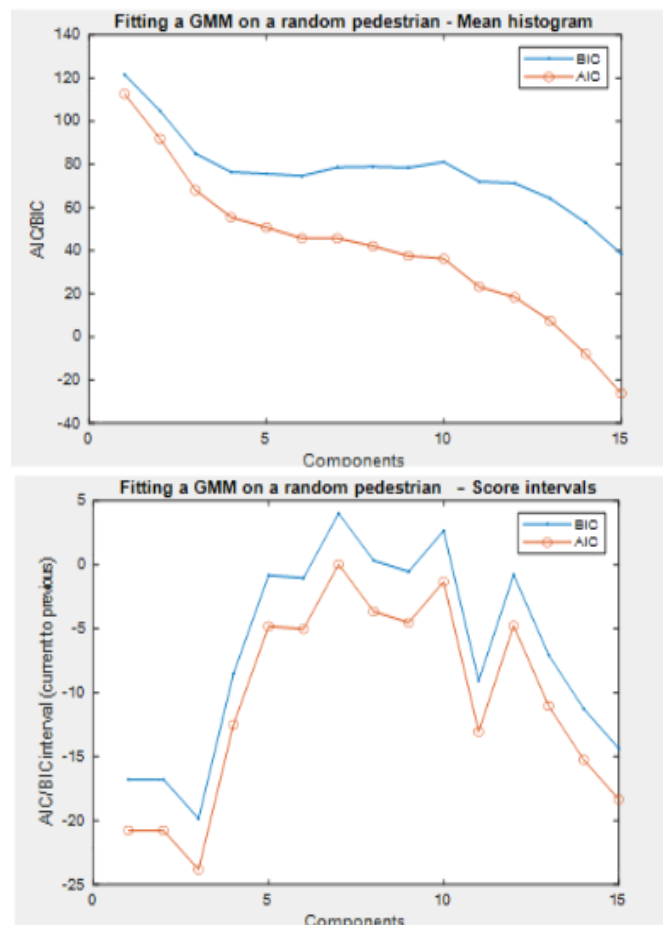
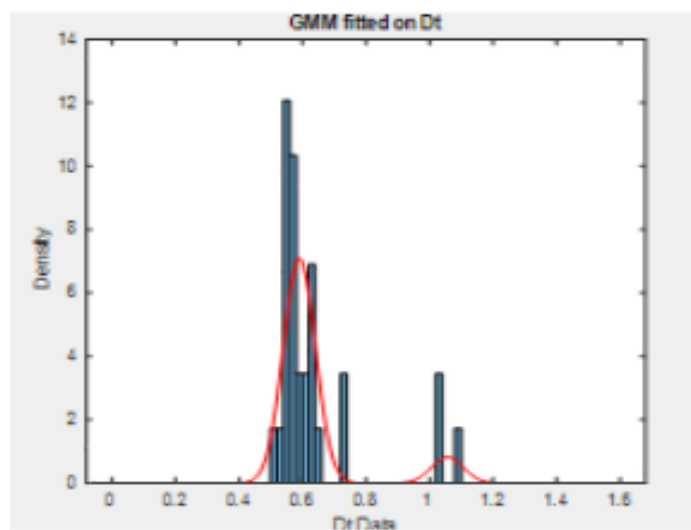
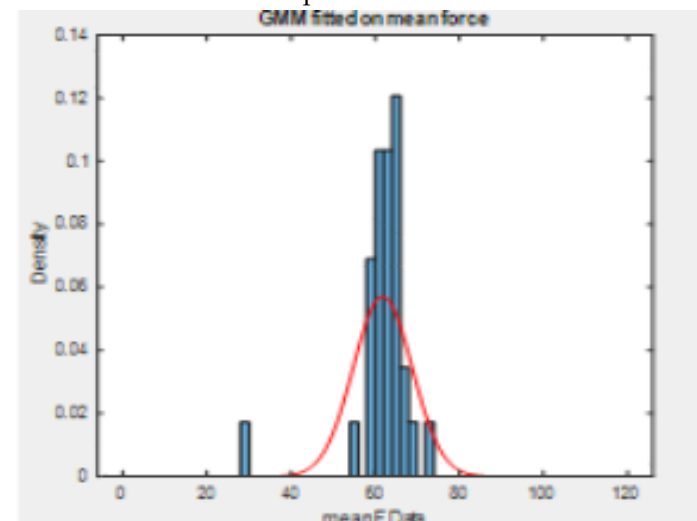


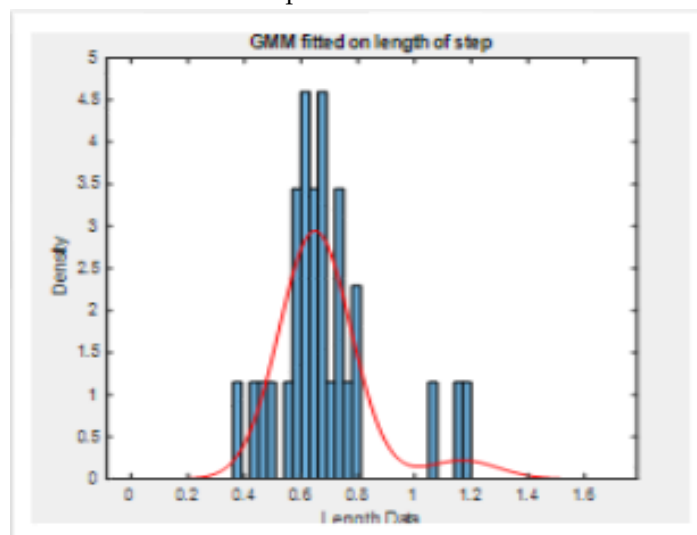
FIGURE 4.16: (a) Mean index evaluation diagram of unified walk data -
(b) Score differential diagram of the unified walk data.



(A) Multivariate GMM of 3 components fitted on interarrival time of step.



(B) Multivariate GMM of 3 components fitted on mean vertical force of step.



(C) Multivariate GMM of 3 components fitted on length of step.

FIGURE 4.17: Multivariate GMM of 3 components fitted in random pedestrian's walk data.

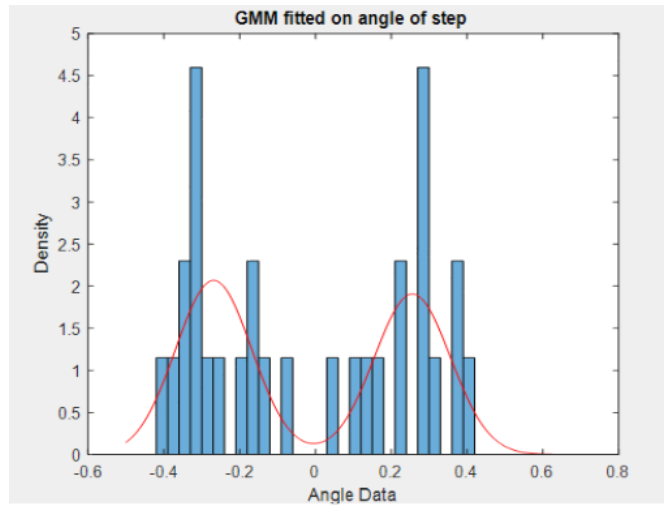


FIGURE 4.18: Univariate GMM of 2 components fitted in random pedestrian's angle of step.

distribution. This result can be considered **sensible** as normal human walking is usually performed in this manner i.e., a footstep in one direction is followed by another footstep in the opposite direction.

4.3 Parameter Modeling

The final goal of this thesis is to create a simulator which will successfully generate a random walk with any given number of steps. This simulator must extract the 4 variables for each step similarly to the provided experimental data based on a **complete statistical model** that describes the human walking process accurately. Therefore, modeling of the parameters of the GMMs describing the variables of human walk is performed.

More specifically, each GMM is characterised by **3 parameters**. Those in fact are the mean table (μ), the variance/covariance matrix Σ (Sigma) and the mixing probability ϕ (component proportion coefficient). The parameters of the 215 GMMs fitted on [section 4.2](#) are mixed and modeling is performed on each using normal distributions in order to model them as accurately as possible.

4.3.1 Statistical Description of the Mean Table

The **mean table (μ) parameter** of a GMM which describes 3 variables with 3 components is a 3×3 table (*components x variables*). Each column corresponds to a different variable and each row describes the mean value of each component on a specific variable. This indicates that each variable (column) must be described by **different Gaussians**.

The procedure followed for the most accurate statistical description of the mu of each variable, will be illustrated using an example. The tables depicted in [Figure 4.21](#) are an example of the mean tables used as parameters on each subject's GMM.

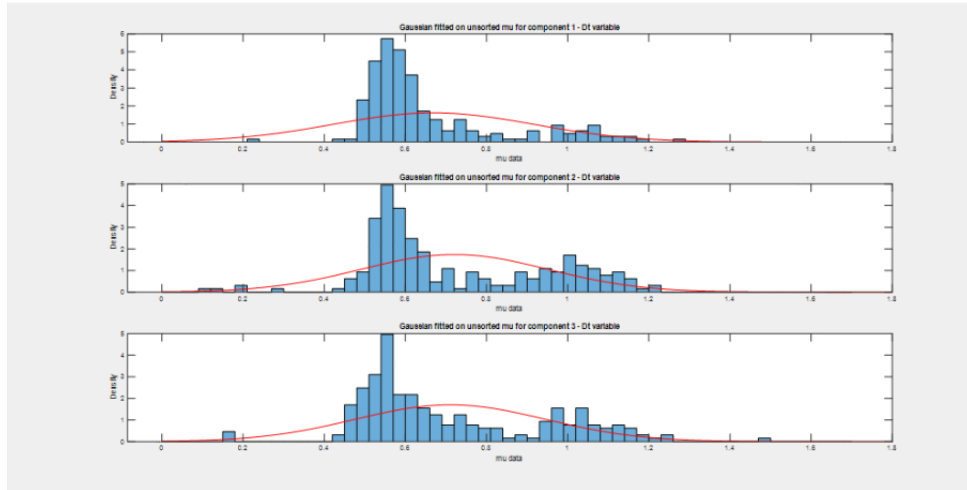
Our approach models each of the 3 mean values describing each variable (Dt, meanF, len) **separately** e.g., each of the first column's values corresponds to the mean value of each GMM component describing Dt. The first step to this approach is to take the 3 or 2 values of each mean table that correspond to the specific variable and put them in a unified 215x3 or 215x2 table (*subjects x components*) for the multivariate (Dt, meanF, len) or univariate (angle) case respectively. We initially **fitted a Gaussian** on each of the mean values of the variable. However, the resulted models **ignore the low values** which play a significant role in the mean table as depicted in [Figure 4.19](#) for Dt, meanF, len and [Figure 4.20](#) for angle.

To counteract this problem, we decided to model the values based on their amplitude i.e., separate the mean values in **different modes with varying amplitudes**. For instance, the distribution of Dt has **3 modes**, leading to 3 mean values in each test case with varying amplitudes. Thus, we organize 3 groups of test model parameters; large, medium and small. This is conducted by sorting each variable's mean values in **ascending order** as presented in [Figure 4.21](#).

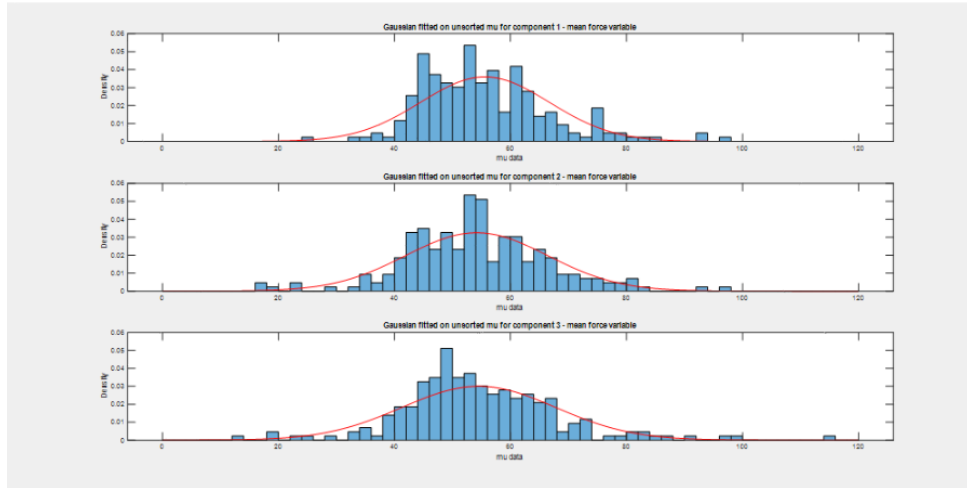
Consequently, each sorted element is then distributed in a corresponding array thus creating 3 arrays containing the mu values of each GMM in ascending order. Lastly, a **Gaussian is fitted in each array** thus creating a model of 3 normal distributions describing the mean values of Dt. The aforementioned are depicted in [Figure 4.22](#). The same procedure is followed for the other 3 variables noting that the **angle** variable is described by a model of 2 normal distributions.

In summary, the modeling of the GMMs' mean table parameter starts at unification and ascending sorting of the mean values. Then, a Gaussian is fitted for each component of each variable. Therefore, Dt, meanF and len are statistically described using 3 normal distributions on each variable while 2 normal distributions are used for the angle resulting in a total of **11 normal distributions**.

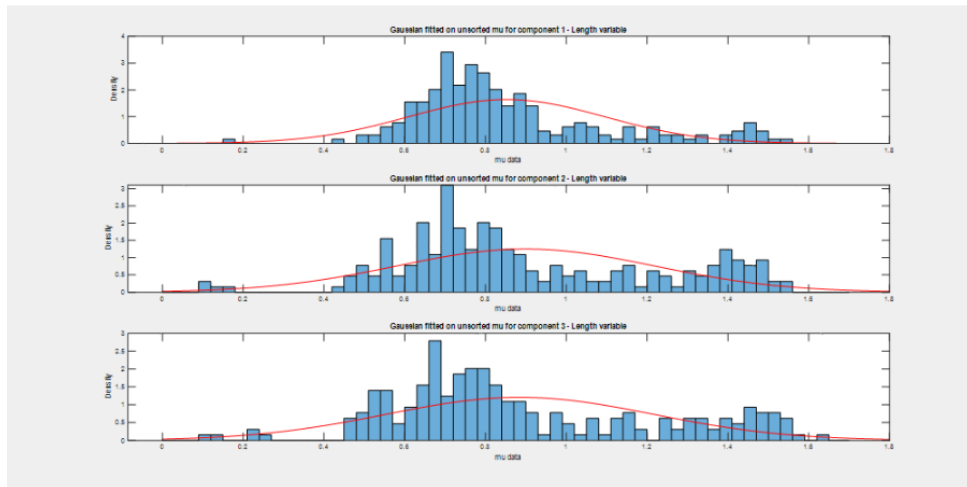
[Figure 4.23](#) depicts the Gaussians fitted on Dt, meanF and len. In this figure we notice that the modeling takes all modes into consideration while the same applies for [Figure 4.24](#) depicting the Gaussians fitted on angle. Moreover, the bivariate nature of angle is modeled using this procedure.



(A) Dt variable.



(B) meanF variable.



(C) len variable.

FIGURE 4.19: Gaussians fitted on mean table for Dt, meanF and len - default method.

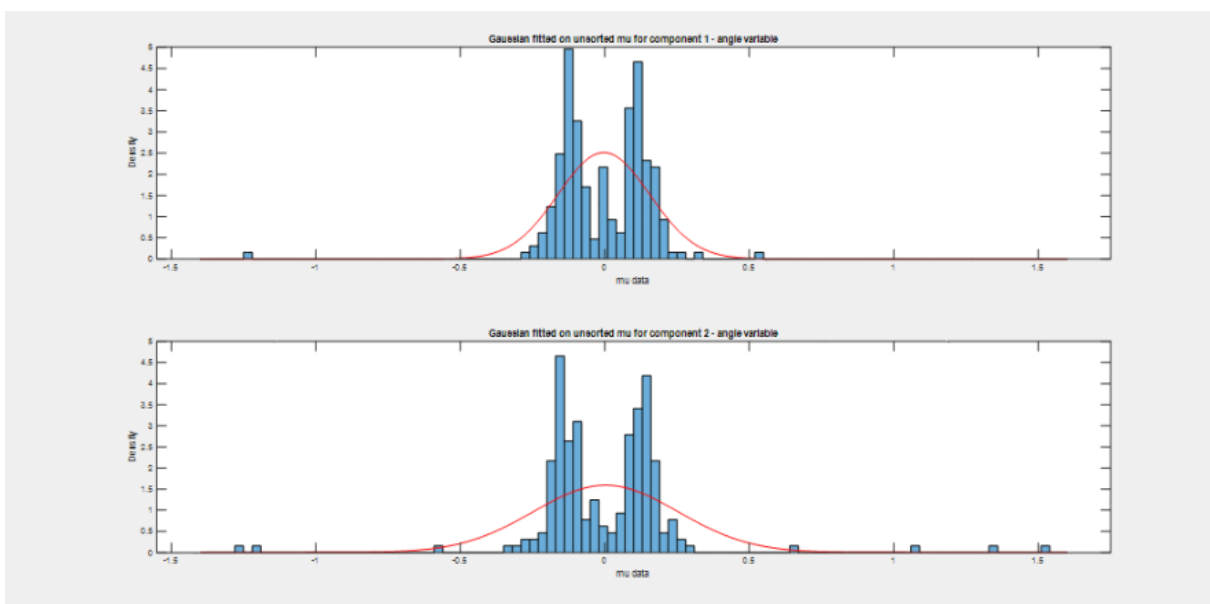


FIGURE 4.20: Gaussians fitted on mean table for angle - default method.

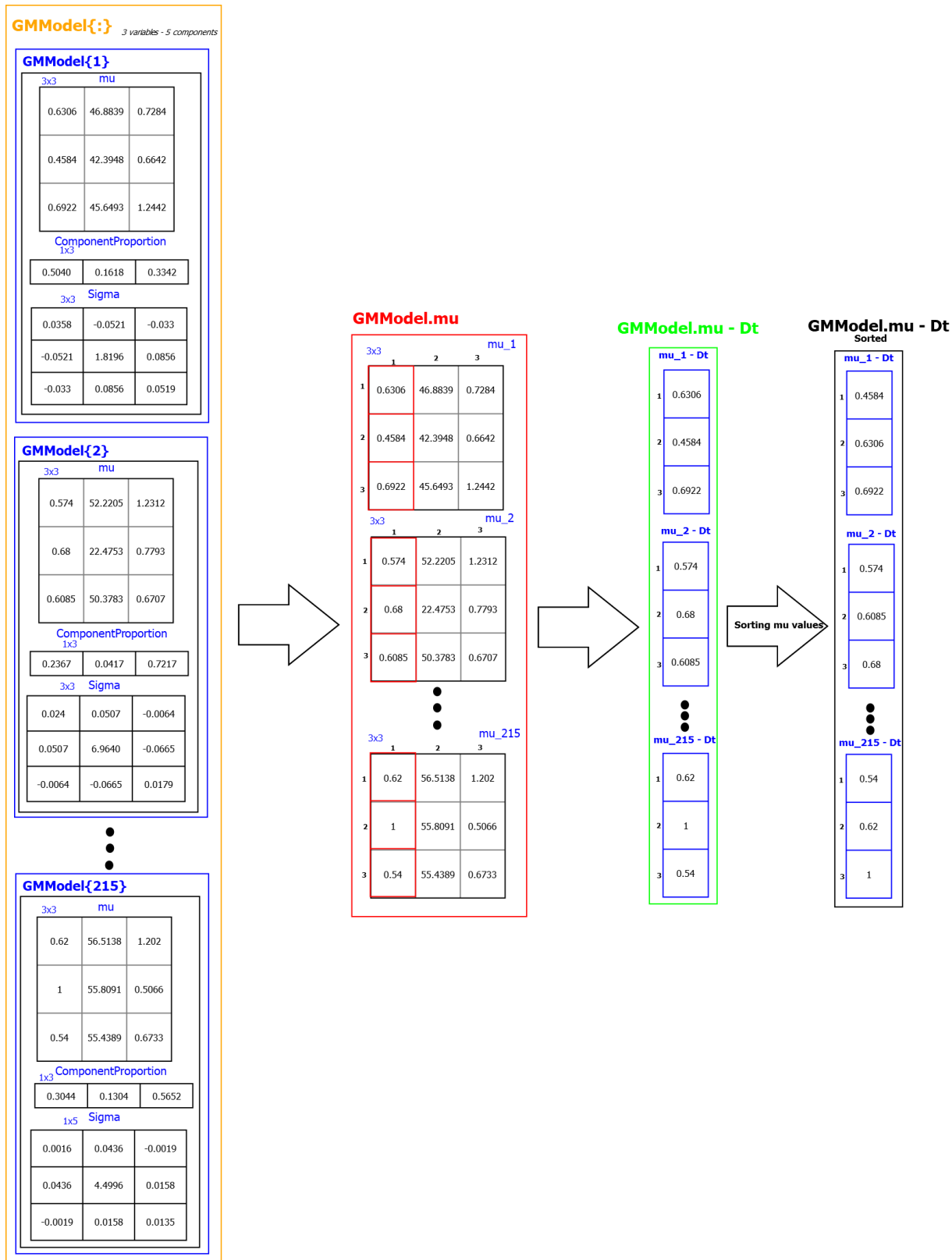


FIGURE 4.21: Mean table's modeling logic for Dt variable - part 1.

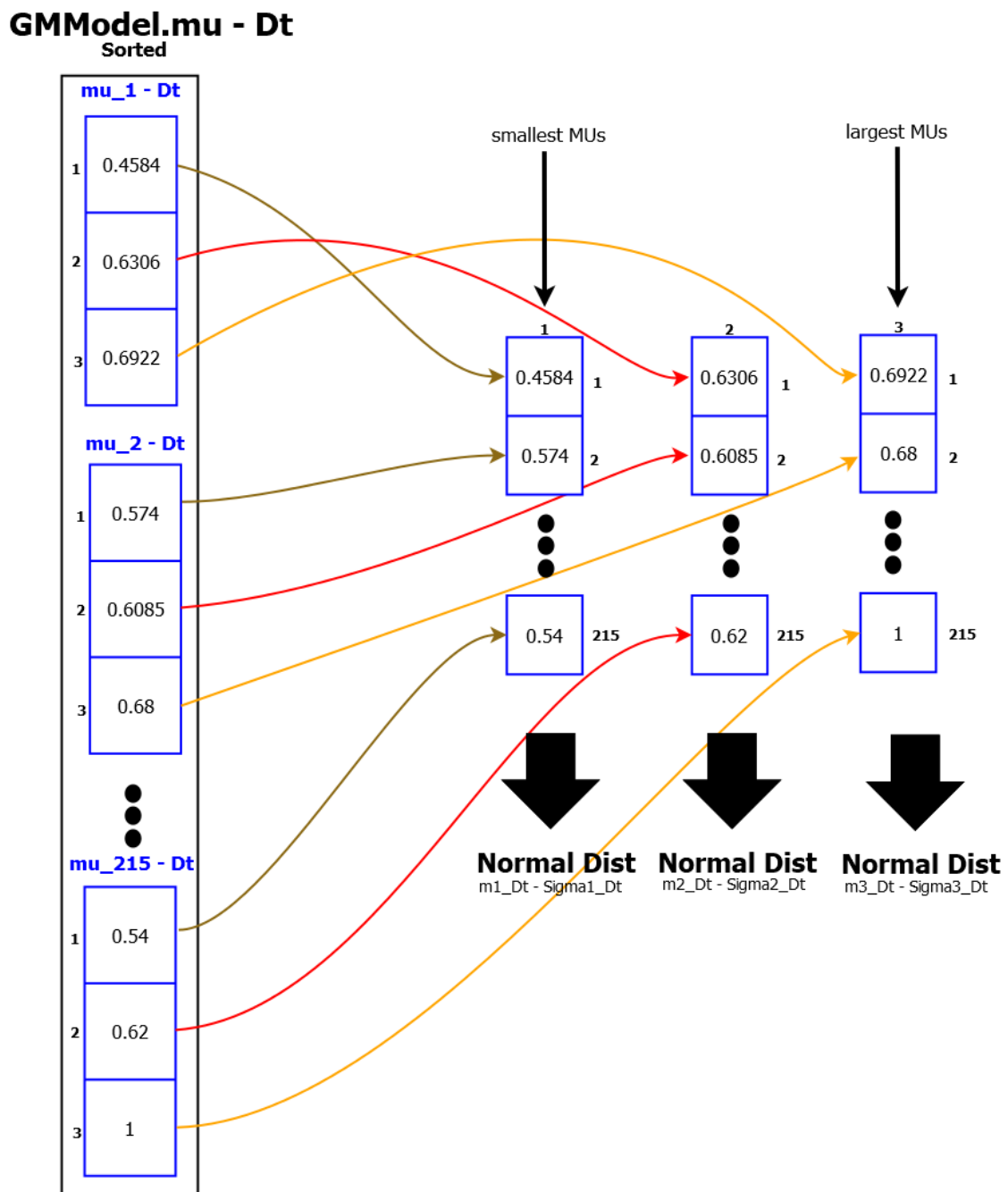


FIGURE 4.22: Mean table's modeling logic for Dt variable - part 2.

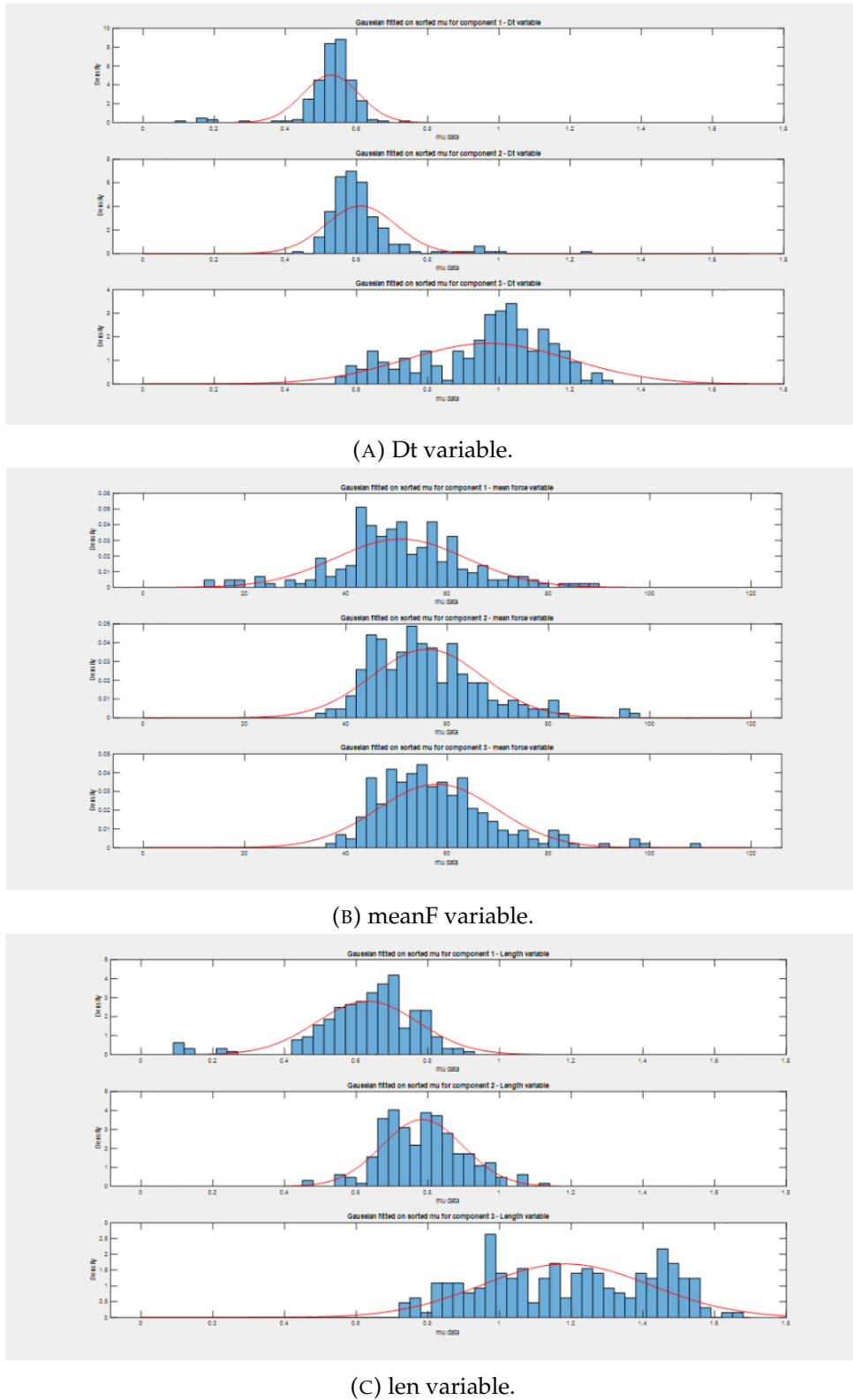


FIGURE 4.23: Gaussians fitted on mean table for Dt, meanF and len.

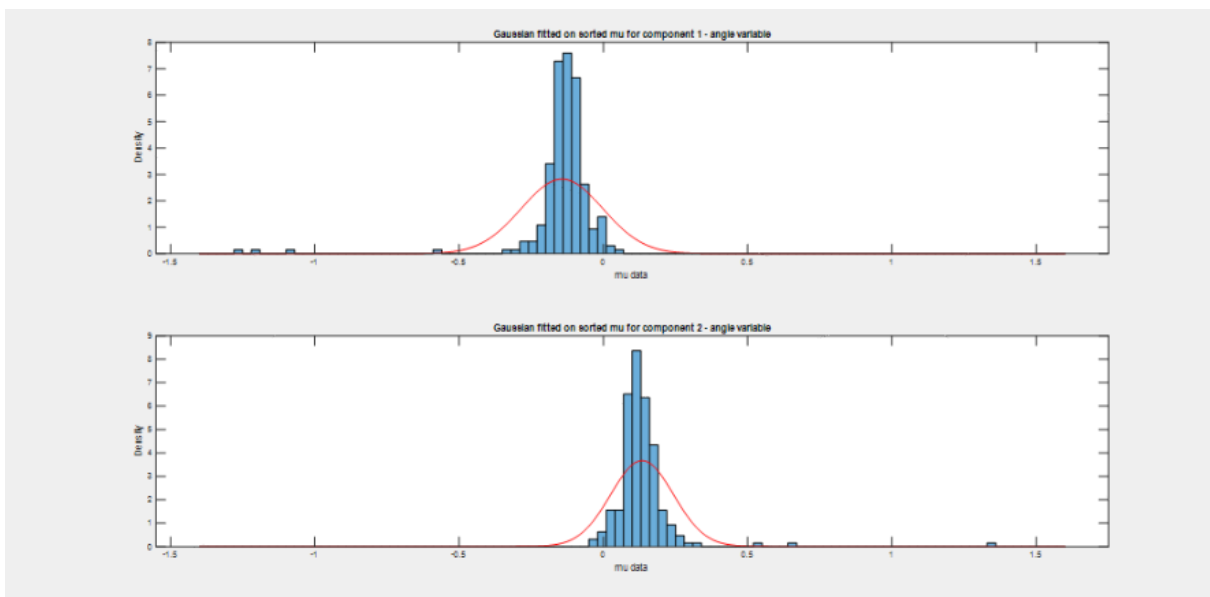


FIGURE 4.24: Gaussians fitted on mean table for angle.

4.3.2 Statistical Description of the Mixing Probability (Component Proportion Coefficients)

The **mixing probability parameter (Component Proportion Coefficients)** of a GMM of 3 components is a 3-tuple array as 3 is the number of GMM's components. Each tuple contains the coefficient describing the proportion of each component and is a number between 0 and 1. The sum of all coefficients is 1. In order to statistically describe this parameter, a Gaussian will be fitted for each component's proportion.

This parameter needs to be in accordance with the component it describes. Thus the approach followed for its statistical description will be conducted alongside the statistical description of the mu table parameter presented in [subsection 4.3.1](#). As if not, the sorting process will **ignore the correlation** between the component proportions and their respective mean values. Subsequently, the component proportions are unified in a 215x3 table for Dt, meanF and len or 215x3 for angle. Then, during the sorting of mu, the coefficients are **shifted** to correspond to each component's mean value as depicted in figure [Figure 4.25](#). This way, the correlation between the component proportions and the mean values will remain after performing the sorting. We characterize this method as **index-fixing**.

Each element is allocated in an array in the same manner as mean table parameter's modeling. A Gaussian is fitted in each array thus creating a model of 3 normal distributions describing the coefficients for Dt, meanF, len and 2 normal distributions for the angle. The aforementioned are depicted in [Figure 4.26](#).

In summary, modeling component proportion coefficients of the GMMs starts at unification and index-fixing of the values. Then, a Gaussian is fitted for each component. Therefore, Dt, meanF and len are statistically described using 3 normal distributions while 2 normal distributions are used for the angle resulting in a total of 5 normal distributions.

[Figure 4.27](#) illustrates the Gaussians fitted on the **mixing probabilities** for the multivariate and univariate model. We notice in the latter that the normal distributions are similar. This result is considered sensible as the probability of a step being performed on each direction is the same.

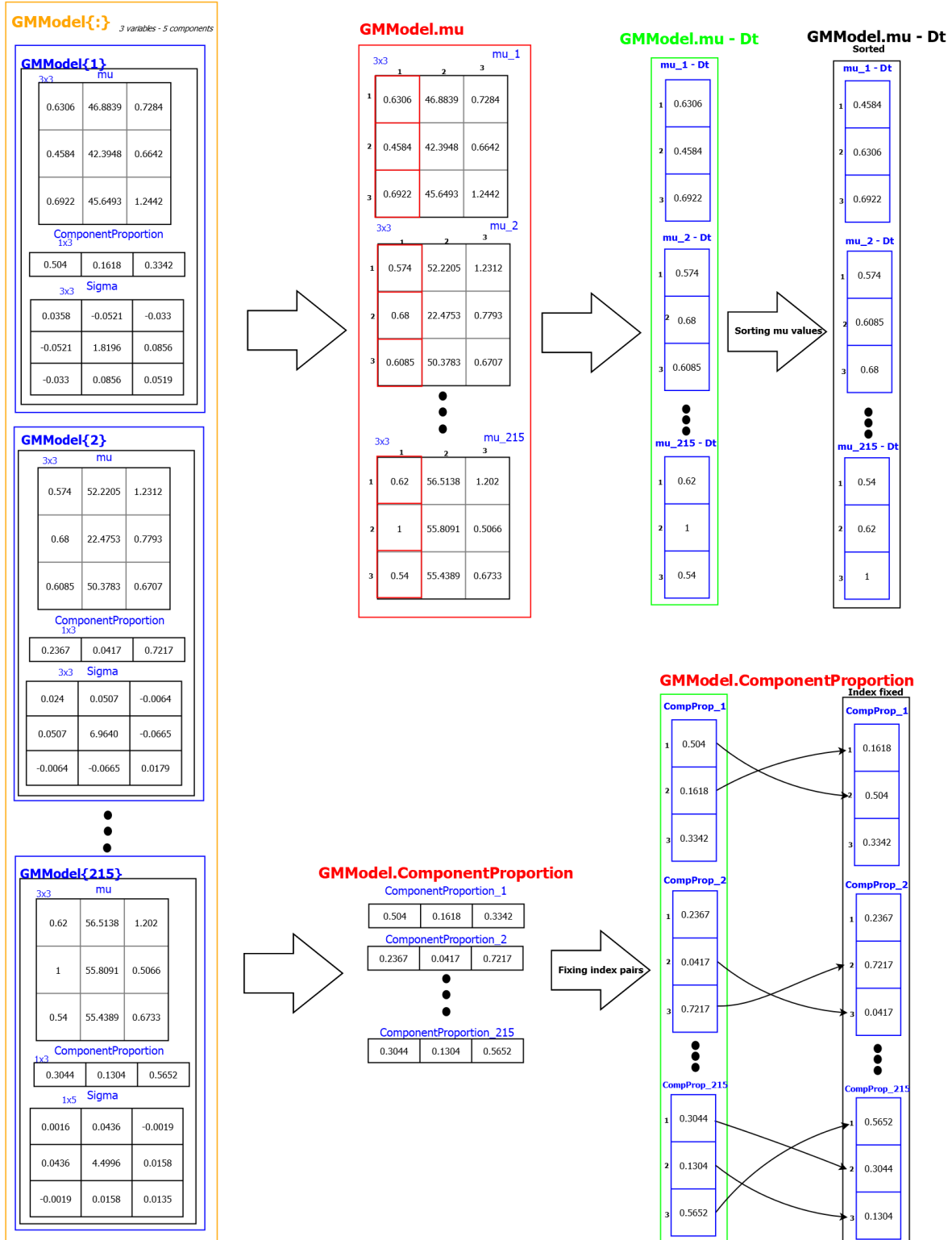


FIGURE 4.25: Mixing probability (Component Proportion Coefficients) modeling logic - part 1.

GMModel.ComponentProportion

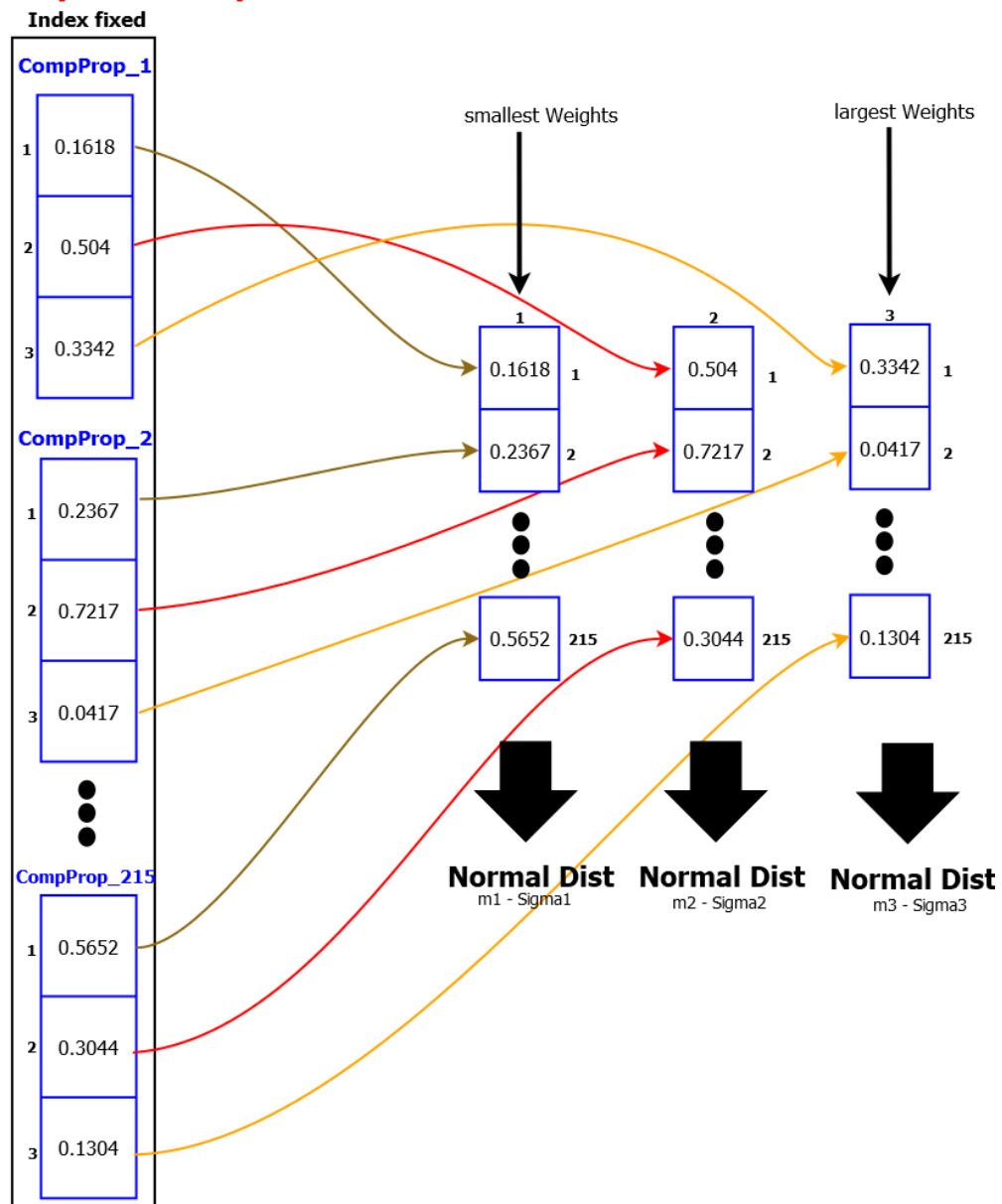
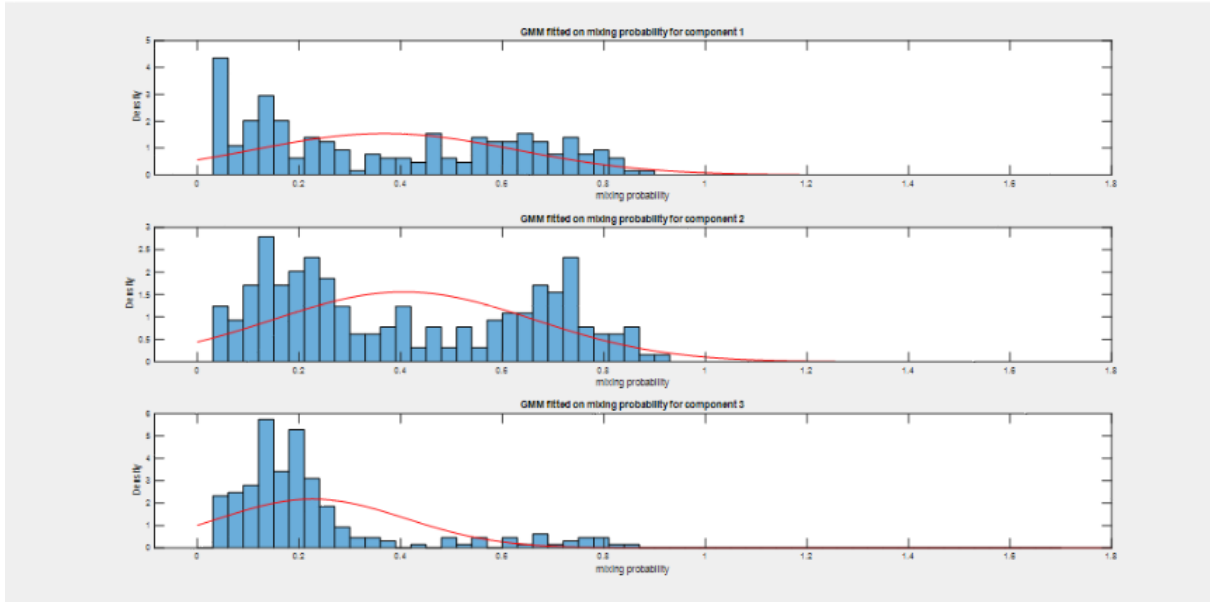
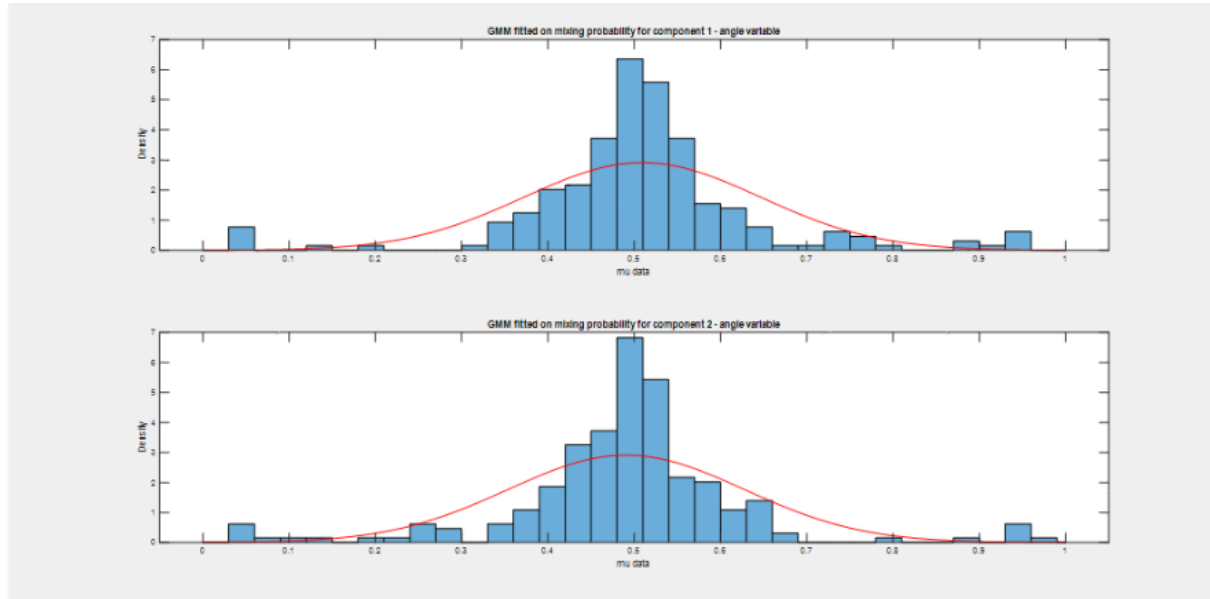


FIGURE 4.26: Mixing probability (component proportion coefficients) modeling logic - part 2.



(A) Multivariate model - Dt, meanF, len variables.



(B) Univariate model - angle variable.

FIGURE 4.27: Gaussians fitted on mixing probabilities.

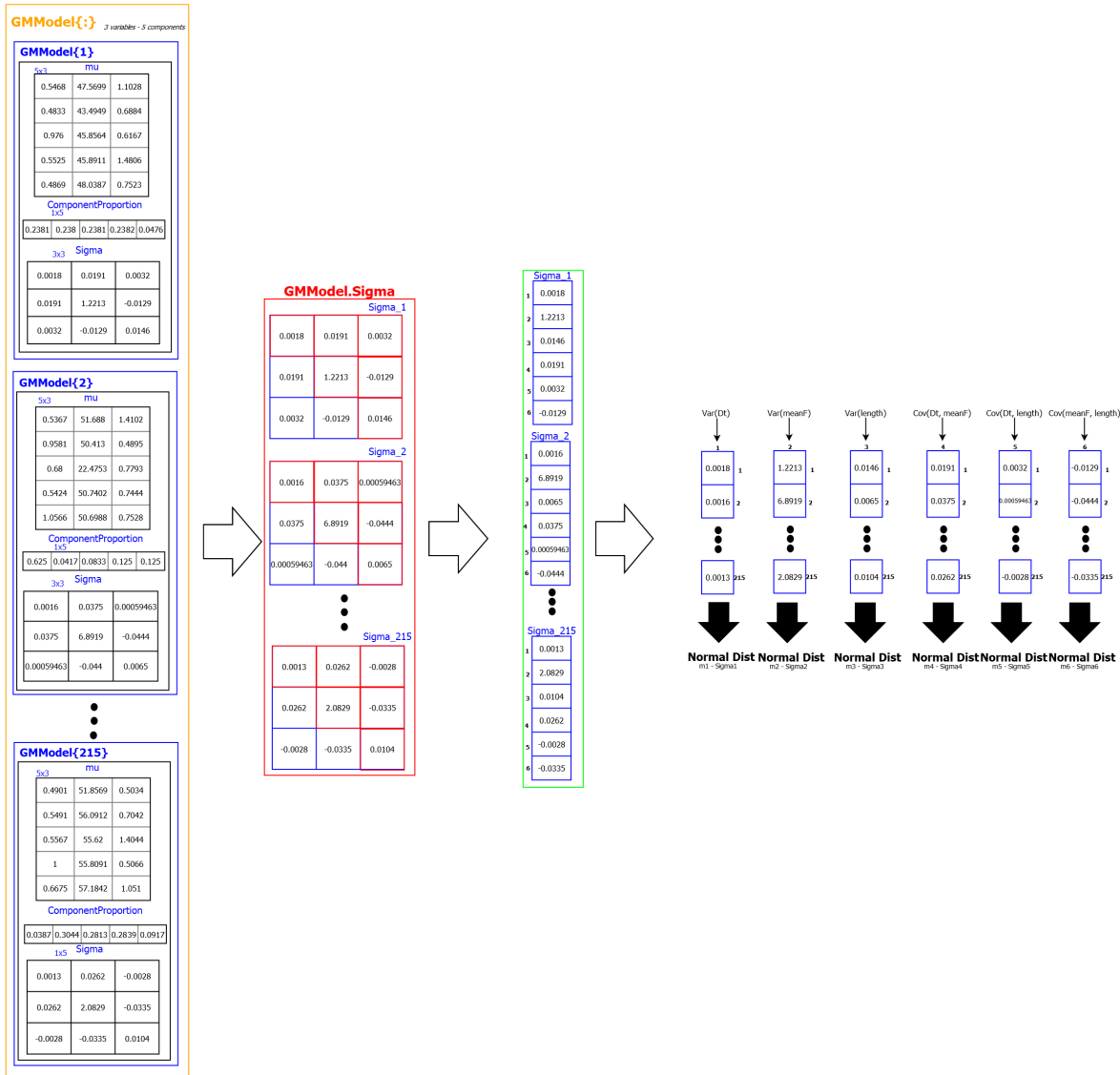
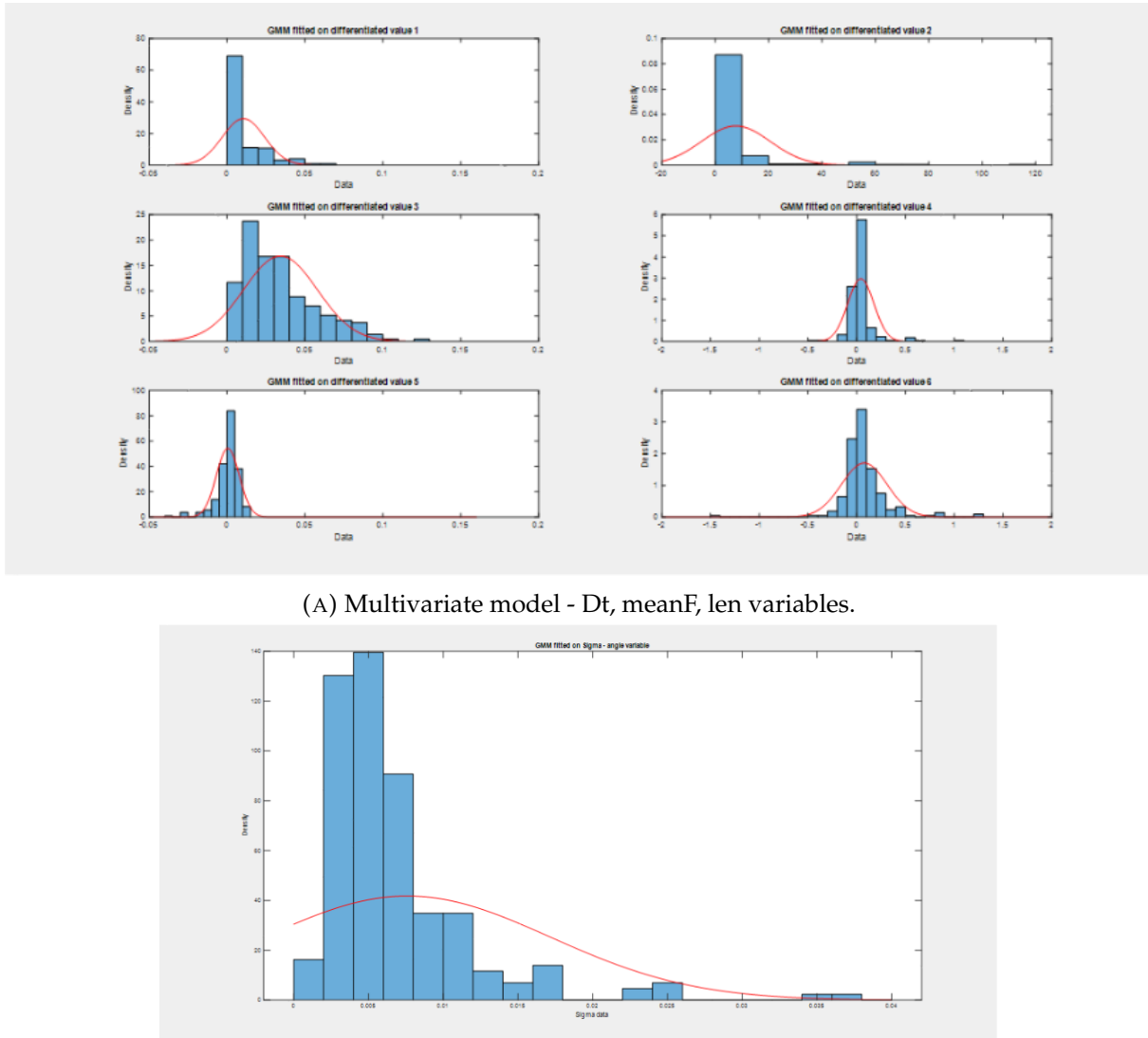


FIGURE 4.28: Variance/Covariance matrix Σ modeling logic.

4.3.3 Statistical Description of the Variance/Covariance Matrix Σ

The **variance/covariance matrix** Σ parameter of a 3-variate GMM is a 3x3 symmetric and positive semi-definite matrix describing the covariance between variables as well as the variances (matrix diagonal), i.e., the covariance of each random variable with itself.

Consequently, the **critical values** of a 3-variate covariance matrix are 6. Those are the 3 diagonal values i.e., the variance of each variable, as well as the covariances between the 1st and 2nd variable, the 1st and 3rd variable and finally, the 2nd and 3rd variable. Thus, for the most accurate statistical description of Σ , a **unified table** containing the 6 differentiated values of all subjects was created and a Gaussian is fitted in each, as illustrated in Figure 4.28.

FIGURE 4.29: Gaussians fitted in variance/covariance matrix Σ .

In summary, modeling variance/covariance matrix Σ of the GMMs starts at unification of its critical values. Then, a Gaussian is fitted for each. Therefore, Dt, meanF and len are statistically described using 6 normal distributions while 1 more is used for the angle as a univariate GMM is described only by its variance. Thus, a total of **7 normal distributions** is required for the modeling of Σ . **Figure 4.29** depicts the Gaussians fitted on the critical values of Σ for the multivariate and the univariate model, respectively.

4.4 Modeling Overview

The **statistical description of the parameters** of the Gaussian Mixture Models concludes the process of modeling the human walk. This modeling was, in summary, implemented following the steps described in the previous sections of [chapter 4](#).

The first step was to **extract the necessary variables** to describe a human walk using the data contained in the provided database. These variables where the interarrival time of each step (D_t), the mean vertical force induced in a step ($meanF$), the length traversed (len) and the angle of each step. Those variables were extracted for each step of each person. Then, 2 GMMs were fitted in each person's walks; a 3-component multivariate for D_t , $meanF$ and len and a 2-component univariate for the angle variable.

Finally, the **statistical description of the parameters** of those GMMs was conducted. More specifically, each GMM is parameterized by its mixing probability (component proportion coefficients), mean table (μ) and covariance matrix Σ . Hence, upon some procedures, these parameters were fitted in GMMs in order to statistically describe them. The statistical description of the multivariate GMM's parameters (describing D_t , $meanF$, len) resulted in:

- **9 Gaussians** to describe the mean table parameter – 3 for each variable as the GMM consists of 3 components.
- **3 Gaussians** to describe the mixing probability (component proportion coefficients) parameter as the GMM consists of 3 components.
- **6 Gaussians** to describe the Σ parameter - each Sigma is a 3×3 symmetric matrix as the GMM describes 3 variables and thus, there are 6 critical values.

While the statistical description of the univariate GMM describing the angle variable resulted in:

- **2 Gaussians** to describe the mean table parameter as the GMM consists of 2 components.
- **2 Gaussians** to describe the mixing probability (component proportion coefficients) parameter as the GMM consists of 2 components.
- **1 Gaussian** to describe the Σ parameter as the GMM describes 1 variable.

The diagram of [Figure 4.30](#) shows an overview of this procedure.

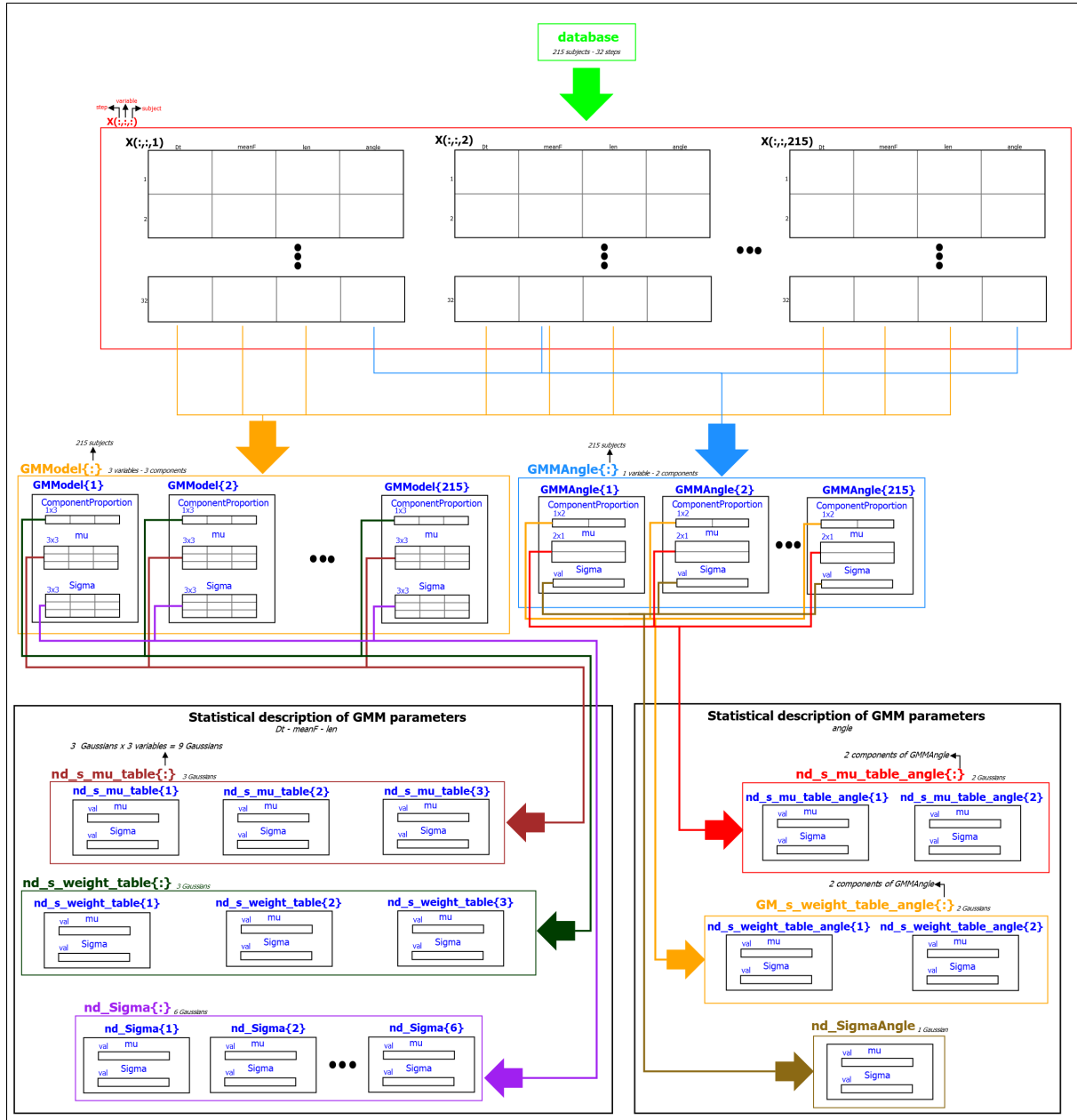


FIGURE 4.30: An overview of modeling human walk.

4.5 The Simulator

The scope of the simulator is to describe a random human walk accurately by extracting n sets of the 4 variables for n desired finite number of steps. In order to achieve this, a **reversed procedure** than the one followed for the modeling will be conducted. More specifically, the goal is to extract a random walk using the statistical description of the parameters acquired through the modeling, as input. Thus, a **random generation** of the parameters is performed using the models describing them. Then, a multivariate and a univariate GMM is fitted using the respective parameters. These GMMs will be used as distributions that best describe the process of human walk. Consequently, using these GMMs, n sets of the Dt, meanF, len and angle random variables will be acquired. Those sets will describe a random walk of n steps. This process is depicted graphically in the diagram of [Figure 4.35](#).

4.5.1 Parameter Estimation

The first step of our implementation is to **generate a set of parameters** to use on the GMM statistically describing the human walk. In the same manner, the multivariate GMM's variables i.e., Dt, meanF, len will be extracted first.

Consequently, using the 3 Gaussians describing the **mean values** of each variable i.e., 9 Gaussians in total, a random value is generated using each one. Thus, the 3 Gaussians produce 3 random values for each of the three random variables and the unification of those produces the final mean table which will be used as a parameter in the simulated GMM ([Figure 4.31](#)).

Likewise, the **mixing probability or component proportion coefficients** parameter of the simulated GMM is generated using the 3 Gaussians created in the modeling. Thus, 3 values are generated and are used as parameters in the simulated GMM ([Figure 4.32](#)). Note that the mixing probabilities must sum to 1. However, since these are randomly generated, this constraint is not always satisfied and therefore, a normalization in the generated mixing probabilities is performed.

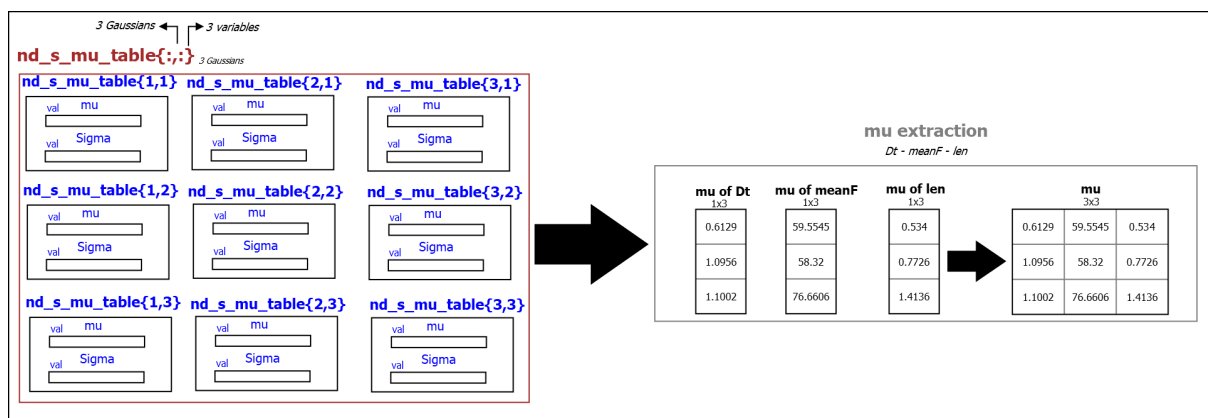


FIGURE 4.31: Generating a random mean table.

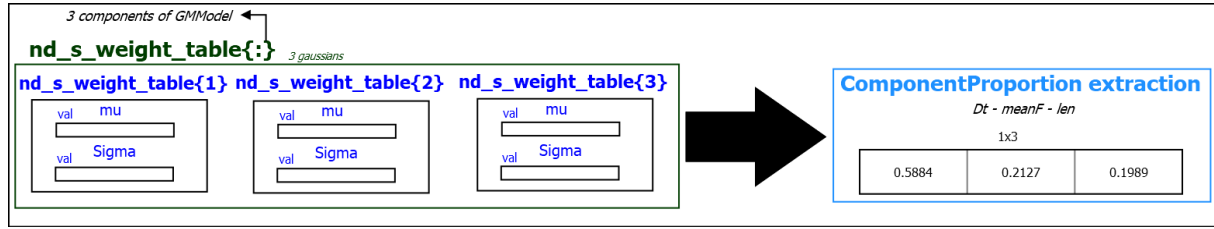


FIGURE 4.32: Generating random mixing probability (component proportion coefficients).

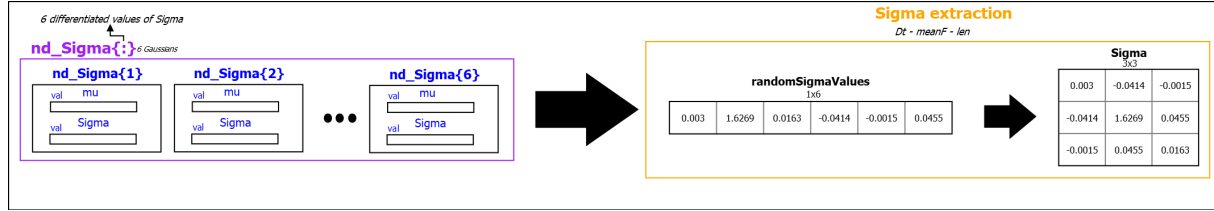


FIGURE 4.33: Generating a random variance/covariance matrix Σ .

Finally, the **variance/covariance matrix** Σ of the simulated GMM is generated using the 6 Gaussians created in the modeling. More specifically, the 6 critical values are randomly generated by these Gaussians. The first 3 values describe the diagonal values of the matrix i.e., variance of each variable, while the fourth describes the covariance between the first and second variable i.e., the values (1,2) and (2,1) of the Σ matrix. Finally, the fifth describes the covariance between the first and the third variable i.e., values (1,3) and (3,1) of the Σ matrix and finally, the sixth describes the covariance between the second and the third variable i.e., values (2,3) and (3,2) of the Σ matrix. This way, a symmetrical covariance matrix is generated (Figure 4.33).

The only constraint in this procedure is that, as it is known by the theory, a covariance matrix, apart from symmetrical, is also positive semi-definite. However, the random generation does not guarantee this. To confront this, a workaround has been implemented and therefore, the random generation is performed in a loop that breaks when the generated matrix is positive semi-definite.

The same procedure is performed for the extraction of the parameters characterizing the simulated univariate GMM describing the random variable of **angle**. In this case, the mean table parameter is determined by randomly generating the 2 necessary values using the 2 Gaussians describing it. The same applies to the extraction of the mixing probability, whereas the 2 values are generated and normalised in order to sum to 1. Finally, the Gaussian describing the variance of the variable is used to randomly generate the value of σ . This procedure is depicted in Figure 4.34

4.5.2 Extraction of the Random Walk

In the final step, two GMMs i.e., a multivariate for Dt, meanF, len and a univariate for the angle, are fitted using the random parameters generated in subsection 4.5.1 as input. Using these GMMs, the random walk is extracted. The multivariate GMM

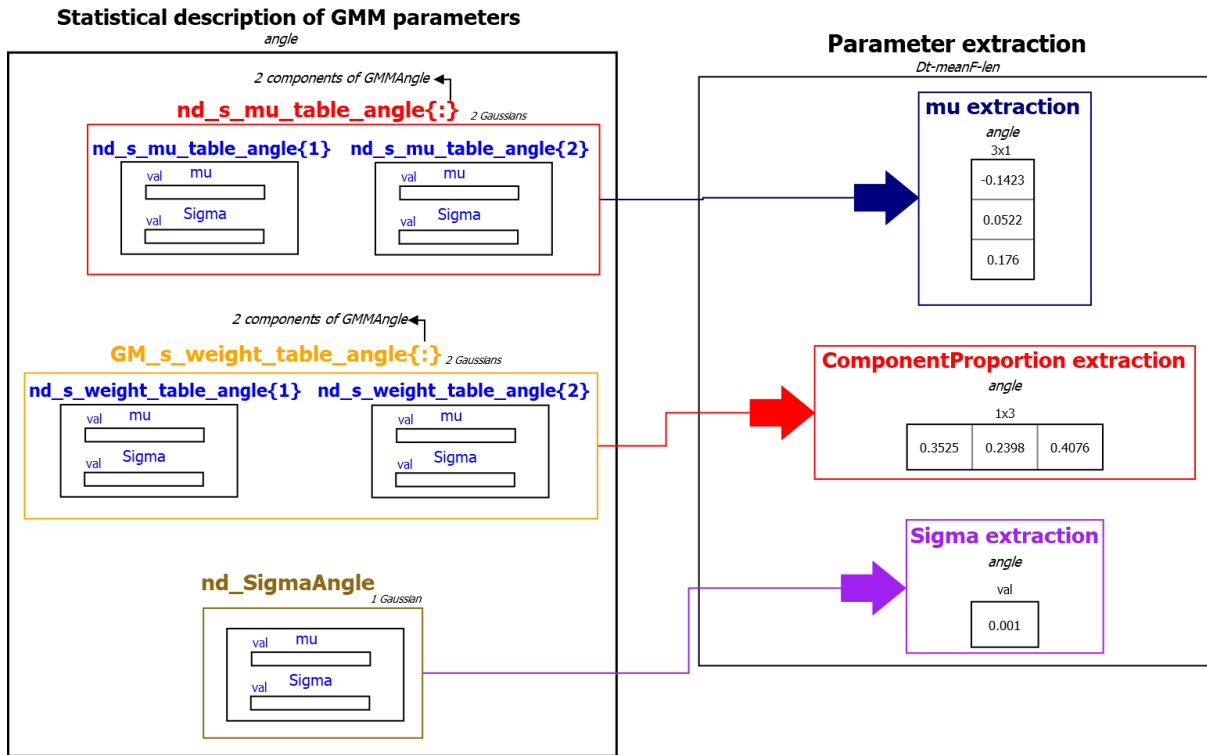


FIGURE 4.34: Generating random parameters for the angle variable.

generates n sets of Dt, meanF and len variables while the GMM describing the angle generates n values of the angle variable. The merging of those describes a **random walk of n steps**.

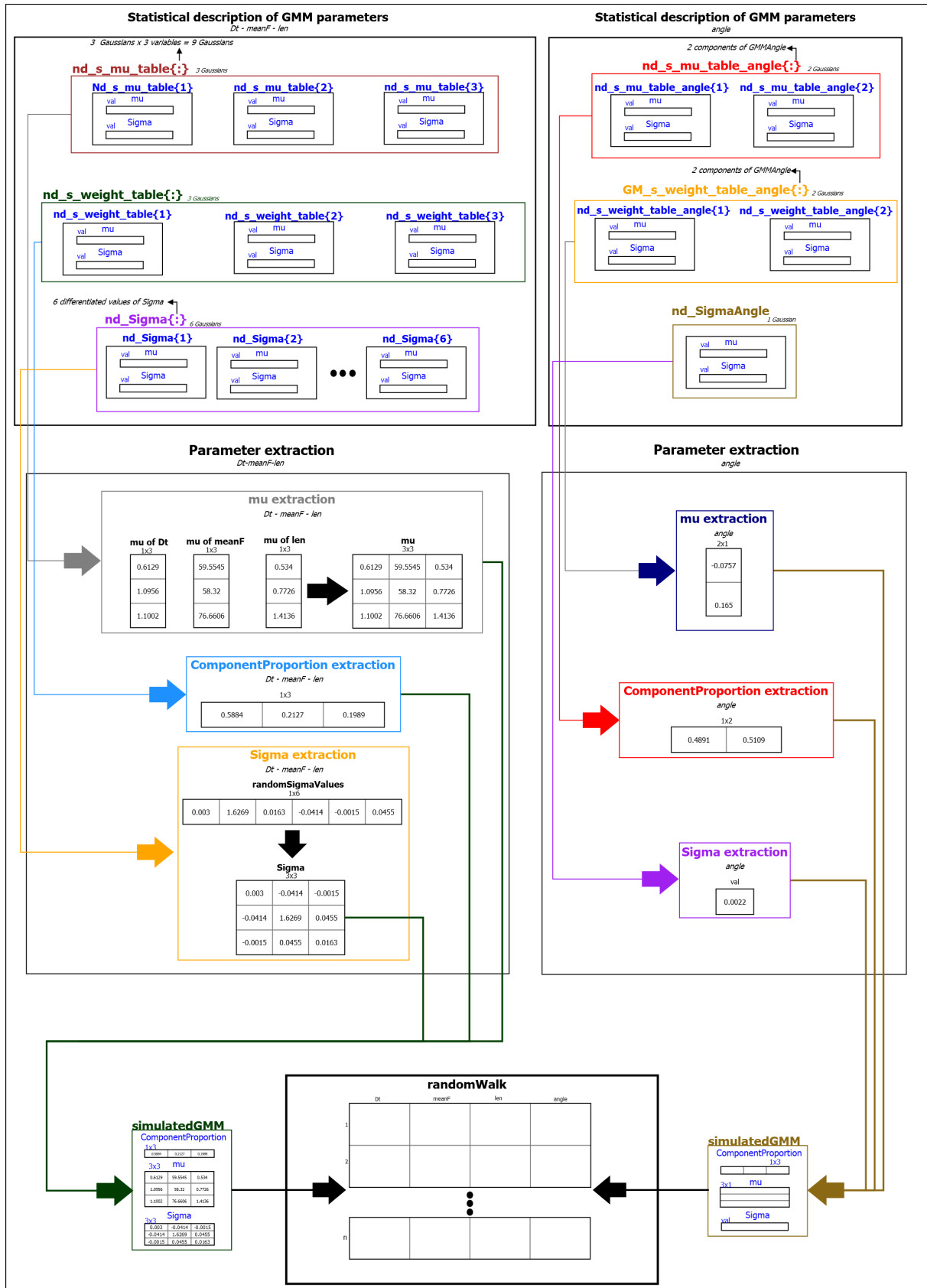


FIGURE 4.35: An overview of the simulator.

Chapter 5

Experimental Setup

5.1 Instruments Used for the Analysis

The data used in this work have been acquired through an experimental campaign [17, 39] conducted at the University of Modena and Reggio Emilia, Department of Engineering “Enzo Ferrari” (Modena, Italy) and were provided beforehand. More specifically, an instrumented floor equipped with a sensor system has been exploited to measure the force, time, and position of each step. The setup used to make the measurements consists of 10 plates that occupy an area of $1m^2$, each, placed sequentially in a horizontal formation yielding an area of 2×5 for a total of $10m^2$ of available surface on the walkway, as illustrated in [Figure 5.1](#). These plates are constructed of stainless steel and covered with waterproof mats made of synthetic material steel.

It is worth pointing out that this approach allows to acquire the quantity of interest directly. Other available methods used in the literature indeed involve uncertainties. An example of this is if, the measurement of the acceleration was acquired using an accelerometer constrained to a foot. In fact, the human body is not a rigid system and the force applied to the floor cannot be simply inferred from the acceleration and the static mass of the person.

Force sensors are installed beneath each vertex of the plates ([Figure 5.2](#)) so that the induced force can be measured. Additionally, the position of the applied force can be inferred through simple trigonometric manipulation. The output of the force sensors is acquired through an acquisition system that consists of a control unit and a computer and is manufactured by National Instrument.

It is important to note that the algorithms, diagrams and extracted results described in [chapter 4](#) and [chapter 6](#) were implemented using MATLAB R2019b Update 7 [29].



FIGURE 5.1: The instrumented floor used in the experiments. [17, 39]



FIGURE 5.2: Force sensors installed beneath the vertices of the plates. [17, 39]

5.2 Critical Factors in the Analysis

The data collected in this study are conditioned by several factors. More specifically, the data relating to the right and left plates were acquired separately. Therefore, the gait of each subject was "guided" towards the center line of the floor.

Secondly, it is important to note that the plates of the instrumented floor could produce noise during the experiments due to the extreme sensitivity of the data. Actually, the software used for the data processing showed some small abnormal variations in the force induced on certain plates.

Thirdly, the subjects tested differed in height and weight i.e. the speed varies on each subject. As known from the literature, as speed varies, the shape of the step changes, hence, a metronome was used to obtain time histories of the step at a fixed rate.

Lastly, the experiments were designed for individuals walking at a normal tempo and thus, the presence of other pedestrians in the walkway, the resonance phenomenon, the contingency of a collision, a random roaming, jogging, running, etc. are not taken into consideration, as a real-world example would require.

Chapter 6

Simulations & Evaluation

Similarly to [Figure 4.11](#), [Figure 6.1](#) depicts an instance of the table extracted by the simulator describing a **randomly generated human gait** of 30 steps. The columns of the table correspond to the variables of interarrival time (Dt), mean vertical force induced (meanF), length (len) and angle of each step, respectively.

As a first deduction by comparing the two tables, the values generated can be considered **comparable** to the values of a random person from the database. The only remarkable difference spotted is in the meanF variable. [Figure 4.11](#) is probably describing a human with large weight whose walking induces a big force on each step. However, the database includes measurements for a variety of body types and sexes and as a result, the simulated values of force contain values with great modulation.

To deepen our understanding about the outcome of the simulator, the **mean speed of gait** was calculated in order to compare it with the theoretical mean speed of human walking at a normal tempo. Using the len and Dt variables, speed can be calculated as:

$$\text{speed} = \frac{\text{length}}{\text{Dt}} \quad (6.1)$$

[Equation 6.1](#) produces the **speed of each step**. The mean speed 1000 random walk simulations of $n = 30$ steps, was calculated as:

$$\text{mean speed} = 5.2 \text{ km/h}$$

The **average speed of human walk** at a normal tempo is ranging from 4.51 km/h to 4.75 km/h for older individuals and from 5.32 km/h to 5.43 km/h for younger individuals [56, 3]. Thus the simulated walk's speed approximates the expected value.

Finally, using the length and the angle of each step acquired by the simulated walk, the x and y positions of each step j were calculated as:

$$x_j = \begin{cases} x_{j-1} + \text{len} \cos(\text{angle}), & \text{if } j > 1 \\ \text{len} \cos(\text{angle}), & \text{if } j = 1 \end{cases} \text{ and } y_j = \text{len} \sin(\text{angle}) \quad (6.2)$$

These positions were scattered in [Figure 6.2](#) in order to visualise the simulated human walk on the walkway.

Finally, [Figure 6.3](#) depicts the first (out of two) walk of the subject of [Figure 4.11](#). Note that the randomly generated walk approximates the pattern of the experimental.

	Dt	meanF	len	angle
1	0.4772	38.6253	0.2384	0.0492
2	0.9901	55.6843	1.2739	-0.4079
3	0.8088	53.9880	1.3394	-0.4177
4	0.7990	60.6444	1.3144	-0.4103
5	0.5119	42.9150	0.5271	0.0385
6	0.7267	68.4648	1.6744	-0.3835
7	0.4080	54.8610	0.7408	-0.3250
8	0.5524	46.7623	0.2481	-0.3857
9	0.7951	56.9033	1.1245	-0.4767
10	0.8785	68.7802	1.5487	-0.3882
11	0.7744	41.0307	0.6300	-0.3817
12	0.2720	55.2004	0.7246	-0.3617
13	0.7673	68.9556	1.2025	-0.3694
14	0.8376	63.4489	1.2532	0.0036
15	0.6809	60.1293	1.6556	-0.0111
16	0.8412	37.3094	0.4857	-0.3886
17	0.6342	41.1686	0.6429	-0.4082
18	0.5698	36.6439	0.5694	-0.3976
19	0.8607	37.1217	0.4648	0.0788
20	0.4331	68.1625	1.0014	-0.3794
21	0.5250	43.7525	0.8476	-0.4437
22	0.4989	38.6265	0.2125	-0.3668
23	0.4420	54.6550	0.9824	-0.4666
24	0.8107	62.5224	1.8612	-0.3315
25	0.3234	60.4584	0.1128	-0.4511
26	0.5733	57.5913	1.5775	-0.3951
27	0.6886	37.3134	0.3525	-0.3833
28	0.8971	61.1870	1.4276	-0.4113
29	0.5228	38.9281	0.8047	0.0604
30	0.5302	53.4987	1.4825	-0.3455

FIGURE 6.1: A random walk generated for $n = 30$ steps.

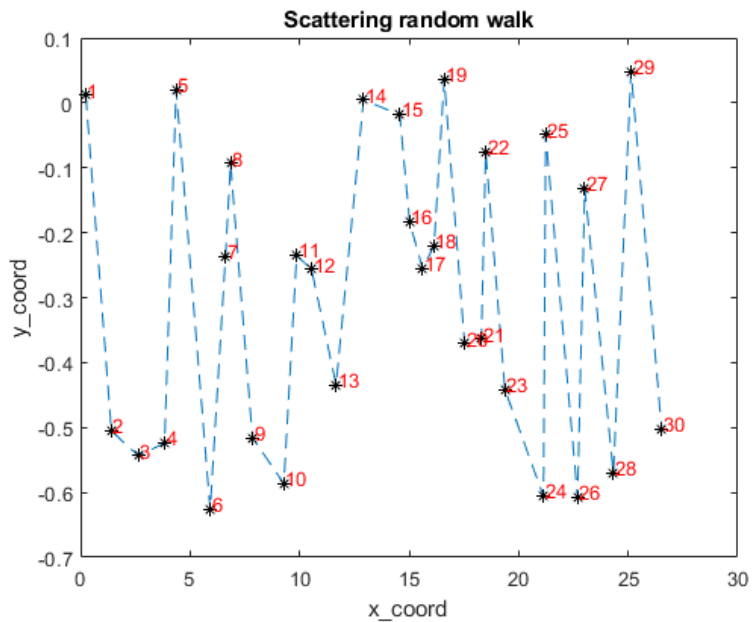


FIGURE 6.2: Scattering a random walk.

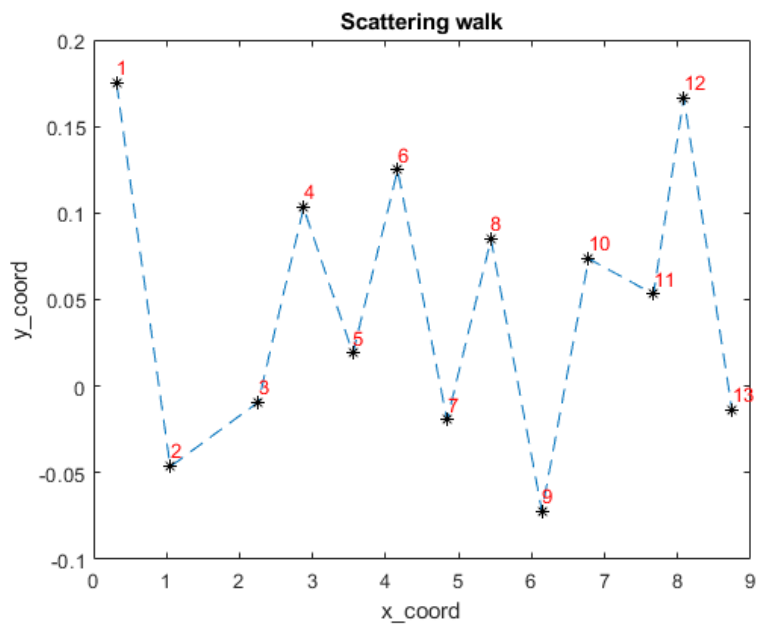


FIGURE 6.3: First walk of the random subject described in Figure 4.11.

In conclusion, it can be inferred that the outcome of the simulator is promising as the data generated match the properties of the experimental quite efficiently. Thus, this simulator is capable of supplementing the experimental procedure in future research.

Chapter 7

Conclusion & Future Work

7.1 Conclusion

In this thesis, we presented an **innovative algorithm** for modeling and simulation of human gait using Gaussian Mixture Models and Normal Distributions. More specifically, we presented a **practical** model to use at the design stage of a walkway that satisfies the requirements of simplicity i.e., the GMMs and Gaussians used require simple calculations, ease of use by engineers as well as accuracy i.e., a large number of experimental samples is used. Furthermore, this algorithm can be considered innovative i.e., we used GMMs and conceived the human walk as a random process, while only a few past researches with a small number of data have done so. Lastly, in the proposed model we accounted the intersubject and intrasubject variability model.

We also implemented a **simulator** that can be used to provide reliable prediction and assessment of floor vibrations under human actions, using the developed models. Thus, using this approach, the experimental procedure can be omitted in future researches.

7.2 Future Work

We conclude this thesis by presenting possible **future extensions** of this work. The next step to our research is to apply the simulator at a digital pedestrian walkway in order to conduct research on bridge oscillations and the resonance effect using simulated walks. This digital pedestrian walkway is developed by the Civil and Environmental Engineering Department of the University of Modena & Reggio Emilia (Dipartimento di Ingegneria "Enzo Ferrari").

Moreover, it would be practical to repeat the experimental campaign using a **bigger instrumented floor** that approximates the dimensions of a real footbridge, thus allowing for more steps at each stride. In this case, the experimental procedure would preferably include more information about the **characteristics** of the subjects e.g., gender, physical characteristics, nation, culture, the environment, etc. These parameters influence the intersubject variability of human walking process as suggested by several researches [23, 62, 66] presented in section 3.3.

Using these information, the model can be extended to include real world occasions e.g., the presence of many pedestrians in the walkway, the synchronization of step

within groups, the contingency of a collision, a random roaming, jogging, running, etc.

Bibliography

- [1] TP Andriacchi, JA Ogle, and JO Galante. "Walking speed as a basis for normal and abnormal gait measurements". In: *Journal of biomechanics* 10.4 (1977), pp. 261–268.
- [2] Andreas Antoniou. *Digital filters: analysis, design, and signal processing applications*. 2018.
- [3] Karen Aspelin and Nick Carey. "Establishing pedestrian walking speeds". In: *Portland State University* (2005), pp. 5–25.
- [4] Ed Ayyappa. "Normal human locomotion, part 1: Basic concepts and terminology". In: *JPO: Journal of Prosthetics and Orthotics* 9.1 (1997), pp. 10–17.
- [5] Hugo Bachmann and Walter Ammann. *Vibrations in structures: induced by man and machines*. Vol. 3. Iabse, 1987.
- [6] Hugo Bachmann et al. *Vibration problems in structures: practical guidelines*. Birkhäuser, 2012.
- [7] J Blanchard, BL Davies, and JW Smith. "Design criteria and analysis for dynamic loading of footbridges". In: *Proceeding of a Symposium on Dynamic Behaviour of Bridges at the Transport and Road Research Laboratory, Crowthorne, Berkshire, England, May 19, 1977*. TRRL Rpt. 275 Proceeding. 1977.
- [8] J MW Brownjohn, Aleksandar Pavic, and P Omenzetter. "A spectral density approach for modelling continuous vertical forces on pedestrian structures due to walking". In: *Canadian Journal of Civil Engineering* 31.1 (2004), pp. 65–77.
- [9] J. M. W. Brownjohn and A. Pavic. "Human-Induced Vibrations on Footbridges". In: *Advances in Bridge Maintenance, Safety Management, and Life-Cycle Performance: Proceedings of the Third International Conference on Bridge Maintenance, Safety and Management (IABMAS), Porto, Portugal* (2015), pp. 263–264.
- [10] James Brownjohn, Vitomir Racic, and Jun Chen. "Universal response spectrum procedure for predicting walking-induced floor vibration". In: *Mechanical Systems and Signal Processing* 70 (2016), pp. 741–755.
- [11] Thomas Caleri. "Sviluppo di un modello matematico per la camminata bipede: Fitting e studio di una distribuzione multivariata che ne approssimi l'andamento". In: Università degli Studi di Modena e Reggio Emilia, 2018.
- [12] Anil K Chopra. "Dynamics of Structures Prentice-Hall". In: *Englewood Cliffs, NJ* zbMATH (1995).

- [13] Brad Davis and Onur Avci. "Simplified vibration serviceability evaluation of slender monumental stairs". In: *Journal of Structural Engineering* 141.11 (2015), p. 04015017.
- [14] Brad Davis, Di Liu, and Thomas M Murray. "Simplified experimental evaluation of floors subject to walking-induced vibration". In: *Journal of Performance of Constructed Facilities* 28.5 (2014), p. 04014023.
- [15] A Ebrahimpour et al. "Measuring and modeling dynamic loads imposed by moving crowds". In: *Journal of Structural Engineering* 122.12 (1996), pp. 1468–1474.
- [16] Per-Erik Eriksson. *Vibration of low-frequency floors-dynamic forces and response prediction*. Chalmers University of Technology, 1994.
- [17] Martina Fornaciari. "Sviluppo di un modello matematico per la camminata bipede: applicazione nello studio di stabilità delle passerelle ciclopedenali". In: Università degli Studi di Modena e Reggio Emilia, 2018.
- [18] FW Galbraith and MV Barton. "Ground loading from footsteps". In: *The Journal of the Acoustical Society of America* 48.5B (1970), pp. 1288–1292.
- [19] F. C. Harper. "The Mechanics of Walking". In: *Res. Appl. Ind* 15.1 (1962), pp. 23–28.
- [20] Jeffrey M Hausdorff. "Gait dynamics, fractals and falls: finding meaning in the stride-to-stride fluctuations of human walking". In: *Human movement science* 26.4 (2007), pp. 555–589.
- [21] EJ Hudson et al. "Active Control of Concert-Induced Vibrations". In: *Geotechnical and Structural Engineering Congress 2016*. 2016, pp. 1729–1741.
- [22] VT Inman, HJ Ralston, and F Todd. "Human walking-Williams and Wilkins". In: *Baltimore, London* (1981).
- [23] Tianjian Ji and Aikaterini Pachi. "Frequency and velocity of people walking". In: *Structural Engineer* 84.3 (2005), pp. 36–40.
- [24] CA Jones, P Reynolds, and A Pavic. "Vibration serviceability of stadia structures subjected to dynamic crowd loads: A literature review". In: *Journal of Sound and Vibration* 330.8 (2011), pp. 1531–1566.
- [25] M Kasperski and C Sahnaci. "Serviceability of pedestrian structures". In: *Proceedings of the International Modal Analysis Conference (IMAC XXC)*, Orlando, USA. 2007.
- [26] Stuart Clifford Kerr. "Human induced loading on staircases". PhD thesis. University of London, 1998.
- [27] H Kramer and HW Kebe. "Man-induced structural vibrations". In: *Der Bauingenieur* 54.5 (1980), pp. 195–199.
- [28] Di Liu and Brad Davis. "Walking vibration response of high-frequency floors supporting sensitive equipment". In: *Journal of Structural Engineering* 141.8 (2015), p. 04014199.

- [29] MATLAB. 9.7.0.1190202 (*R2019b*). Natick, Massachusetts: The MathWorks Inc., 2018.
- [30] Y Matsumoto et al. "A study on design of pedestrian over-bridges". In: *Transactions of JSCE* 4 (1972), pp. 50–51.
- [31] Jack C McCormac and Stephen F Csernak. *Structural steel design*. pearson prentice hall Upper Saddle River, 2008.
- [32] Neil Messenger. "Moving the human machine: understanding the mechanical characteristics of normal human walking". In: *Physics Education* 29.6 (1994), pp. 352–357.
- [33] CJ Middleton and JMW Brownjohn. "Response of high frequency floors: A literature review". In: *Engineering Structures* 32.2 (2010), pp. 337–352.
- [34] TM Murray, DE Allen, and EE Ungar. "Design guide 11, floor vibrations due to human activities". In: *American Institute of Steel Construction (AISC)*, Chicago, IL (2003).
- [35] Karl M Newell and Andrew B Slifkin. "The Nature of Movement". In: *Motor behavior and human skill: A multidisciplinary approach* (1998), p. 143.
- [36] Antonio Occhiuzzi, Mariacristina Spizzuoco, and Francesco Ricciardelli. "Loading models and response control of footbridges excited by running pedestrians". In: *Structural Control and Health Monitoring: The Official Journal of the International Association for Structural Control and Monitoring and of the European Association for the Control of Structures* 15.3 (2008), pp. 349–368.
- [37] Antonio Occhiuzzi, Mariacristina Spizzuoco, and Francesco Ricciardelli. "Loading models and response control of footbridges excited by running pedestrians". In: *Structural Control and Health Monitoring: The Official Journal of the International Association for Structural Control and Monitoring and of the European Association for the Control of Structures* 15.3 (2008), pp. 349–368.
- [38] Sven V Ohlsson. *Floor vibrations and human discomfort*. Chalmers University of Technology, Division of Steel and Timber Structures, 1982.
- [39] Milani Pancaldi Bassoli and Vincenzi. "A Statistical Approach for Modelling Individual Walking Forces". In: Elsevier MSSP, 2020.
- [40] A Pavic et al. "Critical review of guidelines for checking vibration serviceability of post-tensioned concrete floors". In: *Cement and Concrete Composites* 23.1 (2001), pp. 21–31.
- [41] Aleksandar Pavic and Paul Reynolds. "Vibration serviceability of long-span concrete building floors. Part 1: Review of background information". In: *Shock and Vibration Digest* 34.3 (2002), pp. 191–211.
- [42] Aleksandar Pavic and Paul Reynolds. "Vibration serviceability of long-span concrete building floors. Part 2: Review of mathematical modelling approaches". In: *Shock and Vibration Digest* 34.4 (2002), pp. 279–297.

- [43] Aleksander Pavic and MR Willford. "Appendix G: Vibration serviceability of post-tensioned concrete floors". In: *Post-tensioned concrete floors design handbook* (2005), pp. 99–107.
- [44] Matjaž Perc. "The dynamics of human gait". In: *European journal of physics* 26.3 (2005), p. 525.
- [45] Vitomir Racic, James Brownjohn, and Aleksandar Pavic. "Dynamic loading factors of individual jogging forces". In: ECCOMAS proceedings. 2013.
- [46] Vitomir Racic and James Mark William Brownjohn. "Stochastic model of near-periodic vertical loads due to humans walking". In: *Advanced Engineering Informatics* 25.2 (2011), pp. 259–275.
- [47] Vitomir Racic, James MW Brownjohn, and Aleksandar Pavic. "Random model of vertical walking force signals". In: *Topics on the Dynamics of Civil Structures, Volume 1*. Springer, 2012, pp. 73–84.
- [48] Vitomir Racic and JMW Brownjohn. "Mathematical modelling of random narrow band lateral excitation of footbridges due to pedestrians walking". In: *Computers & structures* 90 (2012), pp. 116–130.
- [49] Vitomir Racic and A Pavic. "Mathematical model to generate near-periodic human jumping force signals". In: *Mechanical Systems and Signal Processing* 24.1 (2010), pp. 138–152.
- [50] Vitomir Racic, Aleksandar Pavic, and JMW Brownjohn. "Experimental identification and analytical modelling of human walking forces: Literature review". In: *Journal of Sound and Vibration* 326.1-2 (2009), pp. 1–49.
- [51] JH Rainer, G Pernica, and David E Allen. "Dynamic loading and response of footbridges". In: *Canadian Journal of Civil Engineering* 15.1 (1988), pp. 66–71.
- [52] C Sahnaci and M Kasperski. "Random loads induced by walking". In: *Proceedings of the sixth European conference on structural dynamics*. Vol. 1. 2005, pp. 441–6.
- [53] J. Simpson and E. Weiner. *The Oxford English Dictionary*. Oxford University Press, 1989. ISBN: 9780191958922.
- [54] Andrew L Smith, Stephen J Hicks, and Paul J Devine. *Design of floors for vibration: A new approach*. Steel Construction Institute Ascot, Berkshire, UK, 2007.
- [55] Steven W Smith et al. "The scientist and engineer's guide to digital signal processing". In: (1997).
- [56] Inc TranSafety. "Study compares older and younger pedestrian walking speeds". In: *Road Management & Engineering Journal* (1997).
- [57] Christopher L Vaughan, Brian L Davis, Jeremy C O'connor, et al. *Dynamics of human gait*. Human Kinetics Publishers, 1992.
- [58] John E Wheeler. "Prediction and control of pedestrian-induced vibration in footbridges". In: *Journal of the structural division* 108.9 (1982), pp. 2045–2065.
- [59] Michael W Whittle. *Gait analysis: an introduction*. Butterworth-Heinemann, 2014.

- [60] M Willford, P Young, and C Field. "Predicting footfall-induced vibration: Part 1". In: *Proceedings of the Institution of Civil Engineers-Structures and Buildings* 160.2 (2007), pp. 65–72.
- [61] Michael R Willford, Peter Young, and MIMechE CEng. *A design guide for footfall induced vibration of structures*. Concrete Society for The Concrete Centre, 2006.
- [62] Richard Wiseman. *Quirkology: the curious science of everyday lives*. Pan Macmillan, 2008.
- [63] Wei-ping Xie, Liang Chang, and Yong Du. "Analysis on vibration isolation of Zhongnan Theater". In: *CHINESE JOURNAL OF GEOTECHNICAL ENGINEERING- CHINESE EDITION-* 29.11 (2007), p. 1720.
- [64] Masahiro Yoneda. "A simplified method to evaluate pedestrian-induced maximum response of cable-supported pedestrian bridges". In: *Proceedings of the International Conference on the Design and Dynamic Behaviour of footbridges*. 2002.
- [65] P Young. "Improved floor vibration prediction methodologies. Engineering for Structural Vibration–Current developments in research and practice Arup Vibration Seminar". In: *Institution of Mechanical Engineers* (2001).
- [66] Stana Zivanovic. "Probability-based estimation of vibration for pedestrian structures due to walking." PhD thesis. University of Sheffield, 2006.
- [67] S Živanović, A Pavic, and Vitomir Racic. "Towards modelling in-service pedestrian loading of floor structures". In: *Topics on the Dynamics of Civil Structures, Volume 1*. Springer, 2012, pp. 85–94.
- [68] Stana Živanović and Aleksandar Pavia. "Probabilistic assessment of human response to footbridge vibration". In: *Journal of low frequency noise, vibration and active control* 28.4 (2009), pp. 255–268.
- [69] Stana Živanović and A Pavic. "Probabilistic approach to subjective assessment of footbridge vibration". In: *The 42rd UK Conference on Human Responses to Vibration*. 2007.
- [70] Stana Živanović, ALEKSANDAR Pavic, and Paul Reynolds. "Vibration serviceability of footbridges under human-induced excitation: a literature review". In: *Journal of sound and vibration* 279.1-2 (2005), pp. 1–74.
- [71] Stana Živanović and Aleksandar Pavić. "Probabilistic modeling of walking excitation for building floors". In: *Journal of performance of constructed facilities* 23.3 (2009), pp. 132–143.
- [72] Stana Živanović, Aleksandar Pavić, and Paul Reynolds. "Probability-based prediction of multi-mode vibration response to walking excitation". In: *Engineering structures* 29.6 (2007), pp. 942–954.